# Energy and Reserve Management in Interconnected Systems including Electric Railway and Public Power Grids: Operation, Market Strategies and Capacity Expansion

THÈSE N$^{O}$ 6672 (2015)

PRÉSENTÉE LE 24 SEPTEMBRE 2015

À LA FACULTÉ DES SCIENCES ET TECHNIQUES DE L'INGÉNIEUR
GROUPE DE SCIENTIFIQUES STI
PROGRAMME DOCTORAL EN GÉNIE ÉLECTRIQUE

ÉCOLE POLYTECHNIQUE FÉDÉRALE DE LAUSANNE

POUR L'OBTENTION DU GRADE DE DOCTEUR ÈS SCIENCES

PAR

Mokhtar BOZORG

acceptée sur proposition du jury:

Prof. F. Rachidi-Haeri, président du jury
Dr S.-R. Cherkaoui, directeur de thèse
Prof. L. Wehenkel, rapporteur
Prof. T. Gomez San Roman, rapporteur
Prof. M. Paolone, rapporteur

ÉCOLE POLYTECHNIQUE
FÉDÉRALE DE LAUSANNE

Suisse
2015

You are educated when you have the ability to listen to
almost anything without losing your temper or self-confidence.
— Robert Frost

Dedicated to my beloved wife, Samira, and to my dear family,
for their unconditional love and support.

# Abstract

For historical reasons, the frequency of Electric Railway Power System (ERPS) in central European countries (e.g., Switzerland, Germany and Austria) is different from the frequency of the public power grid. To feed such a low frequency (i.e., 16.7 Hz) system, Electric Railway Companies (ERCs) operate their own low frequency generators. Moreover, ERPSs are connected to the public power grids through both static and rotating converters.

The power and energy demand at ERPS substations is highly fluctuating, due to the movement of trains (mobile demands). Hence, ERC has to provide enough reserve services either from its generators or from interconnecting converters in order to ensure a secure and reliable operation of the system. The interconnection presents great advantages for both of the power grids. The most important benefits are reliability enhancement, sharing reserve service resources and energy trading opportunities due to the temporal diversity of the peak demand.

Within the above context, the following three main problems referring to the operation of ERPSs, strategies for participating in electricity markets and capacity expansion of interconnecting converters have been studied in this thesis.

First, the problem of joint energy and reserve scheduling in an ERPS has been addressed. This problem has been formulated as a two-stage optimization problem including first (day-ahead scheduling) and second (real-time balancing) stages. In this problem, the variation of energy demand at each substation from its forecast value is an important uncertain parameter. To investigate the characteristics of this uncertain parameter, a short term load forecast method based on time series has been applied using realistic data from Swiss ERPS. Next, two mathematical approaches, namely, adaptive robust optimization and stochastic optimization have been proposed for dealing with uncertainties in this scheduling problem. The numerical results show that ERC can effectively utilize its generators and interconnecting converters to: 1) ensure security of its supply and 2) reduce its energy and reserve provision cost.

Second, we propose a robust offering strategy method for ERC to participate in energy and reserve markets, in the sense that uncertainties in energy demand at ERPS substations would not threaten its security of supply. In this respect, a discrete robust optimization technique is used to solve the robust energy and reserve scheduling problem. Afterward, a reserve offering curve construction algorithm based on the solution of robust energy and reserve scheduling is proposed. This algorithm takes into account the correlation between upward and downward tertiary reserve prices. To show the effectiveness of the proposed method, a realistic case study based on the characteristic of Swiss ERPS has been presented.

Third, we propose and investigate methods to assess the capacity expansion of the interconnecting converters. In this respect, the effect of increasing the capacity of the interconnecting converters on the daily operation cost of ERC has been studied. Afterward, the effect of adding new interconnecting converters on the short circuit ratio of ERPS substations has been investigated. Finally, a cost-reliability approach has been proposed to find the optimal size and location of new interconnecting converters. This method has allowed us to provide ERC with a set of optimal solutions according to the different economic and technical criteria.

**Key words:** Electric Railway, Interconnected Power Systems, Electricity Markets, Reserve Services, Uncertainty Management, Robust Optimization, Stochastic Optimization, Capacity Expansion, Load Forecast, Frequency Converters, Power System Reliability.

# Résumé

Pour des raisons historiques, la fréquence du système d'alimentation électrique des chemins de fer (Electric Railway Power System, ERPS) dans certains pays européens (par exemple la Suisse, Allemagne et Autriche) est différente de la fréquence du réseau électrique public. Pour alimenter un tel système à basse fréquence (soit 16,7 Hz), les compagnies de chemin de fer (ERCs) exploitent leurs propres générateurs à basse fréquence. En outre, ERPSs sont connectés aux réseaux publics d'électricité au travers de convertisseurs soit statiques soit tournants.

La demande en puissance et en énergie dans les postes ERPS est très fluctuante, en raison de la circulation des trains (demandes mobiles). Par conséquence, l'ERC doit se procurer suffisamment de réserve à partir de ses générateurs et des stations de conversion afin d'assurer un fonctionnement sûr et fiable du système. L'interconnexion présente de grands avantages pour les deux réseaux électriques. Les avantages les plus importants sont l'amélioration de la fiabilité, le partage des ressources en matière de réserve et des opportunités de négoce d'énergie en raison de la diversité temporelle de la demande de pointe.

Dans le contexte présenté ci-dessus, les trois principaux problèmes suivants se rapportant à l'exploitation des ERPSs sont étudiés dans cette thèse. Ces problèmes concernent respectivement l'établissement des programmes de production d'énergie et de réserve des ERPS, les stratégies d'offre pour la participation au marché d'électricité, et l'expansion de la capacité totale de conversion.

Le premier problème est formulé en terme de problème d'optimisation considérant deux étapes : le jour d'avant et l'équilibrage en temps réel. Dans ce problème, la variation de la demande d'énergie par rapport à la prévision à chaque poste d'ERPS est un paramètre incertain important. Pour étudier les caractéristiques de cette incertitude, une méthode de prévision de charge à court terme sur la base de séries temporelles (time series) est appliquée en utilisant des données réalistes dans le cas du ERPS suisse. Ensuite, deux approches mathématiques, à savoir, l'optimisation adaptative robuste (adaptive robust optimisation) et l'optimisation stochastique sont proposées pour solutionner le problème d'optimisation tout en considérant les incertitudes précitées. Les résultats numériques montrent qu' ERC peut utiliser efficacement ses générateurs et les convertisseurs d'interconnexion de façon à : 1) assurer la sécurité de son approvisionnement et 2) à réduire le coût de la fourniture de l'énergie et de la réserve.

Pour le deuxième problème, est proposée une méthode robuste de stratégie d'offre pour ERC afin de participer à des marchés de l'énergie et de réserve et de sorte que les incertitudes de la demande d'énergie dans les postes ERP ne menacent pas la sécurité d'approvisionnement. À cet égard, une technique d'optimisation discrète robuste est utilisée pour résoudre le problème robuste de planification en matière d'énergie et de réserve. Ensuite, sur cette base, un algorithme de construction de la courbe d'offre pour la réserve est proposé. Cet algorithme prend en compte la corrélation entre les prix de la réserve quand elle augmente et respectivement diminue. Pour démontrer l'efficacité de la méthode proposée, une étude de cas réaliste fondée sur la caractéristique de l'ERPS suisse est présentée.

Pour le troisième problème, on propose et étudie des méthodes pour évaluer l'expansion de la capacité totale de conversion. A cet égard, l'effet de l'augmentation de la capacité des convertisseurs d'interconnexion sur le coût de fonctionnement journalier des ERC a été étudié. Ensuite, l'effet de l'ajout de nouveaux convertisseurs d'interconnexion sur le ratio de court-circuit dans les postes ERPS est examinée. Enfin, une approche coût-fiabilité est proposée afin de trouver la taille optimale et l'emplacement de nouveaux convertisseurs d'interconnexion. Cette méthode permis de donner à ERC un ensemble de solutions optimales en fonction de différents critères économiques et techniques.

**Mots clefs :** Chemin de fer électrique, réseaux électriques interconnectés, marché de l'électricité, service de reserve, Gestion de l'incertitude, Optimisation robuste, Optimisation stochastique, expansion de la capacité, Prévisions de charge, Convertisseur de fréquence, Fiabilité du système d'alimentation.

# Zusammenfassung

In vielen europäischen Ländern (z.B. der Schweiz, Deutschland und Österreich) unterscheidet sich aus historischen Gründen die Frequenz des Bahnstromsystems (Electric Railway Power System, ERPS) von derjenigen des öffentlichen Stromnetzes. Um ein solches Niederfrequenzsystem (16.7 Hz) versorgen zu können, unterhalten viele Bahnnetzbetreiber (Electric Railway Companies, ERCs) eigene Niederfrequenzgeneratoren. Des Weiteren ist das ERPS über Konverter (Frequenzumrichter und –umformer) mit dem öffentlichen Stromnetz verbunden.

Da sich die Züge immerzu fortbewegen (bewegliche Lasten / mobile demands), fluktuiert der Leistungs- und Energiebedarf in den Unterwerken eines ERPS sehr stark. Um einen sicheren und zuverlässigen Betrieb des Systems gewährleisten zu können, muss ein ERC daher mittels Generatoren oder über Konverter jederzeit genügend Regelreserven bereithalten. Die Kopplung über die Konverter ist für beide Stromnetze von Vorteil. Die wichtigsten Vorteile sind hierbei die Verbesserung der Zuverlässigkeit, das Teilen der Ressourcen für die Bereitstellung der Regelreserven sowie die Möglichkeit, aufgrund der zu unterschiedlichen Zeitpunkten auftretenden Lastspitzen Energiehandel zu betreiben.

In dieser Dissertation werden drei Probleme im Bezug auf den Betrieb eines ERPS, Strategien zur Teilnahme am Stromhandel sowie den Kapazitätsausbau der Konverter untersucht.

Erstens wird betrachtet, wie die Generatoren und Konverter optimal eingesetzt werden können, um Energie und Regelreserven bereitzustellen. Dieses Problem wird als zweistufiges Optimierungsproblem formuliert (im ersten Schritt “day-ahead scheduling”, im zweiten Schritt “real-time balancing”). In diesem Zusammenhang ist die Abweichung des effektiven Energiebedarfs in jedem Unterwerk vom prognostizierten Wert ein wichtiger Unsicherheitsfaktor. Um diesen Unsicherheitsfaktor genauer charakterisieren zu können, wird eine Methode zur kurzfristigen Vorhersage der Last basierend auf Zeitreihenanalyse angewandt, wobei reelle Daten aus dem Schweizer ERPS verwendet werden. Es werden zwei mathematische Ansätze

vorgestellt, um mit der Unsicherheit in diesem Optimierungsproblem umgehen zu können: adaptive robuste Optimierung (adaptive robust optimization) und stochastische Optimierung (stochastic optimization). Die Resultate zeigen, dass ein ERC seine Generatoren und Konverter auf effektive Art und Weise einsetzen kann, um 1) die Versorgungssicherheit zu gewährleisten und 2) seine Kosten für die Bereitstellung von Energie und Regelreserven zu verringern.

Zweitens stellen wir eine robuste Angebotsstrategie vor, mit der ERCs in Märkten für Energie und Systemdienstleistungen teilnehmen können. Die Methode ist robust in dem Sinn, dass Unsicherheiten beim Lastaufkommen in den Unterwerken die Versorgungssicherheit nicht beeinträchtigen. Eine diskrete robuste Optimierungsmethode (discrete robust optimization) wird verwendet, um das Problem der zuverlässigen Energie- und Regelreservenallozierung zu lösen. Basierend darauf wird ein Algorithmus zur Berechnung einer Angebotskurve für die Regelreserven vorgeschlagen, der die Korrelation zwischen den Preisen für positive und negative Regelreserven berücksichtigt. Um den Nachweis für die Effektivität der entwickelten Methode zu erbringen, wird eine realistische Fallstudie basierend auf dem Schweizer ERPS vorgestellt.

Drittens werden Ansätze vorgestellt und diskutiert, mit deren Hilfe der Kapazitätsausbau der Konverter beurteilt werden kann. Zunächst wird untersucht, wie sich eine Kapazitätserweiterung auf die Betriebskosten eines ERC auswirkt. Des Weiteren wird beleuchtet, wie das Hinzufügen zusätzlicher Konverter das Kurzschlussverhältnis (short circuit ratio) der Unterwerke beeinflusst. Schliesslich stellen wir einen kosten- und zuverlässigkeitsbasierten Lösungsansatz vor, mit Hilfe dessen zusätzliche Konverter optimal dimensioniert und platziert werden können. Diese Methode hat es uns ermöglicht, einem existierenden ERC einen Satz nach verschiedenen wirtschaftlichen und technischen Kriterien optimierter Lösungen bereitzustellen.

**Stichwörter:** Bahnstromsystems, Stromhandel, Regelreserven, Kapazitätsausbau, Robuste Optimierung, Stochastische Optimierung, Frequenzumrichter und –umformer, Vorhersage der Last.

# Acknowledgements

I would never have been able to finish my dissertation without the guidance of my jury members, help from colleagues and friends, and support from my family and wife.

First of all, I would like to express my deepest gratitude to my thesis director, Prof. Rachid cherkaoui, for his invaluable help and support. Rachid gave me the freedom to explore on my own way, while guiding me into right directions. During the past four years, I found him not only as an excellent adviser but also as a friend that I can always count on him.

My sincere thanks goes to the president of jury, Prof. Farhad Rachidi, who offered his generous help and support whenever I needed. Indeed, he is one of the nicest person that I have ever known and it was a great pleasure for me to be with Farhad in the same laboratory.

I would like to thank the jury member, Prof. Mario Paolone, for his technical support and insightful comments on my work. He has a broad knowledge on different topics related to electrical power systems and I learned a lot from him during our discussions.

I would also like to express my gratitude to the jury members, Prof. Louis Wehenkel and Prof. Tomas Gomez for their valuable comments and discussions during and after the PhD exam.

I must mention that my doctoral study has been part of a larger research project founded by Swiss Federal Railways (SBB/CFF/FFS), Swissgrid, Swiss Electric Research, ABB and Léclanche. Hereby, the financial and technical support provided by aforementioned companies and institutes is gratefully acknowledged. In particular, I would like to thank Dr. Walter Sattinger, Dr. Marec Zima and Dr. Ali Ahmadi Khatir from Swissgrid and Mr. Martin Aeberhard, Dr. Alain Bart and Mr. Rene Vollenwyder from SBB, for their constructive technical comments during our meetings.

I would like to extend my appreciation to my former and new colleagues and friends in ELL building who provided an excellent and delightful atmosphere for me during my doctoral study (listed in order of appearance for me): Andrée Moinat, Jean-Michel Buemi, Dr. Lazar Bizumic, Dr. Omid Alizadeh Mousavi, Dr. Carlos Alberto Romero, Alexander Smorgonskiy, Dr.

Felix Vega, Nicolas Mora, Gaspar Lugrin, Paolo Romano, Stela Sarri, Reza Razzaghi, Mostafa Nick, Maryam Bahramipanah, Konstantina Christakou, Dr. Dimitri Torregrossa, Daniel Lopez, Negin Sohrabkhani, Marco Pignati, Lorenzo Reyes, Lorenzo Zanni, Sophie Flynn, Mohammad Azadifar, Georgios Sarantakos, Dr. Fabrizio Sossan, Emil Namor, Sadegh Azizi and Enrica Scolari. Special thanks also goes to my labmate, Andreas Kettner, for helping me to provide the German version of the abstract of my thesis.

I would like also to thank my friends in Lausanne who always have been sharing good moments and many help on so many levels. In particular, many thanks goes to Ehsan Kazemi, Mohammad Amin Shoaie, Sommayeh Rahimian, Mahdi Aminian, Majid Bastankhah, Arizu Ghiasaleh, Farhang Nabiei, Amir Hesam Salavati, Samira Asgari, Mohammad Razzaghi, Mehdi Gholam-Rezaie, Mahdi Khoramshahi and Farnaz Eslami.

I am greatly indebted to my dear parents, Akbar and Robabeh Bozorg who always encouraged and supported me to pursue my studies with their infinite patience and compassion. Indeed, it was under their watchful eye that I gained so much drive and an ability to tackle challenges head on. Special thanks also goes to my brother, Mohsen Bozorg, and to my sister, Monireh Bozorg, for their spiritual support and empathy.

Finally, from the bottom of my heart, I would like to thank my beloved wife, Samira Kouchali. Her support, encouragement, quiet patience and unconditional love were undeniably the bedrock upon which the past four years of my life have been built.

*22 July 2015*
*Lausanne, Switzerland*

# Contents

# List of Figures

# List of Tables

# Notations

The notation used in this dissertation is listed below. For the sake of clarity, the symbols used to formulate the proposed energy and reserve scheduling in Chapters 4 and 5 are stated below separately for quick reference. Others are defined as required in the text.

## List of Symbols Used in Chapter 4

### Indices and sets

| | |
|---|---|
| $h$ | Index for hydroelectric power plant |
| $i, j$ | Index for railway power network bus |
| $k$ | Index for interconnecting frequency converter |
| $m$ | Index for dam or water reservoir |
| $q$ | Index for time interval in 15 minutes (quarter of an hour) $q = 1, 2, 3, 4$ |
| $t, \tau$ | Index for time interval in hour |
| $\mathscr{C}_i$ | Set of interconnecting frequency converters connected to bus $i$ |
| $\mathscr{G}_i$ | Set of hydroelectric power plants connected to bus $i$ |
| $\mathscr{G}^s, \mathscr{C}^s$ | Set of available hydroelectric power plants and interconnecting converters after realization of scenario $s$ in the balancing stage |
| $\mathscr{H}_m^{\text{in}}, \mathscr{H}_m^{\text{out}}$ | Set of hydroelectric power plants that are upstream/downstream to reservoir $m$, respectively |
| $\mathscr{N}_i$ | Set of adjacent buses connected through transmission line to bus $i$ |
| $\mathscr{S}$ | Set of remained scenarios after scenario reduction |

## Variables

| | |
|---|---|
| $p_{ht}$ | Energy dispatch for hydroelectric power plant $h$ during time interval $t$ [MWh] (day ahead stage) |
| $r^{+}_{ht}, r^{-}_{ht}$ | Upward/downward reserve dispatch for hydroelectric power plant $h$ during time interval $t$ [MW] (day ahead stage) |
| $r^{\mathrm{d}+}_{ht}, r^{\mathrm{d}-}_{ht}$ | Part of upward/downward reserve dispatch for hydroelectric power plant $h$ during time interval $t$ [MW] that is kept for the ERC internal frequency control scheme (day ahead stage) |
| $p^{+}_{htq}, p^{-}_{htq}$ | Upward/downward energy redispatch for hydroelectric power plant $h$ during quarter $q^{\mathrm{th}}$ of time interval $t$ [MWh] (balancing stage) |
| ${p_{htq}}^{s}$ | Energy redispatch for hydroelectric power plant $h$ during quarter $q^{\mathrm{th}}$ of time interval $t$ [MWh] after realization of scenario $s$ (balancing stage) |
| $c^{SU}_{ht}$ | Start up cost for hydroelectric power plant $h$ during time interval $t$ [CHF] (day ahead stage) |
| $p^{\mathrm{c}}_{kt}$ | Energy dispatch for interconnecting converter $k$ during time interval $t$ [CHF] (day ahead stage) |
| $p^{\mathrm{buy}}_{kt}, p^{\mathrm{sell}}_{kt}$ | Energy dispatch for interconnecting converter $k$ on the public grid side during time interval $t$ [MWh] (day ahead stage) |
| $p^{\mathrm{ER}}_{kt}$ | Energy dispatch for interconnecting converter $k$ on the electric railway side during time interval $t$ [MWh] (day ahead stage) |
| ${p^{\mathrm{ER}}_{ktq}}^{s}$ | Energy redispatch for interconnecting converter $k$ on the electric railway side during quarter $q^{\mathrm{th}}$ of time interval $t$ after realization of scenario $s$ [MWh] (balancing stage) |
| ${p^{\mathrm{long}}_{tq}}^{s}$ | Aggregated long energy imbalance (negative) over all interconnecting converters during quarter $q^{\mathrm{th}}$ of time interval $t$ after realization of scenario $s$ [MWh] (balancing stage) |
| ${p^{\mathrm{short}}_{tq}}^{s}$ | Aggregated short energy imbalance (positive) over all interconnecting converters during quarter $q^{\mathrm{th}}$ of time interval $t$ after realization of scenario $s$ [MWh] (balancing stage) |

$p_{tq}^{\mathrm{im}\,s}$ Aggregated energy imbalance (positive or negative) over all interconnecting converters during quarter $q^{\mathrm{th}}$ of time interval $t$ after realization of scenario $s$ [MWh] (balancing stage)

$p_{ktq}^{\mathrm{in}\;\;s}, p_{ktq}^{\mathrm{out}\,s}$ Energy redispatch for interconnecting converter $k$ on the public grid side during quarter $q^{\mathrm{th}}$ of time interval $t$ [MWh] (balancing stage)

$p_{ktq}^{\mathrm{c}^+}, p_{ktq}^{\mathrm{c}^-}$ Upward/downward energy redispatch in interconnecting frequency converter $k$ during quarter $q^{\mathrm{th}}$ of time interval $t$ [MWh] (balancing stage)

$r_{kt}^{\mathrm{c}^+}, r_{kt}^{\mathrm{c}^-}$ Upward/downward capacity reserve in interconnecting frequency converter $k$ during time interval $t$ [MW] (day ahead stage)

$r_{kt}^{\mathrm{dc}^+}, r_{kt}^{\mathrm{dc}^-}$ Part of upward/downward capacity reserve in interconnecting frequency converter $k$ during time interval $t$ [MW] that is is kept for ERC internal frequency control scheme (day ahead stage)

$\delta_{it}^{0}$ Voltage angle for bus $i$ during time interval $t$ [rad] (day ahead stage)

$\delta_{itq}$ Voltage angle for bus $i$ during quarter $q^{\mathrm{th}}$ of time interval $t$ [rad] (balancing stage)

$\delta_{itq}^{s}$ Voltage angle for bus $i$ during quarter $q^{\mathrm{th}}$ of time interval $t$ after realization of scenario $s$ [rad] (balancing stage)

$l_{itq}^{\mathrm{sh}}$ Load shedding at bus $i$ during quarter $q^{\mathrm{th}}$ of time interval $t$ [MWh] (balancing stage)

$l_{itq}^{\mathrm{sh}\;\;s}$ Load shedding at bus $i$ during quarter $q^{\mathrm{th}}$ of time interval $t$ after realization of scenario $s$ [MWh] (balancing stage)

$\Delta l_{itq}$ Energy demand variation at bus $i$ during quarter $q^{\mathrm{th}}$ of time interval $t$ [MWh] in the redispatching (second stage) problem

$w_{ht}^{\mathrm{d}}, w_{ht}^{\mathrm{s}}$ Water flow discharge/spillage for hydro power plant $h$ during time interval $t$ $\left[\frac{\mathrm{m}^3}{\mathrm{s}}\right]$ (day ahead stage)

$u_{ht}$ Binary 0,1 variable denoting the on-off state of hydro power plant $h$ during time interval $t$ (day ahead stage)

$v_{mt}$ Water level for reservoir $m$ during time interval $t$ $\left[\mathrm{m}^3\right]$ (day ahead stage)

$r_{t}^{\mathrm{sell}^+}, r_{t}^{\mathrm{sell}^-}$ Quantity of Upward/downward tertiary reserve ERC can sell in the reserve market during time interval $t$ [MW] (day ahead stage)

| | |
|---|---|
| $\overline{p}^{+}_{ht}, \overline{p}^{-}_{ht}$ | Upper bound of upward/downward energy redispatch for hydroelectric power plant $h$ during time interval $t$ [MWh] (balancing stage) |
| $\overline{p}^{c^+}_{kt}, \overline{p}^{c^-}_{kt}$ | Upper bound of upward/downward energy redispatch in interconnecting frequency converter $k$ during time interval $t$ [MWh] (balancing stage) |

## Parameters

| | |
|---|---|
| $\pi^{p}_{t}$ | Price of energy during time interval $t$ $\left[\frac{\text{CHF}}{\text{MWh}}\right]$ |
| $\pi^{+}_{t}, \pi^{-}_{t}$ | Price of upward and downward tertiary reserve during time interval $t$ $\left[\frac{\text{CHF}}{\text{MW}}\right]$ |
| $\pi^{\text{long}}_{t}, \pi^{\text{short}}_{t}$ | Price of long/short energy imbalances during time interval $t$ $\left[\frac{\text{CHF}}{\text{MWh}}\right]$ |
| $C_h$ | Cost coefficient of power generation for hydro power plant $h$ $\left[\frac{\text{CHF}}{\text{MWh}}\right]$ |
| $C^{+}_{h}, C^{-}_{h}$ | Cost coefficient of upward and downward reserve provision for hydro power unit $h$ $\left[\frac{\text{CHF}}{\text{MW}}\right]$ |
| $C^{\text{sh}}$ | Cost of load shedding $\left[\frac{\text{CHF}}{\text{MWh}}\right]$ |
| $L_{it}$ | Energy demand forecast at railway substation connected to bus $i$ during time interval $t$ [MWh] |
| $\underline{\Delta L}^{\text{Q}}_{itq}, \overline{\Delta L}^{\text{Q}}_{itq}$ | Upper/Lower bounds of energy demand variation at railway substation connected to bus $i$ during quarter $q^{\text{th}}$ of time interval $t$ [MWh] |
| $\underline{\Delta L}^{\text{H}}_{it}, \overline{\Delta L}^{\text{H}}_{it}$ | Upper/Lower bounds of hourly energy demand variation at railway substation connected to bus $i$ during time interval $t$ [MWh] |
| $\underline{\Delta L}^{\text{QT}}_{tq}, \overline{\Delta L}^{\text{QT}}_{tq}$ | Upper/Lower bounds of energy demand variation at whole ERC system during quarter $q^{\text{th}}$ of time interval $t$ [MWh] |
| $B_{ij}$ | Longitudinal suseptance of transmission line between bus $i$ and bus $j$ $\left[\Omega^{-1}\right]$ |
| $T^{\max}_{ij}$ | Maximum power flow limit for transmission line between bus $i$ and bus $j$ [MW] |
| $P^{\max}_{h}, P^{\min}_{h}$ | Maximum and Minimum output power for hydro power plant $h$ [MW] |
| $R^{\text{up}}_{h}, R^{\text{down}}_{h}$ | Upward/downward ramp rate for hydro power plant $h$ $\left[\frac{\text{MW}}{\text{h}}\right]$ |
| $P^{\text{c}^{\max}}_{k}$ | Rated power in both direction for interconnecting converter $h$ [MW] |
| $V^{0}_{m}$ | Initial volume of water in reservoir $m$ $\left[\text{m}^3\right]$ |
| $V^{\max}_{m}, V^{\min}_{m}$ | Maximum and minimum allowable volume of water in reservoir $m$ $\left[\text{m}^3\right]$ |

$W_h^{\max}$ Maximum water flow for hydroelectric power plant $h$ $\left[\frac{\mathrm{m}^3}{\mathrm{s}}\right]$

$\xi_{mt}$ Natural water inflow of reservoir $m$ during time interval $t$ $\left[\frac{\mathrm{m}^3}{\mathrm{s}}\right]$

$\eta_h$ Rate of water flow to power conversion for hydro power plant $h$ $\left[\frac{\mathrm{MWs}}{\mathrm{m}^3}\right]$

$\eta_k$ Energy efficiency for interconnecting converter $k$ $\left[\frac{\mathrm{MWs}}{\mathrm{m}^3}\right]$

$P_h^{\mathrm{fix}}$ Internal power demand for hydroelectric power plant $h$ [MWh]

## List of Symbols Used in Chapter 5

### Indices and sets

$i, j$ Index for railway power network bus

$t, \tau$ Index for time interval in hour

$h$ Index for hydroelectric power plant

$m$ Index for dam or water reservoir

$k$ Index for interconnecting frequency converter

$\mathscr{N}_i$ Set of adjacent buses connected through transmission line to bus $i$

$\mathscr{G}_i$ Set of hydroelectric power plants connected to bus $i$

$\mathscr{C}_i$ Set of interconnecting frequency converters connected to bus $i$

$\mathscr{H}_m^{\mathrm{in}}, \mathscr{H}_m^{\mathrm{out}}$ Set of hydroelectric power plants that are upstream/downstream to reservoir $m$, respectively

$J_0^{\mathrm{p}}, J_0^{+}, J_0^{-}$ Set of time $t$ when the price of energy, upward and downward reserves are not known in advance, receptively.

### Variables

$p_{ht}$ Energy dispatch for hydroelectric power plant $h$ during time interval $t$ [MWh]

$r_{ht}^{+}, r_{ht}^{-}$ Upward/downward reserve dispatch for hydroelectric power plant $h$ during time interval $t$ [MW]

$c_{ht}^{SU}$ Start up cost for hydroelectric power plant $h$ during time interval $t$ [CHF]

| | |
|---|---|
| $p^{c}_{kt}$ | Energy dispatch for interconnecting converter $k$ during time interval $t$ [CHF] |
| $r^{c^+}_{kt}, r^{c^-}_{kt}$ | Upward/downward capacity reserve in interconnecting frequency converter $k$ during time interval $t$ [MW] |
| $\delta_{it}$ | Voltage angle for bus $i$ during time interval $t$ [rad] |
| $w^{d}_{ht}, w^{s}_{ht}$ | Water flow discharge/spillage for hydro power plant $h$ during time interval $t$ $\left[\frac{m^3}{s}\right]$ |
| $u_{ht}$ | Binary 0,1 variable denoting the on-off state of hydro power plant $h$ during time interval $t$ |
| $v_{mt}$ | Water level for reservoir $m$ during time interval $t$ $\left[m^3\right]$ |
| $q^{+}_{t}, q^{-}_{t}$ | Quantity of Upward/downward tertiary reserve offer from the electric railway company to the ancillary service market during time interval $t$ [MW], respectively. |
| $l_{it}$ | Auxiliary variable related to the energy demand of railway substation connected to bus $i$ during time interval $t$, which is used in the construction of the robust counterpart problem. |

## Parameters

| | |
|---|---|
| $\pi^{p}_{t}$ | Price of energy during time interval $t$ $\left[\frac{CHF}{MWh}\right]$ |
| $\pi^{+}_{t}, \pi^{-}_{t}$ | Price of upward and downward tertiary reserve during time interval $t$ $\left[\frac{CHF}{MW}\right]$ |
| $C_h$ | Cost coefficient of power generation for hydro power plant $h$ $\left[\frac{CHF}{MWh}\right]$ |
| $C^{+}_{h}, C^{-}_{h}$ | Cost coefficient of upward and downward reserve provision for hydro power unit $h$ $\left[\frac{CHF}{MW}\right]$ |
| $L_{it}$ | Energy demand of railway substation connected to bus $i$ during time interval $t$ [MWh] |
| $B_{ij}$ | Longitudinal suseptance of transmission line between bus $i$ and bus $j$ $\left[\Omega^{-1}\right]$ |
| $T^{max}_{ij}$ | Maximum power flow limit for transmission line between bus $i$ and bus $j$ [MW] |
| $P^{max}_{h}, P^{min}_{h}$ | Maximum and Minimum output power for hydro power plant $h$ [MW] |
| $R^{up}_{h}, R^{down}_{h}$ | Upward/downward ramp rate for hydro power plant $h$ $\left[\frac{MW}{h}\right]$ |
| $P^{c^{max}}_{k}$ | Rated power in both direction for interconnecting converter $h$ [MW] |

| | |
|---|---|
| $R_t^+, R_t^-$ | Internal upward/downward reserve demand of the ERC during time interval $t$ [MW] |
| $V_m^0$ | Initial volume of water in reservoir $m$ $\left[\mathrm{m}^3\right]$ |
| $V_m^{\max}, V_m^{\min}$ | Maximum and minimum allowable volume of water in reservoir $m$ $\left[\mathrm{m}^3\right]$ |
| $W_h^{\max}$ | Maximum water flow for hydroelectric power plant $h$ $\left[\frac{\mathrm{m}^3}{\mathrm{s}}\right]$ |
| $\xi_{mt}$ | Natural water inflow of reservoir $m$ during time interval $t$ $\left[\frac{\mathrm{m}^3}{\mathrm{s}}\right]$ |
| $\eta_h$ | Rate of water flow to power conversion for hydro power plant $h$ $\left[\frac{\mathrm{MWs}}{\mathrm{m}^3}\right]$ |
| $P_h^{\mathrm{fix}}$ | Internal power demand for hydroelectric power plant $h$ [MWh] |
| $Q_t^{+^{\min}}$ | Minimum allowable quantity for upward reserve offer from the railway power company to the reserve market during interval $t$ [MW] |
| $Q_t^{-^{\min}}$ | Minimum allowable quantity for downward reserve offer from the railway power company to the reserve market during interval $t$ [MW] |

# 1 Introduction

## 1.1 Thesis Motivation and Aims

For historical reasons, the frequency of Electric Railway Power System (ERPS) in many European countries is different from the frequency of the public power grid. The single-phase, low frequency (i.e. 16.7 Hz) electric railway system has been in operation for over a century in central European (Germany, Austria and Switzerland) and Scandinavian (Sweden and Norway) countries. To feed such a system, Electric Railway Companies (ERCs) have their own generators operating at 16.7 Hz. These generators are connected to the ERPS substations through a transmission and a distribution system in order to feed the end point power demands (i.e. trains). At the transmission system level, ERPSs are also connected to the public power grids through interconnecting frequency converters. For illustrative purpose, figure 1.1 shows the structure of ERPS in Switzerland where generators are installed in cascaded hydro power plants.

The ERPS demand in terms of power and energy is distinct from the conventional loads in the public grid according to two attributes. First, fast and large fluctuations at the load of each substation as well as the total system load and second, the predictable temporal and spatial correlations between the loads of substations that is derived from the time table and the schedule of trains.

Referring to the strong load fluctuations, ERCs have to provide enough reserve services in order to ensure the reliable operation of the system. The required reserve services can be provided from either the ERC's generators or the interconnecting frequency converters.

Most of the interconnecting converters (specially in central European countries) can be used to exchange energy in both directions from 50 Hz to 16.7 Hz system, and vice versa. The bidirectional capability of converters allows ERCs to effectively participate in energy and

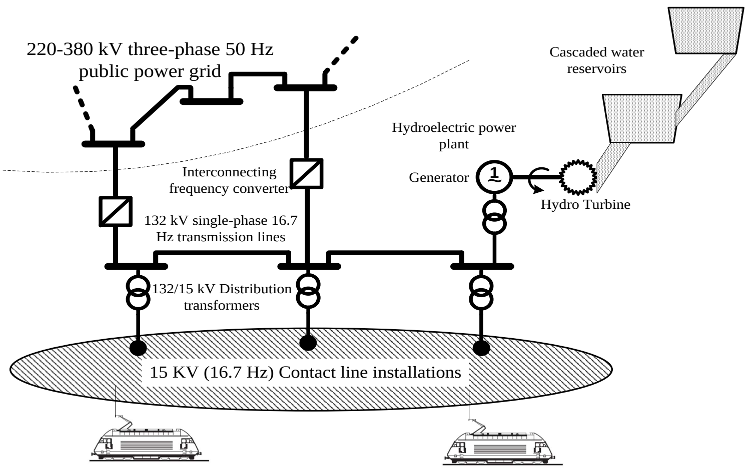


Figure 1.1 – Centralized electric railway power system configuration in Switzerland

reserve markets. In addition, the interconnecting converters permit the electric railway and public power grids to exchange reserve services. Indeed, due to the load diversity, each system can be operated with less reserve services than it could normally be required for isolated operation.

Within the above context, the first aim of this thesis is to develop appropriate methods and strategies aiming to allocate and dispatch the energy and reserve services in the interconnected system including electric railway and public power grids.

From one hand, the railway companies (in particular ERCs) aim to improve the commercial railway transportation services in order to increase the number of passengers and the amount of freight services. As a result, the power demand of ERPSs increases year by year.

On the other hand, the total capacity of ERC's generators is not expected to rise in the future. These generators are mainly installed in the hydro power plants and its expansion is limited due to geographical and environmental factors. Despite, the generation expansion in public grid side is more feasible and economic. In fact, the interconnection enables ERCs to access the vast and diverse generation resources that are connected to the public grid. Therefore, the capacity expansion of the interconnecting converters, plays a decisive role for ERCs to satisfy their increasing long term power demand.

Hence, the second aim of this thesis is to propose and to assess models aiming to find the optimal interconnecting converter capacity expansion in order to maximize the benefits that can be delivered from the interconnection.

## 1.2 Problem Description

Following power industry deregulation and restructuring in recent decades, electrical energy markets have been emerged in which the power producers and consumers compete to maximize their profit. Moreover, the generation and transmission activities of the traditional vertically integrated utilities are unbundled. Hence, to ensure the reliable and secure operation of the system, independent transmission system operators (TSOs) have been emerged. In fact, TSOs are responsible for secure transmission of electrical power from the power producers to the consumers over public grids. For this purpose, TSOs have to procure some ancillary services such as reserve services (frequency control reserves) and voltage control, according to the operating condition.

In power systems, the power has to be generated at the same time as it is consumed. TSOs must be aware to remove any deviation from this power equilibrium. In this respect, some generators must have sufficient reserve capacity to change their generation level when it is required. "Reserve services" or shortly "reserve", which refer to this reserve capacity of generators, is an essential component for secure and reliable operation of the system.

Reserve markets have been developed in many countries along with the electrical energy markets. The reserve market permits the TSO to obtain the required resources to maintain the security of the system at minimum cost. Beside, the reserve service providers seek to maximize their profit by participating in reserve markets [1].

From technical point of view, the operation of ERPSs is similar to the operation of public grids. However, the economic structure of ERPSs are totally different. As mentioned earlier, public grids are operated under open market rules. In contrast, ERPSs are operated by a single company, we name it ERC (electric railway company), in a monopoly way. ERC is responsible for generating, transmitting and distributing electrical power from generators and interconnecting converters to the electric trains.

Before describing the main problems of this thesis, we should clarify two points: 1) the role of ERC in energy market and 2) the relationship between ERC and TSO.

The ERC is a price-taker in the energy market where the prices do not change by any action of any participant like ERC. The energy market operator (e.g. EPEX[1] in central European countries) accepts demand or generation offers (i.e. a price and quantity pair) from the market participants including ERC, and determines the market-clearing price (MCP) at which energy is bought and sold. Participation in the energy market permits ERC to allocate its generation

[1] The European Power Exchange which is an exchange for power trading in Germany, France, Austria and Switzerland.

sources in the most economic way. Note that any energy transaction (sell or buy) has to be delivered or received through the interconnecting converters.

In this thesis, we follow the central European electricity market structure in which the reserve market is operated by TSO, independently from the operation of electrical energy market. The TSO is the only buyer in the market, hence, ERC can sell some reserve services from its generators to the TSO. Nevertheless, ERC has to provide enough reserve services to ensure secure and reliable operation of its own system.

Considering the above context and the thesis motivation presented in section 1.1, this dissertation addresses the three main problems below:

1. Joint energy and reserve scheduling for an electric railway power system under uncertainties (Operation)
2. Offering strategy methods for an electric railway company in energy and reserve markets (Market Strategy)
3. Capacity expansion of the interconnecting converters in interconnected system including electric railway and public power grids (Capacity Expansion)

Next, in this section, these problems have been described more in detail.

### 1.2.1 Joint energy and reserve scheduling for an electric railway power system under uncertainties

One of the main tasks of ERC, as the operator of electric railway power system, is to maintain the frequency of the system in an allowable range. For this purpose, ERC has a two level hierarchical frequency control scheme to follow the railway power demand fluctuations. Here, the primary frequency control is directly implemented in hydroelectric power plants using traditional frequency droop control. The public power grid through interconnecting converters could also support the railway power system, in case of strong fluctuations in the railway power demand [2]. As a result, the exchanged energy through the interconnecting converters deviates from its scheduled value during a given time step (e.g. 15 min). To remove this energy imbalance, the role of secondary frequency control, is to adjust the power set points of the ERC's generators and the interconnecting converters. Note that ERC is charged by the TSO for the energy imbalances through interconnecting converters during each 15 minutes time step.

To ensure the proper functioning of the above mentioned frequency control scheme, ERC has to provide both upward and downward reserve from its own generators and part of the capacity of the interconnecting converters.

Within the above context, the aim of this study is to find the joint energy and reserve schedule of the ERC's generators and the interconnecting converters for a given set of energy and reserve market prices. This scheduling problem is formulated as a two stages optimization problem.

The first (dispatching) stage deals with day-ahead decision variables considering the forecast of energy demand of railway substations. For each generator and interconnecting converter, day-ahead decision variables includes the hourly output power set point, part of provided reserve to be used for ERC's frequency control scheme and part of provided reserve to be sold in the reserve market.

Since, in real-time, the energy demand (load) of electric railway substations is not equal to its forecast value, the second (balancing) stage is required to ensure the security of supply. In the second stage, the provided reserves (from first stage) are activated in order to maintain the power balance in the system.

The load forecast error is an uncertain parameter in the problem. In this study, a short term load forecast method based on ARIMA (auto-regressive integrated moving average) time series is applied to find the load forecast of ERPS substations. Moreover, this load forecast technique is applied to capture the temporal and spatial correlations between the loads of ERPS substations.

To handle uncertainties in the joint energy and reserve scheduling problem, two mathematical approaches, namely, two-stage stochastic optimization and adaptive robust optimization, are investigated in this study.

#### Adaptive Robust Optimization Approach

In recent years, this uncertainty management approach has been received lots of attention in power system area [3, 4]. In robust optimization the uncertainty model is not stochastic, but rather deterministic and set-based. The decision-maker constructs a solution that is not only feasible for all realizations of the uncertain parameters within the uncertainty set (e.g. confidence intervals) but also optimal for the worst realization of such uncertain parameters. Here, the uncertainty set includes the variation of energy demand at ERC substations from its forecast values. Both of the temporal and spatial correlation of variation of energy demand at ERC substations are effectively considered in this approach.

In fact, in the second stage, the energy demand variations are optimization variables rather than determined parameters (represented by scenarios). To obtain the robust solution, in the second stage, we are looking for the minimum balancing cost while the energy demand variation at each substation is varying in a way to maximally affect the objective function.

This approach requires only moderate information about the underlying uncertainty, such as the mean and the range of the uncertain parameter. Moreover, the adaptive robust model constructs an optimal solution that is immune against all realization of the uncertain data within the deterministic uncertainty set. This robustness is desirable for electric railway power systems where the penalty associated with the infeasible solution is very high. Hence the concept of robust optimization is consistent with the risk-averse fashion in which the electric railway power systems are operated.

However, the main drawback of this approach is that the second stage problem has to be modeled in a linear way (including only continuous variables). Otherwise, the dual of the second stage problem can not be obtained and consequently we can not solve the adaptive robust problem.

The adaptive robust optimization approach is discussed in details in chapter 4.

#### Two-Stage Stochastic Optimization Approach

In terms of modeling limitations, stochastic optimization approach is more flexible in the sense that both of the first and second stage formulation can contain binary variables. As a results, some detailed technical considerations such as interconnecting converter losses and the aggregation of energy imbalances over all converters can be simply included in the problem formulation.

Stochastic programming is a mathematical framework for dealing with problems under uncertainties. Here, in the second (balancing) stage, Monte Carlo simulation is used to generate scenarios including the energy demand of railway substations and the availability of generators and interconnecting converters.

Energy demand scenarios are generated using normal distribution for the energy demand forecast error at each substation. Scenarios for the availability of generator and converter units are generated using sequential Monte Carlo simulation based on exponential distributions. Here a two-state continuous-time Markov chain model is applied to represent available and unavailable states of each unit [5].

Since computation requirements for solving scenario-based optimization models depends on the number of scenarios, a scenario reduction technique based on k-medoids clustering algorithm [6] is adapted for a trade off between solution accuracy and computation burden.

The main advantage of this approach is that there is no limitation on the second stage modeling. However, the stochastic optimization approach suffers from some difficulties such as:

- For capturing uncertainties, in stochastic optimization, we need to estimate the probability distribution function of the uncertain parameter.
- To have an accurate solution, we need to generate many scenarios which leads to huge computation time.
- The final aggregated solution of stochastic optimization approach, might not be optimal or even feasible for some severe realization of uncertain parameters.

The stochastic optimization approach is discussed in details in chapter 4. Moreover, a complete comparison between stochastic optimization approach and adaptive robust optimization approach concerning the joint energy and reserve scheduling problem for an electric railway power system is presented in that chapter.

**Offering strategy methods for an electric railway company in energy and reserve markets**

As we already discussed, ERCs are interested to participate in energy and reserve markets as they see an opportunity to optimally allocate their generation resources in a most economic way.

It should be noted that the main objective of an ERC is to ensure the security of supply of its own demand. Afterward, ERC is interested to maximize its profit from participating in energy and reserve markets. Therefore ERC is looking for a robust offering strategy to participate in the markets, in the sense that uncertainties in energy demand of its own substations would not threaten its security of supply.

In this study we follow an electricity market structure where the reserve market is cleared before the energy market clearing. Hence, the day ahead energy market prices are not known when ERC has to submit the upward and downward reserve offering curves to the reserve market. For illustrative purpose, figure 1.2 shows the role of ERC in energy and reserve market. Note that the variations of day ahead energy prices from the forecast values can move the solution of the energy and reserve scheduling problem from an optimal point (minimum total cost) to any suboptimal point. Therefore, besides the security of supply, the reserve offering strategy of ERC should be robust against the uncertainty in the upcoming day ahead energy

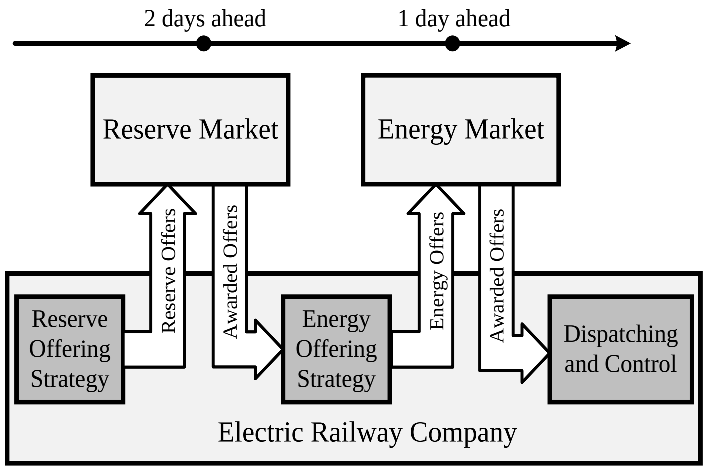


Figure 1.2 – ERC in energy and reserve market structure

market prices.

Within the above context, the aim of this study is: 1) to propose an appropriate offering strategy method for an ERC to participate in reserve markets and 2) to find optimal energy offering curve taking into account the outputs (accepted reserve offers) of the reserve market. Both the proposed energy and reserve offering strategies are using the solutions of a robust energy and reserve scheduling of ERC generators and converters.

To find the offering strategy for ERC in reserve markets; first, we solve the joint energy and reserve self-scheduling problem of ERC. Solving this scheduling problem, we obtain the optimum quantity of reserve that ERC can offer to the reserve market for the given energy and reserve prices. Then we could construct the hourly reserve offering curves based on the solutions of the self-scheduling problems for different levels of reserve price.

The multi period self-scheduling problem for an ERC considering generators, interconnecting converters and network constraints is a mixed integer linear programming (MILP) problem. In this optimization problem, both of the cost coefficients (energy and reserve prices) and the data involved in the constraints (energy demands of substations) are subject to uncertainty. Referring to these uncertainties, the previous study (presented in section 1.2.1 and chapter 4), is mainly dedicated to consider uncertainties in the constraints and hence, a sophisticated two-stages problem formulation is proposed. In contrast, the study presented in this section, is mainly dedicated to consider uncertainties in the cost coefficients. Therefore, a more simple single-stage formulation is proposed in this study.

Next, a discrete (mixed integer) robust optimization technique, relying on [7], is applied to solve the above mentioned single-stage self-scheduling problem taking into account uncertainties in the energy and reserve prices as well as uncertainties in the energy demand of railway substations. This proposed robust energy and reserve scheduling model allows controlling the degree of conservatism of the solution and moreover it is computationally tractable.

Afterward we propose an effective algorithm for constructing the upward reserve offering curve by iteratively solving the above mentioned robust energy and reserve scheduling problem for different levels of upward reserve price. For each level of upward reserve price, the robust scheduling problem is solved, taking into account the energy price and downward reserve price uncertainties as well as energy demand uncertainties.

Finally we present an energy offering curve construction algorithm taking into account some fixed amount of reserve that ERC has to sell into the reserve market. This algorithm is relying on the solution of energy and reserve self scheduling problem while the set of energy prices is the only uncertain parameter in the objective function

The proposed energy and reserve offering strategy methods are presented in details in 5.

### 1.2.2 Capacity expansion of the interconnecting converters in interconnected system including electric railway and public power grids

The power demand of ERPS is expected to increase in the next years. Increasing the capacity of the interconnecting converters is a reasonable solution to deal with this problem. The aim of this chapter is: 1) to investigate the technical effect and economic effect of increasing the capacity of interconnecting converters and 2) to propose a preliminary model to find the optimal location and size of new converters as well as the size of capacity expansion of the existing converters.

To investigate the economic effect of increasing the capacity of the interconnecting converters, the daily energy and reserve scheduling problem under given set of prices have been solved, taking into account different values for the capacity of the interconnecting converters.

The value of short circuit Ratio (SCR) at a substation, implicitly depicts the strength and the capabilities of the grid on the substation. Hence, SCR is considered as a technical criteria to investigate the technical effect of expanding the interconnecting converters.

Finally an optimization formulation based on a cost-reliability approach is proposed to address the capacity expansion problem. Solving the optimization problem, the possible solutions which satisfy a list of technical constraints, are evaluated under two main criteria:

- Minimizing the investment cost of the interconnections
- Achieving an acceptable reliability level

This study is presented in details in chapter 6.

## 1.3 Thesis Contributions

Most of researches in low frequency electric railway power systems has focused more on technical problems (i.e. stability [8], converter control [9]-[10], system simulation and modeling [11], etc.) than economic and market issues. Among few studies, in mid 1990s, Ollofsson et al. in [12] and [13] solve the load flow and optimal power flow problems for the Swedish electric railway system considering controlled and uncontrolled interconnecting converters.

In general, this thesis aims to partially fill the gap between technical studies in electric railway power systems and the technical and economic studies in power system area. For instance, to the best knowledge of the author of this thesis, the problem of energy and reserve scheduling for an ERC for participating in energy and reserve markets has not been reported in the literature.

Referring to the problem description presented in section 1.2, the original contributions of this thesis are summarized below.

1. Regarding the joint energy and reserve scheduling problem (chapter 4), the contributions are:

    (a) to model the multi-period self-scheduling problem of an ERC in two stages (day ahead dispatching and real time balancing) considering cascaded hydro plants, interconnecting converters and internal transmission network constraints in a linear way;

    (b) to apply a short term load forecast technique based on time-series to obtain the uncertainty characteristics of energy demand forecast error of the ERC substations;

    (c) to propose an adaptive robust optimization technique to solve the above two stages (1.(a)) scheduling problem considering the spatial and temporal correlations between energy demand forecast error uncertainty of the ERC substations;

    (d) to propose an enhanced two stages self scheduling problem formulation that considers detailed technical considerations in addition to (1.(a)) using binary variables;

(e) to propose a two stages stochastic optimization technique to solve above (1.(d)) two stage scheduling problem considering energy demand forecast error uncertainty and the availability of the generators and interconnecting converters.

2. Regarding offering strategy methods for participating in energy and reserve market (chapter 5), the contributions are:

   (a) to propose a discrete robust optimization technique to solve a single stage scheduling problem considering price and demand uncertainties (uncertain parameters in objective function and constraints);

   (b) to propose offering curve construction algorithm for participating in reserve market based on the robust energy and reserve self-scheduling considering the correlation between upward and downward reserve prices;

   (c) to present energy offering curve construction algorithms for participating in energy markets considering the awarded reserve offers from the output of the reserve market.

3. Regarding the capacity expansion problem (chapter 6), the contributions are:

   (a) to analyze the effect of increasing the capacity of the interconnecting converters on the energy and reserve provision cost;

   (b) to investigate the effect of increasing the capacity of interconnecting converters on the short circuit ratio of ERPS substations;

   (c) to propose a cost-reliability approach to find the size and location of new interconnecting converters;

   (d) to incorporate reliability index calculation within the optimization formulation in the above cost-reliability approach.

## 1.4 Thesis Outline

This thesis dissertation is organized as follows.

**Chapter 2** The aim of this chapter is to review the most important characteristics of electric railway power systems (ERPSs). First, the technical differences of the existing ERPS are introduced. Since this thesis is more dedicated to low frequency (i.e., 16.7 Hz) ERPS, they have been studied more in details. In this respect, the basic elements of these systems including the generation system, interconnecting converters and transmission and distribution systems have been investigated. Finally, special characteristics of power and energy demands of ERPS in comparison with the demands of conventional power systems are presented.

**Chapter 3** The aim of this chapter is to introduce reserve services which are essential for secure operation of power systems and to investigate the role of reserve services in interconnected systems including electric railway and public power grids. In this respect, different types of reserve services are described and reserve services provision methods have been reviewed. Next, the structure of reserve markets with focus on Swiss reserve market is presented. Finally reserve services from electric railway power system point of view has been investigated.

**Chapter 4** The aim of this chapter is to investigate methods for finding the day-ahead schedule of ERC's generators and interconnecting converters for a given set of energy and reserve market prices. First, the joint energy and reserve scheduling is formulated as a two stage optimization problem. In this optimization problem, the forecast of energy demand at railway substations is subject to uncertainty. Hence, the load forecast uncertainty is analyzed to provide a realistic uncertainty representation for the scheduling problem. Afterward, an adaptive robust optimization method is proposed for dealing with energy demand uncertainty in the scheduling problem. Next, a two stage stochastic optimization method is proposed for dealing with the problem uncertainties. Here, in addition to the energy demand forecast error, the availability of the ERC generators and the interconnecting converters are subject to uncertainty. Finally to demonstrate the effectiveness of the proposed robust and stochastic methods, a realistic case study based on the characteristic of ERPS in the western part of Switzerland is presented. Moreover, a discussion on the advantages and drawbacks of each method considering the characteristics of the ERPS is provided.

**Chapter 5** This chapter proposes appropriate offering strategy methods for an ERC to participate in energy and reserve markets. In this respect, first the problem of energy and reserve scheduling for ERC is modeled in based on a single-stage formulation. Next, a discrete robust optimization technique is used to solve the problem taking into account the uncertain energy and reserve prices as well as the uncertain hourly energy demand of ERC's substations. Afterward, a reserve offering curve construction algorithm based on the solution of robust energy and reserve scheduling is proposed. This algorithm takes into account the correlation between upward and downward reserve prices. Moreover, an appropriate energy offering curve construction algorithm is presented. Finally, to show the effectiveness of the proposed methods, a realistic case study based on the characteristic of an ERC in Switzerland is presented.

**Chapter 6** The aim of this chapter is to propose and to investigate methodologies to assess the capacity expansion of the interconnecting converters. In this respect, the effect of increasing the capacity of the interconnecting converters on the daily operation cost of ERC has been studied. Afterward, the effect of adding new interconnecting converters on the short circuit ratio of ERPS substations has been investigated. Finally, a cost-reliability approach has been proposed to find the optimal size and location of new interconnecting converters.

**Chapter 7** This chapter concludes the studies presented in this dissertations. Moreover, it suggests some interesting topics for future research.

# 2 Electric Railway Power Systems

## Chapter Overview

*The aim of this chapter is to review the most important characteristics of electric railway power systems (ERPSs). First, the technical differences of the existing ERPS are introduced. Since this thesis is more dedicated to low frequency (i.e., 16.7 Hz) ERPS, they have been studied more in details. In this respect, the basic elements of these systems including the generation system, interconnecting converters and transmission and distribution systems have been investigated. Finally, special characteristics of power and energy demands of ERPS in comparison with the demands of conventional power systems are presented.*

## 2.1 General Overview

### 2.1.1 Definitions

In this thesis, the term "electric railway power system (ERPS)" or "electric traction power system" as suggested in [8] is used to describe the total system of components used for the generation/conversion, transmission and consumption of energy for electric railway transport. Moreover, the term "electric railway company (ERC)" is used to describe the company which is responsible for the operation of the electric railway power system. Note that ERC might own partially or totally the ERPS components including the generators and converters as well as the transmission and distribution system components.

### 2.1.2 History and Classification

The history of railway electrification and its extensiveness is well documented in the technical literature [14, 15]. In short, *Siemens* displayed the first electrically powered locomotive in 1879 at the Berlin Commerce Fair. The locomotive was driven by a 2.2 KW direct current (DC) motor, which was fed from a current -carrying rail placed between two main rails. The first fully electrified railway was opened in 1895 by the *Baltimore & Ohio RR* in United States of America [14].

In the past, DC power supplies were widely used, due to the ease of control and hyperbolic traction/speed curve of the series commutator motors. The main drawbacks of DC supplies are; the low voltage level which leads to high currents to transmit the required traction power, the feeding distance limitation and finally the expensive power supply equipment. However, over half of all electric traction systems in the world still use direct current.

At the beginning of the twentieth century, efforts were made to combine the traction advantages of the series motor with the transforming capability of alternating current. In Germany, development efforts led to single-phase AC supply with a frequency of 50/3 = 16 2/3 Hz, where the electrical energy is generated and distributed as single phase in a separate railway high-voltage network. AC supply was also adopted by Austria, Switzerland, Norway and Sweden and has proven to be particularly powerful and effective for the electrical power supply of high-speed and high-capacity traffic. Note that, in 2000, Austrian, German and Swiss railways changed their nominal frequency from 16 2/3 Hz to 16.7 Hz [15].

Initial experience with an AC 50 Hz traction power supply was gained at the Hollental-balm in Germany starting in 1940. Due to the enormous progress made in the field of power electronics, the technical problems for using AC 25 kV 50 Hz for traction application has been resolved.

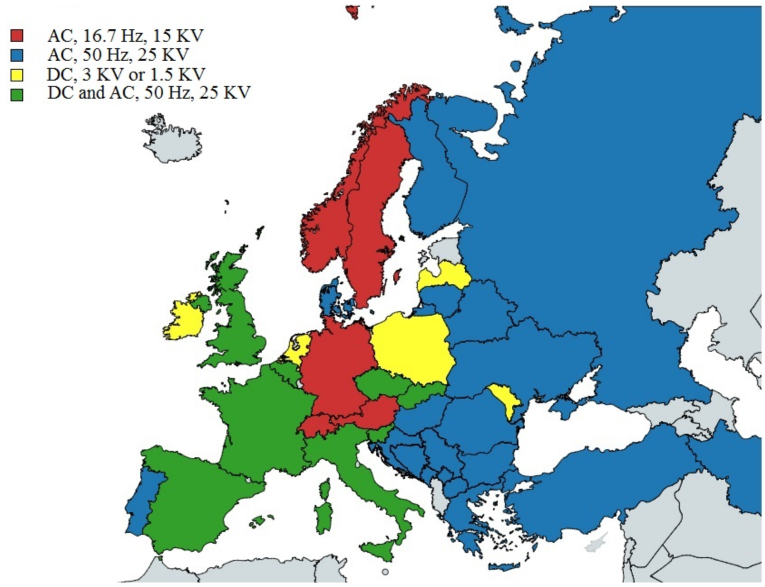


Figure 2.1 – Electric railway power system classification in European countries

Nowadays most of high speed railway lines are supplied by the AC 25 KV, 50 Hz system.

In summary, the most common electric railway power systems are:

- Direct current 0.6 kV, 0.75 kV, 1.5 kV and 3 kV.
- Alternating current 16.7Hz 15 kV.
- Alternating current 50 Hz 25 kV.

Figure 2.1, which is depicted based on data from [15], shows the different types of electric traction power systems for mainline railways in Europe. In the countries highlighted in green, the conventional railway lines are supplied by DC system (e.g. DC 0.75 KV in the United Kingdom, DC 1.55 KV in the Netherlands and France and DC 3 KV in Italy, Spain and Belgium) while the AC 50 Hz 25 KV system is used to supply the high speed railway lines.

It should be noted that this thesis is mainly dedicated to the low frequency (i.e., 16.7 Hz) electric railway power systems which are widely operated in the central Europe and Scandinavian countries. As mentioned earlier, the low frequency electrified railway system has been in operation for over a century in Switzerland, Sweden, Germany, Norway and Austria. With the modern day power electronics technology available for frequency conversion, and the high power quality demanded by the utility power customers, the low frequency system is likely to make the railway electrification system more affordable and desirable [16].

## 2.2 Low Frequency Electric Railway Power System Configuration

Two kinds of 16.7 Hz single-phase power supply have been evolved in Europe, namely, the centralized and the decentralized configurations. The central traction power supply has existed in Germany, Austria, Switzerland since 1913 and late in Norway and can be characterized according to [15]

- Power generation using 16.7 Hz single-phase generators installed in hydroelectric, thermal and nuclear power plants and driven by water or steam turbines. It can be also supplied by public power grid through rotating or static converters.

- Transmission of electrical energy with 110 or 132 kV overhead line network with a nominal frequency of 16.7 Hz from the power plants to the substations. This single-phase network mostly incorporates two circuits and has a feed and return conductor for each system.

- Distribution of single-phase electricity in railway substations, where the voltage is converted from 110 kV or 132 kV to the nominal voltage of the contact line installation of 15 kV.

- Contact line installations, which finally feeds the trains.

As an example of a centralized power supply system, figure 2.2 shows the configuration of Swiss railway power system in which the cascaded hydro power units and interconnecting frequency converters provide the required power demand of the system.

The decentralized traction power supply has been operated since mid 1920 in Sweden and Norway and afterward since 1968 in the former East Germany. In general its structure is similar to that of centralized power supply system. The main difference is the existence of decentralized converter which directly connects the electric railway distribution substations to the public 50 Hz grid. Here, the majority of the energy consumed by trains is supplied directly from the 50 Hz grid by means of the decentralized converters.

From technical point of view, both centralized and decentralized power supply systems safely and reliably deliver the power to the railway systems. However, from economic point of view, the centralized power system can provide more flexibility for the operating company to tackle the high, short-term load peaks at the railway substations.

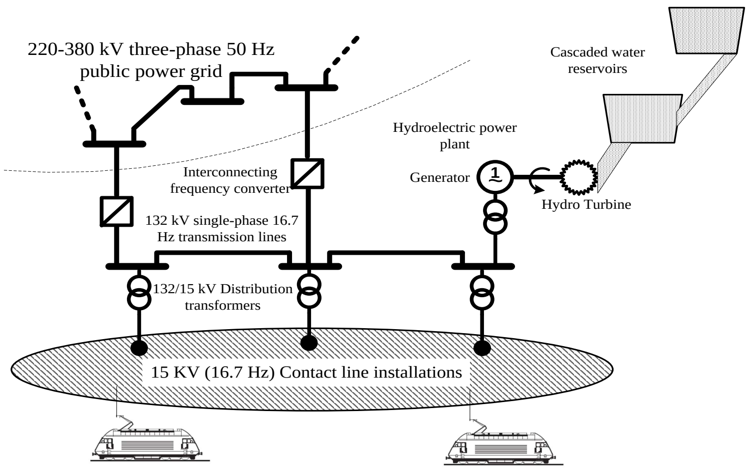


Figure 2.2 – Centralized electric railway power system configuration in Switzerland

## 2.3 Hydro Power Generation System

Due to the historical-technical reasons as well as the availability of water reservoirs, the generation system of most of ERPSs is dominated by hydro power units. In this respect, this section first reviews the most important characteristics of a hydro dominant power system then it provides a general formulation to model cascaded hydro power units in the energy and reserve scheduling problems.

Some important characteristics of hydro dominant systems must be taken into account by the ERC for energy and reserve scheduling. First, the main component of the generation cost is the opportunity cost of having less water available for future periods [17]. Second, hydro producers must take into account the fact that their generation capacities depend on the amount of stored water in the reservoirs and the water inflows [18].

### 2.3.1 Hydrological Model of Cascaded Hydro Units

In general, a cascaded hydro units is a sequence of dams which are connected through a river or a water channel. Thus, the water released at the upstream dam goes into the reservoir of the downstream dam. The head reservoir is typically quite large and used as a buffer, while the other reservoirs are smaller and are used for electricity production. There is a time lag between the water release and its arrival at the downstream reservoir. Thus it takes a few hours for all water to arrive at the lowest dam after its release from the highest reservoir. This phenomenon called “river routing effects” can be modeled using lag coefficients. These coefficients represent the fraction of the water released upstream that arrives at the downstream dam every hour after the release. Natural inflows are also important, like those coming from snow melting, rain, runoff water and natural river flow (for the head reservoir). These inflows are stochastic, but are handled here in a deterministic way, by using hourly averages provided by a natural inflow forecast model. This deterministic approximation is acceptable here referring to the short-term horizon considered (24 h). That is, reservoir levels are not likely to be significantly modified by unexpected natural inflows. The water level at each dam must lie between a minimum and a maximum value, which are the same throughout the year [19].

### 2.3.2 Assumptions on the Operation of Units

Each dam, apart from the first one, has a certain number of units with a given capacity (in MW). The amount of electricity produced by each unit is a function of the water head, unit flow and unit type. Each dam possesses a mechanism to spill a large quantity of water, if necessary. However, spilling should be avoided as much as possible, given that no electricity is produced in this case. There is a start-up cost associated with each unit, as they suffer some wear due to the huge water pressure applied on them.

Besides producing electricity, a unit can also be in "reserve" which means that some of its power capacity is put aside to provide electricity in case of a shortcoming somewhere over the network. A revenue is earned through this practice depending on the type of reserve under consideration, which can be either secondary or tertiary reserves. These types of reserve are related to the time required to bring the energy into use and the physical behavior of the facilities that provide it. A complete discussion on different types of reserve is provided in chapter 3.

### 2.3.3 Simple Cascaded Hydro Model

The cascaded hydro power generators in the hydro system imposes several constraints into the scheduling problem. To model these constraints, a state space model for cascaded hydro power units including several reservoirs and one connecting river is proposed based on the pioneering work of [20]. As simply depicted in figure 2.3, $v_{mt}$ and $w_{mt}$ are the water level of reservoir $m$ and the downstream water flow into the reservoir $m$ at time $t$. If we neglect the delay time of downstream water discharge between two reservoirs regarding to the optimization time step, the water level of reservoir can be calculated as (2.1).

$$v_{mt} = V_m^0 + \sum_{\tau=1}^{\tau=t} (w_{m-1,t} - w_{mt}) \tag{2.1}$$

where $V_m^0$ is the initial amount of water in reservoir $m$.

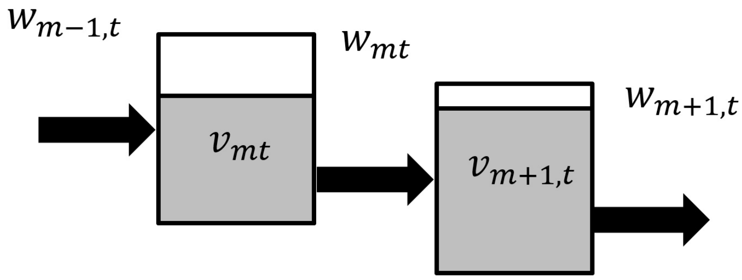


Figure 2.3 – Simple cascaded hydro power units

To consider the delay time of downstream water discharge, equation (2.1) can be modified as (2.2).

$$v_{mt} = V_m^0 + \sum_{\tau=1}^{\tau=t} (w_{m-1,t-td_{m-1}} - w_{mt}) \tag{2.2}$$

Here, $td_{m-1}$ is the delay time of water flow between upstream reservoir $(m-1)$ and downstream reservoir $m$. In general, if we consider that several cascaded hydro units are connected through different rivers and water channels, $v_{mt}^{\text{in}}$ (the net amount of input water into reservoir $m$ at time $t$) can be calculated as (2.3).

$$v_{mt}^{\text{in}} = \sum_{n \in \mathscr{R}} \left(A_{mn} w_{n,t-td_{mn}}\right) - w_{mt} + \zeta_{mt} \tag{2.3}$$

where $A$ is the reservoir connection matrix while $A_{mn}$ ($A_{mn} \in \{-1, 0, 1\}$) represents the possible connection and its direction between reservoirs $m$ and $n$ and $\mathscr{R}$ is the set of all reservoirs. Moreover, $\zeta_{mt}$ is the natural inflow water into reservoir $m$ at time $t$. Therefore, equation (2.2) can be extended as 2.4.

$$v_{mt} = V_m^0 + \sum_{\tau=1}^{\tau=t} \left( \sum_{n \in \mathscr{R}} \left(A_{mn} w_{n,\tau-td_{mn}}\right) - w_{m\tau} + \zeta_{m\tau} \right) \tag{2.4}$$

### 2.3.4 General Cascaded Hydro Model

In this section, we extend the simple cascaded hydro power units formulation to model the water circulation in a more complicated hydro power system. In general, the hydro system includes rivers, water channels, reservoirs as well as hydro power turbines and pumps. For illustrative purpose, figure 2.4 shows the schematic of a hydro system in the western part of Switzerland that is owned by Swiss Federal Railway company (SBB/CFF/FFS). Here, the

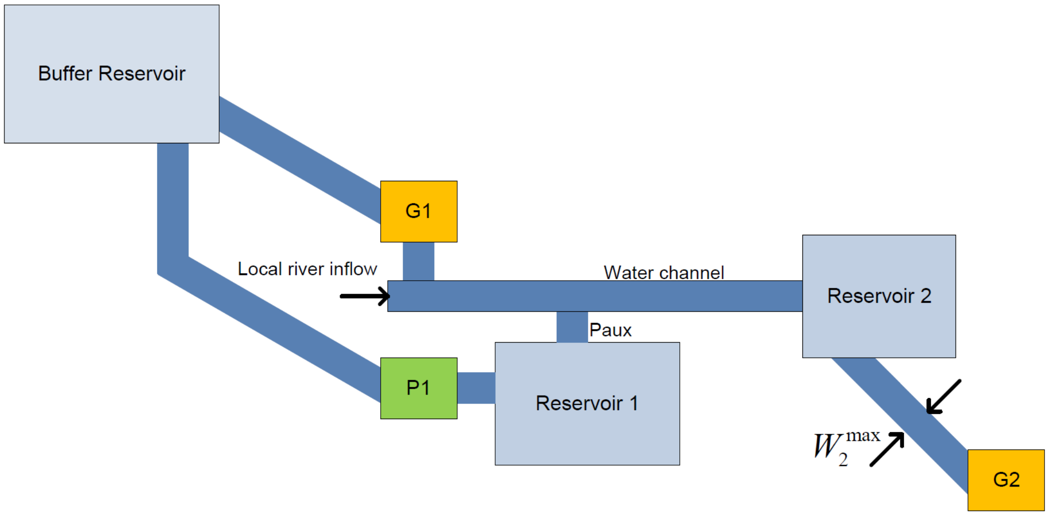


Figure 2.4 – Schematic of SBB cascaded hydro power units in western part of Switzerland

system is composed of two main hydro power units (G1 and G2) and a pump (P1) that directly connects the buffer reservoir (i.e. the Emosson lake) to the first down stream reservoir. The natural water inflow of the local river is also feeding the water channel that connects the first and the second reservoirs. There is a small auxiliary pump that is used to pump water from the first reservoir to the connecting water channel. There are two types of hydro units, namely, hydro-power turbine and pump. To model the water circulation in the hydro system, a water flow variable $(w)$ can be assigned to each hydro unit. For the hydro-power turbine units, this variable is composed of two positive variables $w^{\mathrm{d}}$ and $w^{\mathrm{sp}}$ that represent the water discharge to produce power (turbined water) and the water spillage, respectively.

In the optimization framework, the water flow variables are the decision variables while the other hydro system variables such as water level in reservoirs could be derived from the set of water flow variables $(w)$. For instance, the variable $v_{mt}$ (the water level in reservoir $m$ at time step $t$) using state space model presented in section 2.3.3 can be formulated as 2.5.

$$v_{mt} = V_m^0 + \sum_{\tau=1}^{\tau=t} \left( \sum_{p\in\mathscr{P}_m^{\mathrm{in}}} w_{p,\tau-td_{mp}} - \sum_{p\in\mathscr{P}_m^{\mathrm{out}}} w_{p\tau} - \sum_{h\in\mathscr{H}_m^{\mathrm{out}}} (w_{h,\tau}^{\mathrm{d}} + w_{h,\tau}^{\mathrm{sp}}) + \sum_{h\in\mathscr{H}_m^{\mathrm{in}}} (w_{h,\tau-td_{hm}}^{\mathrm{d}} + w_{h,\tau-td_{hm}}^{\mathrm{sp}}) + \zeta_{mt} \right) \tag{2.5}$$

Where

| | |
|---|---|
| $t,\tau$ | Index for time |
| $m,n$ | Index for reservoirs |

| | |
|---|---|
| $p$ | Index for pumps |
| $h$ | Index for hydro power units |
| $\mathscr{R}$ | Set for reservoirs |
| $\mathscr{P}_m^{\text{out}}$ | Set of pumps that pump out the water from reservoir $m$ |
| $\mathscr{P}_m^{\text{in}}$ | Set of pumps that pump water into reservoir $m$ |
| $\mathscr{H}_m^{\text{in}}$ | Set of upstream hydro-power units that flow into the reservoir $m$ |
| $\mathscr{H}_m^{\text{out}}$ | Set of downstream hydro-power units that flow out of reservoir $m$ |
| $w_{ht}^{\text{d}}$ | Water flow discharge (turbined water) for the hydro unit $h$, at time $t$ |
| $w_{ht}^{\text{sp}}$ | Water flow spillage for the hydro unit $h$, at time $t$ |
| $w_{pt}$ | Water flow pumped by the pump $p$, at time $t$ |
| $td_{mp}, td_{mh}$ | Delay time between pump $p$ or hydro power unit $h$ and the reservoir $m$ |

In the rest of this section, we present the most important constraints that have to be considered in energy and reserve scheduling problem in following chapters 4 and 5 for a hydro dominant system.

#### Reservoir level limit

$$V_m^{\min} \leq v_{mt} \leq V_m^{\max}, \quad \forall m \in \mathscr{R}, \forall t \tag{2.6}$$

where $V_m^{\min}$ and $V_m^{\max}$ are the minimum and the maximum allowable level of water for reservoir $m$ during the scheduling period.

#### Reservoir level at the end of scheduling period

$$v_{mT} = V_m^{\text{T}}, \quad \forall m \in \mathscr{R} \tag{2.7}$$

where $V^{\text{T}}$ is the desirable level of water for reservoir $m$ at the end of the scheduling period $(t = T)$.

**Water flow limit** The water flow variables $w^{\mathrm{d}}_{ht}$, $w^{\mathrm{sp}}_{ht}$ and $w_{pt}$ are positive variables which are also limited by the capacity of hydro-power units and pumps as (2.8) and (2.10).

$$w^{\mathrm{d}}_{ht}, w^{\mathrm{sp}}_{ht} \leq W^{\max}_{h}, \quad \forall h, \forall t \tag{2.8}$$

$$w_{pt} \leq W^{\max}_{p}, \quad \forall p, \forall t \tag{2.9}$$

where $W^{\max}_{h}$ and $W^{\max}_{p}$ are the maximum allowable water flow for the hydro power unit $h$ and the pump $p$, respectively.

An uncontrollable pump is a pump that works with its nominal capacity if the pump is switched on, otherwise it does not pump any water. In other words, the pump water flow variable cannot be controlled continuously from zero to the nominal capacity of the pump as formulated in (2.10). In this case, a binary variable $u_{pt}$ can be used to model the water flow variable as (2.10).

$$w_{pt} = W^{\max}_{p} u_{pt}, \quad \forall p \in \mathscr{P}^{\mathrm{UC}}, \forall t \tag{2.10}$$

Where binary variable $u_{pt}$ ($u_{pt} = \{0, 1\}$) represents the on-off state of the uncontrollable pump $p$ and $\mathscr{P}^{\mathrm{UC}}$ is the set of all uncontrollable pumps.

**Hydro power generation constraints** The output power of a hydro power unit is a function of its discharge water flow. A linear function as presented in (2.11) can simply model the relation between the water flow of the hydro power unit and its generated power.

$$p_{ht} = \rho g H_h w^{\mathrm{d}}_{ht}, \quad \forall h, \forall t \tag{2.11}$$

where $p_{ht}$ is the output power of the hydro unit $h$. Moreover, $H_h$ is the height of the dam, $\rho$ is the specific weight of water ($\rho = 1000\frac{kg}{m^3}$) and $g$ is the gravitational constant ($g \approx 9.8\frac{m}{s^3}$). In the energy and reserve scheduling problem for a hydro dominant system, equation 2.11 connects the water flow and water reservoir variables to the electric power system variables.

## 2.4 Interconnecting converters

Although the railways have their own power plants, the strong fluctuation in power demand often makes it necessary for the supply systems to also be connected to the public grid. In Germany, for example, interconnecting converters exist between the traction power supply and the public power grid at about 40 locations [21]. In Switzerland, there exists 6 interconnecting converters with the total capacity of 540 MW while the total capacity of Swiss railway hydro power generation system is around 800 MW. Besides meeting considerable part of the railways' total power demand, these interconnecting converters also allow the traction power supplies to be stabilized. Moreover, since most of them can be used to exchange energy in both directions (i.e., from the 50 Hz to the 16.7 Hz system, and vice versa), traction power generation can be scheduled in a more economic way.

There are two types of interconnecting frequency converters, namely rotatory and static converters. The traditional rotatory converter consists of two electrical machines that are coupled mechanically [9]. In recent decades, the increasing reliability of power semiconductor devices, and particularly the successful introduction of Gate Turn-Off (GTO) thyristors, has made static converter installations the preferred option [21]. Moreover, the high initial and maintenance costs of rotatory converters persuades the ERCs to move to the utilization of static converters [14]. The static converters, are normally back-to-back voltage source inverters with a DC-link capacitor. The static converters are fully controllable for exchanging energy in both directions using efficient control methods (e.g. pulse width modulation method).

Next in this section, the characteristics of rotatory and static converters are briefly reviewed.

### 2.4.1 Rotatory Converters

A rotatory converter is mainly combined of two electrical machines that are coupled mechanically: one three-phase synchronous or asynchronous machine with 3p pole pairs (machine 1) and a single-phase synchronous machine with p pole pairs (machine 2), both are combined on a common shaft so that they feature the same mechanical frequency $f_{mech}$ [9]. Figure 2.5 shows the diagram of a rotatory converter based on a 16.7 Hz single phase synchronous generator that is connected to a 50 Hz induction motor.

The converter have to operate at a varying frequency to enable the ERC operator to adjust a power-frequency control scheme independently from the public power grid. In this respect usually machine 2 is a four-pole single phase synchronous generator that is driven by a twelve-pole induction motor (machine 1). The synchronous single phase machine has a strong winding damper to alleviate as much as possible the negative sequence rotatory field. Moreover, the stator of this machine has to be suspended on rotatory-springs supports to mitigate the remaining 2 × 16.7 Hz torque oscillations. In general, the size of single phase synchronous generators are three times larger than conventional 50 Hz synchronous generators of equal nominal power, due to single phase and low frequency character [14].

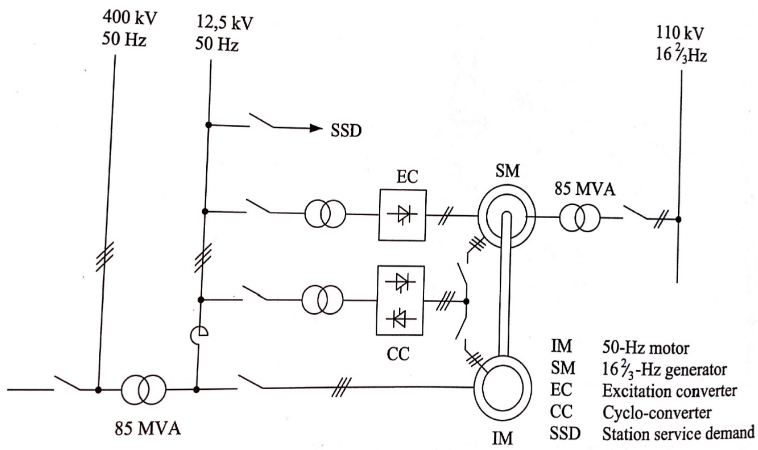


Figure 2.5 – Diagram of an 80-MW rotatory converter[14]

Using single phase synchronous generators make the modeling of rotatory converters different from the conventional power system elements. Robertson and Rogers [22] first in 1948 investigate the performance of a single phase synchronous generator based on steady state voltage-current model. In recent studies, it is prevalent to model the dynamic behavior of this converter using state space models. For instance, the authors in [9] provide the rotatory converter stability analysis based on a state space model that uses the DQ variables and parameters of synchronous machine. Moreover, Danielson et al. in [23, 8] investigate the stability problem taking into account the interaction between the rotatory converter and electric railway vehicles.

The most important characteristics of a single phase synchronous machine in comparison with conventional three phase synchronous machines are 1) the existence of stator suspending springs, that connect the stator to the building foundation to absorb the $2 \times 16.7$ Hz torque oscillations and 2) the existence of large rotor damper winding to induce flux in the rotor, thereby minimizing rotor-body currents and back emf (electromotive force) induced into the dc excitation system.

### 2.4.2 Static Converters

The static converters also known as power-electronic based converters are implemented and used for many applications such as domestic, industrial and IT applications. From technical point of view, the static converters are divided into two types, namely, the voltage source converters (VSC) and the current source converters (CSC). The VSCs are widely used in the low frequency electric railway power systems, specially after the emergence of powerful turn-off semiconductors in the form of GTOs (gate turn-off thyristors) and IGCTs (integrated gate

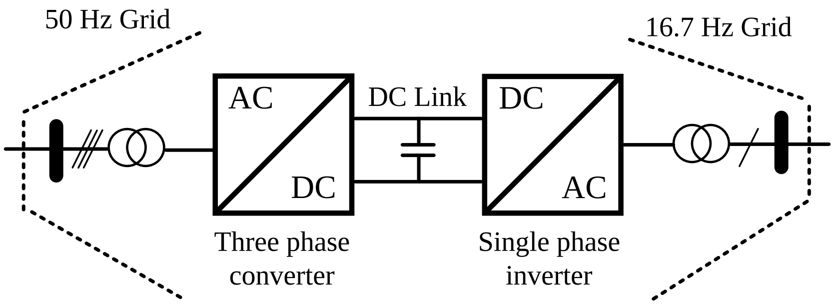


Figure 2.6 – Static Converter Scheme

commutated thyristors) [24, 21].

A VSC based static converter as depicted in figure 2.6 composed of two main parts,namely, a three phase AC-DC voltage source converter that is connected to the 50 hz public grid side and a single phase DC-AC inverter that is connected to the 16.7 Hz electric railway side. In both sides the corresponding transformers are usually used to adjust the level of voltage with the nominal transmission system voltage level.

The basic control mechanism of a three phase AC-DC converter (rectifier) is to keep the dc-link voltage at a desired reference value, using a feedback control loop. The dc-link voltage is measured and compared with the reference. The error signal generated from this comparison is used to switch on and off the power electronic switches of the converter. For instance, when the dc load current is positive (rectifier operation), the capacitor is discharged, and the error signal becomes positive. In this case, the control block takes power from the 50 Hz grid by generating the appropriate PWM (pulse width modulation) signals for the six power switches of the rectifier. Hence, the current flows from AC to DC side, and the capacitor voltage is recovered [25]. This specific topology provides the following advantages: regulation of the dc output voltage, low harmonic distortion, power factor correction and bidirectional power flow that is the reason why it is one of the most popular topologies [26].

In the inverter side, in order to produce a sinusoidal output voltage waveform at the desired frequency (i.e., 16.7Hz), the PWM method is used. Here a sinusoidal control signal at the desired frequency is compared with a triangular waveform. The frequency of the triangular waveform establishes the inverter switching frequency, which is generally kept constant as well as its amplitude.

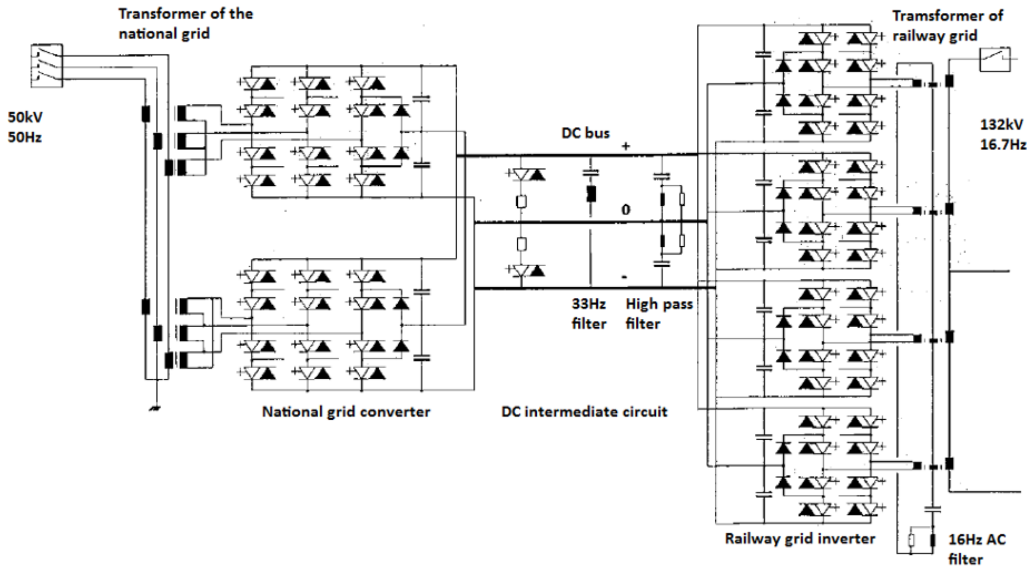


Figure 2.7 – Diagram of a 4 × 20 MW, static converter [27]

A schematic of an 80 MW converter that is operated in Switzerland is depicted in figure 2.7. Here, on the public grid side, two 3-arm bridge rectifiers are converting the 3-phase, 50 kV voltage to DC voltage. DC connection consists of two filters which are decreasing the voltage distortion by cutting off second and lower harmonic of the final output voltage at frequency of 16.7 Hz. On the electric railway grid side, there are four 2-arm bridge inverters. Finally there are four transformers, in series connection, to increase the voltage level to 132 kV.

## 2.5 Transmission and Distribution Systems

Connecting the electric railway substations, converter stations and low frequency generators through a high voltage transmission system brings several advantages. First, the load can be shared by several converter stations since the transmission line provides a strong connection. Moreover the variation of the converter station loadings are decreased and less installed MVA is needed in the system. Other advantages are better voltage profile along the contact line, reduced system losses and fewer disturbances in the train power supply [12].

The transmission system of ERPS in Switzerland is depicted in figure 2.8. The back bone of the system is a 132 KV network that connects 57 substations to 6 interconnecting converters (depicted in orange) as well as 6 hydro power plants (depicted in blue). Moreover, the thick, thin and dashed lines represent the 132 kV, 66 kV and 33 kV transmission lines, receptively.

The function of ERPS distribution system is to supply the contact lines (i.e., 15 KV overhead

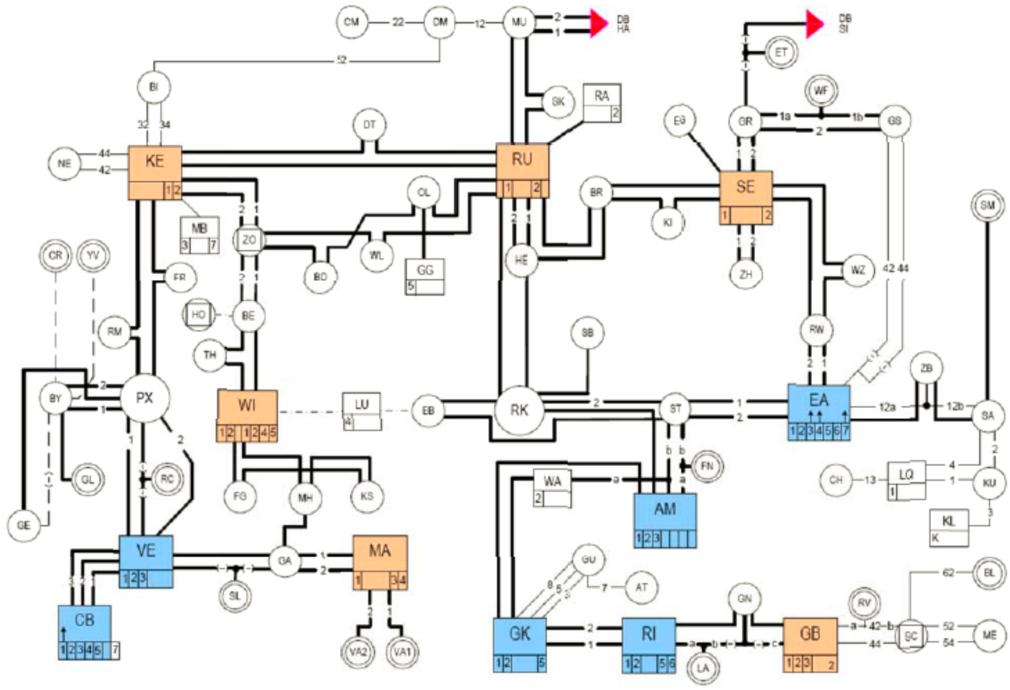


Figure 2.8 – Swiss electric railway transmission network [28]

catenaries) from the above mentioned high voltage substations. The main elements of a ERPS distribution system are as follows:

- *Power transformer stations (substation)* which converts the voltage from the transmission network into the nominal voltage of the contact line network. Here and after in this thesis the terms "substations" or " ERPS substations" refer to this power transformer stations.

- *decentralized converter stations* which convert the three phase 50 Hz power from public grid directly into the contact line (catenary) network. These stations are only applicable in a decentralized ERPS configuration.

- *Switching posts and coupling posts* which receive the power from other substations and feed the contact line network or interconnecting different sections of the contact line network and switching these sections on or off.

It should be noted that in the scope of this thesis, the energy and reserve management approaches consider the transmission system as well as the substations (power transformer stations).

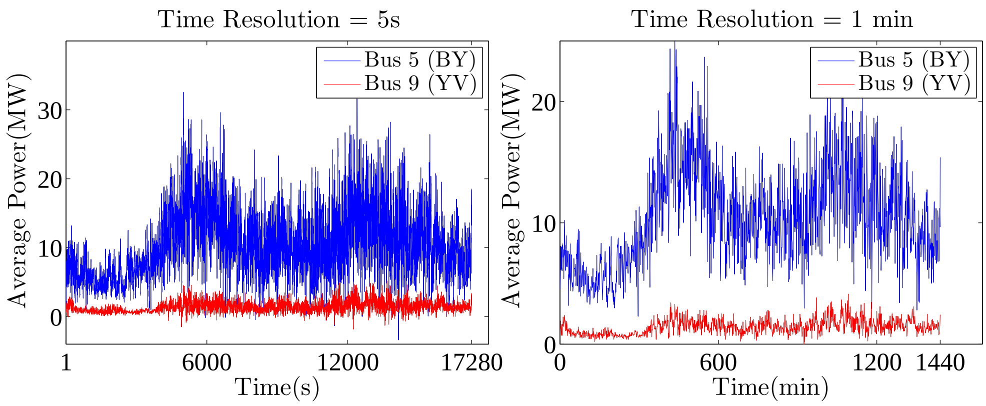


Figure 2.9 – Power demand of Swiss ERPS substations at Bussigny and Yverdons-les-bains on October, 8, 2013

## 2.6 Power and Energy Demand

The power demand of electric railway power system is mostly influenced by the timetable and the schedule of trains. The problem of power demand estimation for the traction loads has been deeply investigated in the literature. For instance, the authors in [29] propose a power demand estimator for high speed railways using DLE (dynamic load estimation) technique. Recently, this technique which is relying on the Lomonossoff's equation is also used for power demand estimation of urban transportation system in [30]. The Lomonossof's equation describes the relation between the speed of the train and its traction or breaking effort based on the mass of the train and some other mechanical parameters.

The ERPS load in terms of power and energy is distinct from the conventional loads in the public grid in two attributes. First, fast and large fluctuations at the load of each substation as well as the total system load and second, the predictable temporal and spatial correlations between the loads of substations that is derived from the time table and the schedule of trains.

In general, each train consumes its maximum power (usually nominal power) during its acceleration period (when the train leaves a passenger station). In contrary, the train consumes no power or even regenerate power during its deceleration period (when the train reaches a passenger station). Beside, the time table of trains are linked to each other to have limited number of trains connected to the contact line in each section of the network. Hence, most of the time the acceleration periods (or deceleration periods) of the trains occurs simultaneously. As a result, the aggregated power consumption of trains connected to a substation is highly fluctuating. Figure 2.9 shows the average power demand of a Swiss ERPS substation at Bussigny and Yverdons-les-bains, for 5s and 1 minute time resolutions.

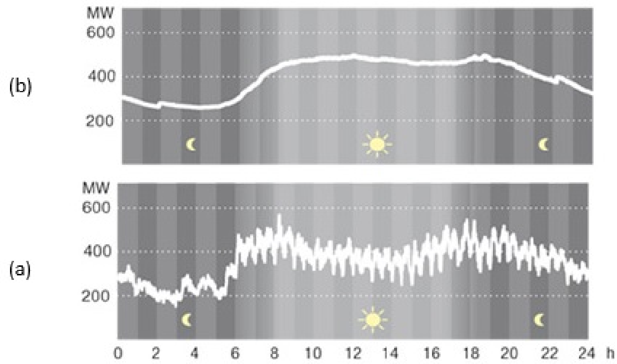


Figure 2.10 – Power demand of (a) Swiss total ERPS and (b) Zurich area in public grid [31]

Clearly the total ERPS load is not as fluctuating as the load of each substation, but it is still highly fluctuating in comparison with the conventional loads. Figure 2.10 shows the difference between the total load of Swiss ERPS and the load of Zurich area in Switzerland for a same day.

As mentioned earlier the load of each substation depends on the position of the trains in the network. In a given region for a given time period, the number of moving trains is limited. Hence an increase in the load of one substation (due to entrance of a train into corresponding section) may lead to decrease the load of the neighboring substation. The term "spatial correlation" refers to this observation. Moreover the load of each substation for consecutive time periods (e.g, 15 minutes) during a day is also correlated to each other depending on the time table and schedule of the trains. The term "temporal correlation" refers to this correlation.

For an ERPS, historical power demand data of substations can be used to quantify the above mentioned temporal and spatial correlations. More insight and analysis concerning the temporal and spatial correlation are provided in sections 4.2.2 and 4.4.1 in chapter 4 aiming to obtain a realistic load forecast analysis for ERPS.

# 3 Reserve Services in Interconnected Systems including Electric Railway and Public Power Grids

## Chapter Overview

*The aim of this chapter is to introduce reserve services which are essential for secure operation of power systems and to investigate the role of reserve services in interconnected systems including electric railway and public power grids. In this respect, different types of reserve services are described and reserve services provision methods have been reviewed. Next, the structure of reserve markets with focus on Swiss reserve market is presented. Finally reserve services from electric railway power system point of view has been investigated.*

## 3.1 Reserve Services

Ancillary services (also known as *system services*) in the power system area are defined as essential services to ensure secure and reliable operation of the system. In general, transmission system operators (TSOs) are responsible for ancillary service procurement. Main ancillary services include [32]:

1. Reserve services (Frequency control reserve)
   (a) Primary control
   (b) Secondary control
   (c) Tertiary control
   (d) Time control
2. Reactive power for voltage support
3. Compensation of active power losses
4. Black start and island operation capability
5. System coordination

In power systems, the active power has to be generated at the same time as it is consumed, otherwise a power deviation occurs. Such power deviation leads to a system frequency deviation resulting from the variation of the kinetic energy of synchronous generators and motors that are connected to the grid. Note that the connected synchronous generators can be operated only in a narrow range of system frequency deviation [33]. Hence, it is crucial for secure operation of the system to maintain power equilibrium in order to control system frequency.

On the other hand, in spite of recent development in electrical storage technologies, there is only very limited possibility of storing electrical energy in large scale which is insufficient for controlling the power equilibrium [34]. In fact, many undesirable events such as generators or transmission lines outages and demand fluctuations can disturb the power equilibrium. As a result, the generators must have sufficient reserve capacity to change their generation level in order to maintain the power equilibrium.

For maximizing the probability of operating a real secure power system, Frequency Control Reserve (FCR) also known as *reserve services* is considered by the system operators to rapidly handle system frequency deviations. FCR could act in both upward and downward ways to compensate the rise or drop of system frequency with activation of upward or downward reserve [35].

### 3.1.1 Definitions and Classifications

As mentioned earlier, *reserve services* can be defined as essential services for maintaining the power equilibrium in power systems. The structure of reserve services is not the same for every power systems. It differs from one system to another system based on its classification, naming, time response, control characteristics, time scales, provision methods, recalling and activation, and so forth.

In this thesis, we follow the structure of reserve services as defined by the European Network of Transmission System Operators for Electricity ENTSO-E (UCTE [1]). FCR is divided into four different types: primary, secondary, tertiary frequency control and time control by ENTSO-E [33]. Next, this structure of reserve services is briefly reviewed.

Primary control restores the balance between power generation and consumption within seconds after deviation occurring. During this operation, the frequency is stabilized within the permissible limit values. The activation takes place directly and automatically in the power plants thanks to the turbine regulators (speed-governor). For each generator, the system frequency is measured and compared with a reference frequency, then the mechanical input power of the generator changes proportionally to the frequency error according to droop characteristic of the turbine regulator. In this respect, the term "primary control reserve" or shortly "primary reserve" refers to the reserve capacity of generators that is used for the operation of primary control.

In an interconnected multi-area power system (e.g. in Europe or North America), the generators in all the areas contribute to the primary frequency control when an imbalance between generation and consumption in a given area occurs. Due to this contribution, the power exchanged between areas deviates from its agreed scheduled value. Therefore, the responsibility of secondary control is, first to restore the system frequency to its reference value and second, to restore the power exchanged between areas to its scheduled value. Needles to say that in an isolated power system the role of secondary control is only to restore the system frequency.

A power plant participates in secondary control by moving (up or down) its droop characteristic. A central controller (installed in TSO), automatically activates the contribution of participating power plants in secondary control. In this respect, the term "secondary control reserve" or shortly "secondary reserve" refers to this reserved capacity of the participating power plants for the operation of secondary control. Following an imbalance event, secondary control is activated after a few seconds (e.g. 30 seconds in Europe) and is typically completed after at most 15 minutes. If the cause of the deviation is not eliminated after 15 minutes,

[1] UCTE was incorporated into ENTSO-E on 1 July 2009 and continues to exist as "Regional Group Continental Europe"

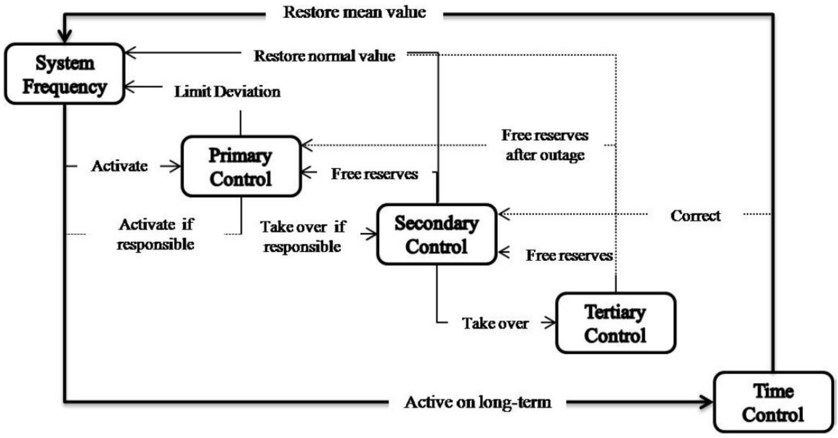


Figure 3.1 – Order of actions for frequency control reserve in ENTSO-E[33]

secondary control is replaced by tertiary control [32].

Tertiary control is any automatic or manual change in the power set points of generators or loads, in order to: 1) guarantee the provision of an adequate secondary control reserve at the right time and 2) distribute the activated secondary control reserve among the participating power plants in the most economic way [33]. In general, the tertiary control reserve is necessary for adjusting major and persistent power deviations, in particular after generator outages or unexpectedly long-lasting load changes. The tertiary control reserve can be provided by power plants or controllable loads. The activation is effected by the TSO dispatcher by means of special electronically transmitted messages to the tertiary reserve providers. The providers must change their power set point as requested by TSO to ensure the supply of tertiary control power within 15 minutes [32].

Counting the number of oscillations of the alternative current of the electrical supply and knowing the nominal frequency of the network (e.g., 50 Hz), one can estimate the time. However, since the frequency of the system actually varies over time, the time given by the electrical network, also called synchronous time, may not be accurate.

Time control corrects time deviation between Universal Coordinated Time (UCT) and synchronized time in the long term using participation of all areas/TSOs in this kind of control. The correction involves the setting of the frequency set-point for secondary control in each control area at 49.99 Hz or 50.01 Hz, depending upon the direction of correction, for full periods of one day (from 0 to 24 hours).

Figure 3.1 shows the order of action of different types of frequency control reserves based on the ENTSO-E reserve structure. For the clarification purpose, figure 3.2 also provides a detailed example of frequency control reserve action following an unexpected power plant

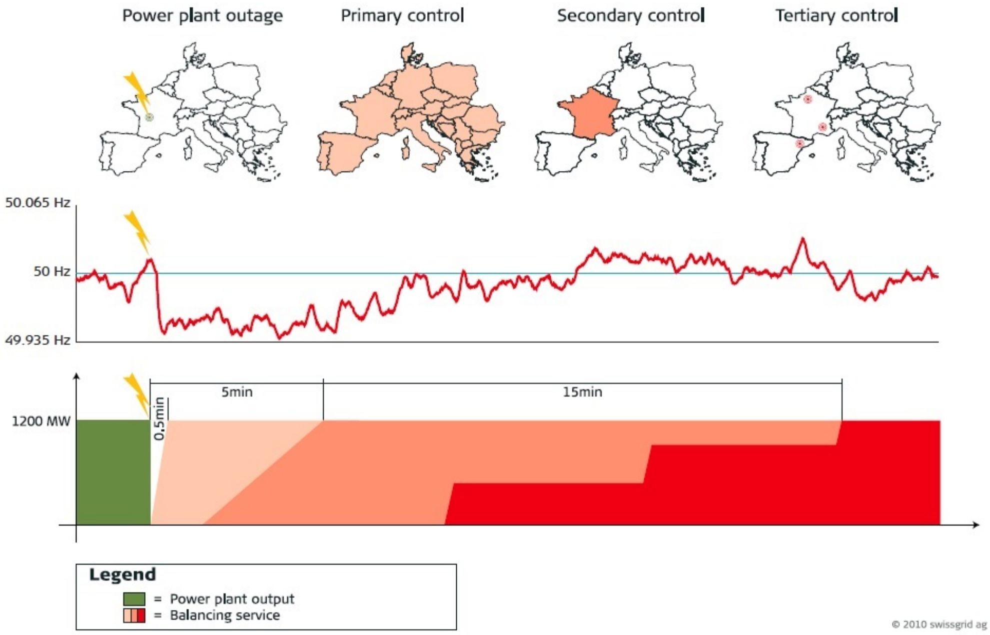


Figure 3.2 – Example of order of actions for frequency control reserve in ENTSO-E[33]

outage in France. Here in the entire UCTE region, primary control is activated directly. After 30 seconds, secondary control power is automatically called up in France, and replaced after 15 minutes by tertiary control, in this example provided by power plants in France and Spain.

Finally it is worth to mention some other reserve service classification which are widely used outside Europe. North American Electric Reliability Council (NERC) classifies the reserve services in two categories, namely, normal reserve services and contingency reserve services. Normal reserve services, which are required for routine operation of the system, includes frequency response, regulation and load following. Contingency reserve services, which are required to handle unexpected outages and contingencies, includes spinning reserve, non spinning reserve and supplement reserves [35]. Here the term "spinning reserve" refers to the reserve capacity of the generators which are connected to and synchronized with the power grid.

The power plants that provide the spinning reserve must start responding immediately to a change in frequency, and the full amount of reserve capacity must be available very quickly. On the other hand, the power plants providing supplemental reserve services do not have to start responding immediately. Depending on local rules, some forms of supplemental reserve services may be provided by units that are not synchronized to the grid but can be brought online quickly [34].

### 3.1.2 Reserve Service Provision

In power system operation and planning, it is important to find out that how much reserve and from which sources should be provided to guarantee the secure functioning of the system in a most possible economic way.

The reserve services provision can be divided into two conceptually different areas, namely, static and operating provisions as suggested by Billinton in [5]. The static provision (i.e., related to long term assessment) is considered as the installed capacity that must be planned and constructed in advance of the system requirement. On the other hand, the operating provision encompasses the efficient management of reserve capacity, provided in long term phase, during the operation period.

In what follows in this section, different reserve provision time scales have been introduced. Afterward, we briefly review the state of the art of reserve service provision methods.

#### Reserve Provision Time Scale

The time frame for reserve service provision can vary from few minutes in real-time operation to some years in long-term capacity expansion planning. In this respect, four time scales (i.e., long-term, mid-term, short-term and real-time) can be considered to study the reserve provision problem.

The reserve services provision in long-term planning (from some years to some decades) is to find the amount of required reserve capacity in long-term capacity expansion planning in order to fulfill the reliability and security criteria. It can be achieved by considering the forced and planned outage rate of generating units, the long term load forecasting uncertainty, the uncertainty in long term penetration of wind turbine and renewable energy sources in the network. It is also affected by financial risks and uncertainties such as interest rate variation, economic signals coming from the energy markets and other factors.

The mid-term (from a month to a year) reserve services provision is the required capacity reserve provision in such a way to consider the maintenance program of generating units, fuel scheduling and allocation, environmental constraints, future development projects, transactions with neighboring power providers, cross border capacity allocation, mid-term load and wind speed forecasting uncertainties, and so forth.

Note that a proper long term and mid-term reserve provisions can give a wider range of options for managing the system security in short term and real-time operations. On the other hand, the power system operation strategies over real-time and short term operation phases can provide efficient signals for long term and mid-term reserve provisions [36].

The reserve services provision in short term (hourly, day-ahead or weekly) operation phase considers the topology of the grid, the transmission flow constraints and the unexpected failure of power system components. It is also influenced by hourly, daily and weekly fluctuations of load demands and intermittent generations. Moreover, the short term load forecasting uncertainties as well as the price uncertainties in energy and reserve markets should be considered in short term reserve provision.

Finally, the real-time (online) reserve services provision consider the unexpected failures of power system components and instantaneous fluctuation of load and generation (for intermittent generation such as wind generation) due to sudden change in weather condition or inaccuracy of forecasting process.

In this thesis, chapters 4 and 5 consider the short term and real-time time scales. In particular, chapter 4 proposes several mathematical modeling and optimization techniques for short term energy and reserve provision for electric railway power systems. In addition, chapter 6 proposes the optimal placement and sizing of new interconnecting converters considering the long-term reserve provision based on some reliability index.

**Reserve Provision Methods**

The problem of reserve provision has been deeply investigated in power system literature and a number of methods have been proposed to find the required reserve for a particular operating condition. From mathematical point of view, these methods can be classified into three categories, namely, deterministic, probabilistic and hybrid (deterministic/probabilistic) approaches.

The deterministic approaches set the required reserve services to a predefined amount equal to the capacity of the largest online generator, to some fractions of the peak load or to any combination of both, so that the system will be able to tolerate any single outage of generating units or some deviation of load demand without causing any constraint violation [37, 5]. For instance, ENTSO-E employs the deterministic approach (3000 MW as a reference incident) to set the required primary reserve services on its whole synchronized area [33]. Next, the system operator allocates the fixed amount of reserve services among different providers, such that a distinctive objective function is optimized [38, 39, 40]. A complete literature review on deterministic reserve provision approaches employed in different power systems is provided in [35] and [41].

Although these techniques can be understood and implemented easily, they do not explicitly and accurately reflect the actual system risk. Probabilistic techniques, however, can provide a comprehensive and realistic evaluation of the risk by incorporating the stochastic nature of the system components and load behavior [42]. The probabilistic methods consider the system risk index such as Loss of Load Probability (LOLP) and Expected Energy Not Supplied (EENS) [43] in the reserve provision problem.

The lack of sufficient information provided by probabilistic index and the difficulties in interpreting the risk index made many system operators considerably reluctant to apply probabilistic technique to evaluate reserve services requirement [35]. The hybrid deterministic/probabilistic approach is then proposed in the literature. It combines accepted deterministic considerations with probabilistic index to overcome the shortcomings of pure probabilistic methods [44, 45].

The probabilistic and hybrid methods can be divided into two categories, namely, statistic-based and optimization-based methods. The static-based methods perform a statistic assessment for all the sources of power imbalance including power plant outage, load demand variation, load forecast errors and forecast errors of intermittent generation. Then the required amount of reserve is obtained, using this statistic assessment, in such a way that a target risk level is satisfied. The authors in [46] applied a statistic-based method for dimensioning of secondary and tertiary control reserve. Moreover, it is applied in [47] for evaluating the proposed integrated pan-European reserve service market.

The main drawback of the statistic-based methods is that satisfying a predefined risk level target might not be economical. In contrary, the optimization-based methods incorporate reliability index (e.g., EENS and LOLP) into an optimization problem, and then the optimum amount of required reserve is achieved solving this problem. Note that the reliability index can be incorporated in two ways. The first one is to impose upper bounds on reliability index as an inequality constraint. This inequality constraint force the system operator to procure reserve services in a scheduling period such that the pre-specified risk target is satisfied. The second way is to add a penalty function, increasing monotonically with EENS, to the objective function of the problem using the so-called Value Of Lost Load (VOLL).

Several litterateurs referenced in [48, 49, 50, 51] incorporate the probabilistic criteria into the unit commitment (UC) problem to determine the optimal required reserve. They solve the problem iteratively; at the first step the UC problem is solved considering an initial required reserve. In the second step, the risk index derived from capacity outage probability table (COPT), is checked to ensure whether it satisfies the target. If not, the initial reserve is updated, and the UC problem is solved again. The basic drawback of the above approaches is that it is not possible to incorporate COPT directly into UC formulation because of its discrete nature;

therefore, it could be computationally intensive since several UC runs may be needed.

References [52, 53] propose an approximated function whose parameters are system-dependent to integrate the risk index into the UC problem as a continuous inequality constraint. The shortcoming of this approach is that the results acquired from are not so accurate. Afterward, the authors in [54, 55] include the risk index into the UC formulation as a continuous variable such that its mathematical form is compatible with Mixed Integer Linear Programming (MILP) algorithm. This methodology was only applied in the case of isolated power system not in the case of interconnected power system.

Note that all the aforementioned approaches determine the required reserve services implicitly. On the other hand, references [56, 57, 58] employ a two-stage stochastic programming technique to provide the required reserve services explicitly. In the explicit reserve services provision model, the reserve requirements are taken into account considering possible realization of different scenarios. Each scenario can include the size and location of a unit outage, demand fluctuation or any other possible disturbance. However, the difficulty with stochastic programming is that the problem size and the computational time increases with the number of scenarios since a large number of scenarios are often required to ensure the quality of the solution.

Robust optimization which is an alternative framework to stochastic optimization for solving problems dealing with uncertainty, is also proposed to solve energy and reserve provision problems (e.g. [3, 4]). In robust optimization the uncertainty model is not stochastic, but rather deterministic and set-based. The decision-maker constructs a solution that is not only feasible for all realizations of the uncertain parameters within the uncertainty set (e.g. confidence intervals) but also optimal for the worst realization of such uncertain parameters [59].

In this thesis, both of the two stage stochastic optimization and the adaptive robust optimization techniques are proposed to find the joint energy and reserve scheduling of an electric railway power system in chapter 4. A complete discussion on the advantages and drawbacks of both methods is also provided in that chapter.

#### Reserve Provision in Interconnected Power Systems

Most electric power systems prefer to be operated as members of an interconnected system for a definite improvement in system adequacy and security. System interconnections permit the electricity market participant to export and/or import electrical energy and TSOs to exchange ancillary services for mutual benefit. In addition, due to the diversity of load demands and the forced outages of generating equipment, each power system can operate with less reserve service than would normally be required for isolated operation [60, 61, 48].

Today in interconnected systems (e.g. UCTE), the national TSOs are responsible for providing reserve services to maintain the security of the system. Hence the required reserve is obtained in a decentralized way by each TSO. The authors in [47] evaluated the reserve requirement of the interconnected European power system using a statistic-based method in a centralized way. It is concluded that the centralized approach leads to a significant reduction of the required reserve. Moreover, the authors in [42, 62] proposed an optimization-based method and showed that The inter-zonal trading in a interconnected power system improves the system efficiency from both the economic and security point of view by sharing the resources (energy and reserves) across the boundaries.

As already mentioned the problem of energy and reserve provision in interconnected systems including electric railway and public power grids is not deeply investigated in the literature. Among few studies, Burger et al. in [2] investigate the amount of required reserve for the Swiss electric railway power system based on a static probabilistic method. This method is relying on the probability of power plant outages and load forecast error to find the required reserve for satisfying an accepted level of deficit (load shedding). It is shown that centralized reserve provision approach leads to 11 MW (2.8%) and 7 MW (4.6%) reduction in required reserve of Swiss TSO and Swiss ERPS, respectively.

## 3.2 Reserve Market Structure

Reserve service markets (ancillary service markets in general) have been developed in many countries along with the liberalization in power industry. Generally TSOs are responsible for the procurement reserve services. The reserve market permits the TSO to obtain the required resources to maintain the security of the system at minimum cost. Beside, the reserve service providers seek to maximize their profit by participating in reserve markets [1]. Due to the technical complexities associated with reserve services, various forms of reserve market structure have been set up [57, 63, 64].

In this thesis we follow the Swiss reserve market structure which has some similarities with other European reserve markets. From January 2009, Swissgrid company (the Swiss TSO) is required to purchase system services in accordance with a transparent, non-discriminatory and market-based procedure. It does this in accordance with the technical specifications of the ENTSO-E as presented in section 3.1.1.

Currently a statistic-based method is used for dimensioning the amount of required reserves.

The probability distributions of power imbalances due to disturbances on the load side, random outages of generators and due to forecast errors are calculated over time horizons of 15 minutes and 1 hour. These times correspond to the operation times of secondary and overall frequency control reserves respectively. The risk index target is that the ACE should regulate to zero at 99.9% of time as recommended by ENTSO-E in [33]. As a result, the required amount of primary, secondary and tertiary reserves are $\pm 66$MW, $\pm 400$MW and $+450/-390$MW respectively [65]. Primary and secondary reserves are auctioned in a monthly and weekly markets respectively, while tertiary reserves can be procured in both daily and weekly auctions.The shares of the weekly and daily markets are fixed to a predefined values based on judgment and experience. However some recent studies such as [66] propose a stochastic optimization approach to determine the optimal dimensions and shares of secondary and tertiary control reserves in each market by minimizing the provision cost subject to the system security index.

The primary and secondary reserve are activated automatically by TSO signals for load following purpose. The reserve providers are not credited for the deployed energy during primary control period. However for the secondary energy deployment, the providers are credited based on a secondary activation price which is 1.2 times the spot market price. The tertiary reserve is activated manually by the TSO dispatchers. Each provider should submit energy deployment price offer along with its tertiary reserve capacity offer. In case of long-lasted imbalances which needs the activation of tertiary reserves, the TSO dispatchers activate the tertiary reserves from the most cheap accepted offer to the the most expensive one.

For billing and accounting purposes, generation units and consumers are organized in BGs (Balanced Groups) which covers any number of feed-in and feed-out points [67]. Each BG submits a day-ahead power exchange schedule to the TSO, i.e., a profile of the BG net position during the next day with a time resolution of 15 minutes. Due to load or generation forecast errors and unexpected events, some BGs may deviate from the submitted schedules during real-time operation [68]. These deviations are balanced by the TSO using the above mentioned provided reserves. After completion of the energy deliveries in real-time operation, Swissgrid calculates the balance energy for each BG. Balance energy is the difference between the schedule sum of the BG and the measured sum (actual) that is determined on the basis of the 15 minutes periods. The balance energy price mechanism is a two-price system in which the prices for balance energy are classified according to the direction of a balance group discrepancy. BGs in surplus (long BGs) receive a credit note, while BGs in deficit (short BGs) are charged accordingly [67]. Generally the short and long balance prices are considerably higher and lower than the day ahead and spot market prices, respectively. The long prices might be even negative in case of low demand events accompanied with high wind and photovoltaic generations.

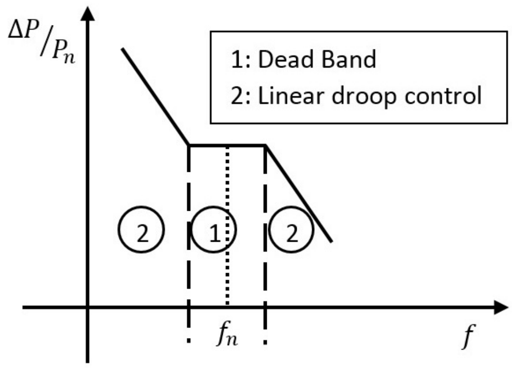


Figure 3.3 – Power-frequency diagram for primary control on hydro power units

## 3.3 Reserve Services in ERPS Side

As already discussed in chapter 2, ERPS suffers from high load fluctuations. Generally the electric railway installations (i.e. generators, converters, etc.) are over sized to reduce the risk of power shortage in case of strong fluctuations in electric railway power demand. Moreover, fast interconnecting converters alongside with fast hydroelectric power plants, allow ERCs to adjust the energy exchanges through the converters to reduce the imbalances in the public power grid.

In Switzerland, SBB company (the Swiss ERPS operator) employ a two level hierarchical frequency control scheme for tackling high load fluctuations. The primary control is directly implemented in hydro power units using traditional droop control as depicted in figure 3.3. The public power grid through interconnecting converters could also support the railway power system, in case of strong fluctuations in the railway power demand. Afterward, the role of secondary frequency control is to adjust the output of the ERC's generator and the set point of the converters to follow the energy demand fluctuations over each 15 minutes time step and to restore the ERPS frequency. In addition, the secondary control considers the energy exchanges between SBB and DB (German ERPS operator) and OBB (Austrian ERPS operator) [69].

Figure 3.4 depicts a general scheme of SBB secondary control system. Here the required secondary control power ($\Delta P$) is obtained by integrating the deviation of power exchanges between SBB and the neighboring ERPSs plus an amplified frequency error signal. Note that SBB is charged by the the TSO for the short or long energy imbalances through interconnecting converters during each 15 minutes time step as discussed in section 3.2. In this respect the role of SCPD (secondary power control dispatcher) block is to dispatch the required $\Delta P$ among generators ($\Delta PG$) and converters ($\Delta PC$), with one minute resolution, in such a way that the

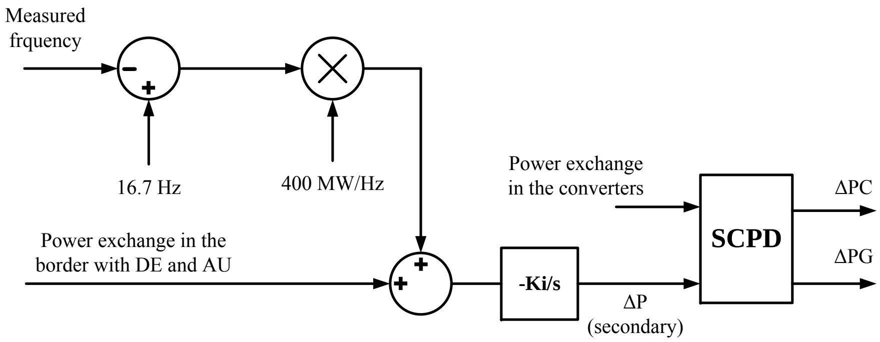


Figure 3.4 – Secondary control scheme of Swiss electric railway power system

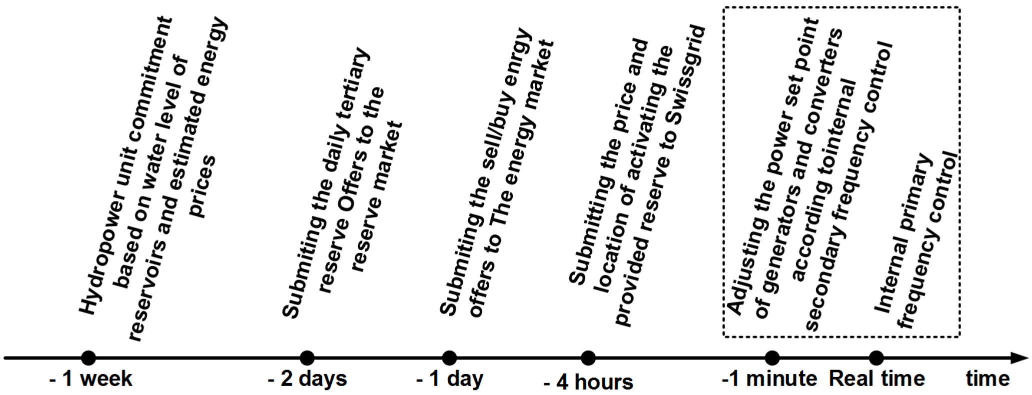


Figure 3.5 – Weekly operation chronology of Swiss electric railway power system

energy imbalances through the converters during each 15 minutes period is minimized.

In order to guarantee the proper operation of primary and secondary control, ERC has to provide both upward and downward reserve from its own generators and part of the capacity of the interconnecting converters. In current practice, the amount of required reserve is obtained in a deterministic way. In chapter 4 of this thesis, we propose two optimization-based methods to find the amount of reserve that should be provided by each generator and converter. After providing the internal required reserve, the ERC is interested to offer the tertiary reserve (upward and downward) to the market from the remaining capacity of its own generators. Chapter 5 proposes a robust offering strategy for an ERC to participate in reserve (and energy) markets in the sense that uncertainties in energy demand of its own substations would not threaten its security of supply.

Needless to say that any optimization-based reserve provision or scheduling method should consider the tight connection between energy and reserve as they are provided from the same generators. Figure 3.5 presents the current short term operation procedure of SBB to demonstrate the connection between energy and reserve provision, scheduling and market strategies.

# 4 Joint Energy and Reserve Scheduling under Uncertainty

## Chapter Overview

*The aim of this chapter is to investigate methods for finding the day-ahead schedule of ERC's generators and interconnecting converters for a given set of energy and reserve market prices. First, the joint energy and reserve scheduling is formulated as a two stage optimization problem. In this optimization problem, the forecast of energy demand at railway substations is subject to uncertainty. Hence, the load forecast uncertainty is analyzed to provide a realistic uncertainty representation for the scheduling problem. Afterward, an adaptive robust optimization method is proposed for dealing with energy demand uncertainty in the scheduling problem. Next, a two stage stochastic optimization method is proposed for dealing with the problem uncertainties. Here, in addition to the energy demand forecast error, the availability of the ERC generators and the interconnecting converters are subject to uncertainty. Finally to demonstrate the effectiveness of the proposed robust and stochastic methods, a realistic case study based on the characteristic of ERPS in the western part of Switzerland is presented. Moreover, a discussion on the advantages and drawbacks of each method considering the characteristics of the ERPS is provided.*

## 4.1 Introduction

One of the main tasks of the railway power system operator, is to maintain the frequency of the system in an allowable range. For this purpose, the ERC has a two level hierarchical frequency control scheme to follow the railway power demand fluctuations as described in section 3.3. In summary, the primary frequency control is directly implemented in hydroelectric power plants using traditional frequency droop control. The public power grid through interconnecting converters could also support the railway power system, in case of strong fluctuations in the railway power demand. Afterward, the role of secondary frequency control is to adjust the output of the ERC's generator and the set point of the converters to follow the energy demand fluctuations over each 15 minutes time step. In this respect, the ERC has to provide both upward and downward reserve from its own generators and part of the capacity of the interconnecting converters.

Within the above context, the aim of this chapter is to investigate methods for finding the day-ahead schedule of the ERC's generators and interconnecting converters for a given set of energy and reserve market prices. Since the ERC is charged by the the TSO for the energy imbalances through interconnecting converters during each 15 minutes time step, the scheduling problem has to consider two stages, namely, the day-ahead dispatching and the balancing stages.

### 4.1.1 Literature Review and Contributions

Most of researches in the electric railway power system operation has focused more on load flow and optimal power flow problems[12, 13, 70, 71] than energy and reserve provision for the system [2].

In the mid 1990s, Ollofsson et al. in [12] and [13] solve the load flow and optimal power flow problems for the Swedish electric railway system considering controlled and uncontrolled interconnecting converters. Afterward, the optimal power flow problem by controlling the power electronic equipment on-board the trains rather than controlling large installed power electronic facilities is investigated in [70]. A probabilistic load flow analysis based on Monte Carlo simulation approach is presented in [71]. Here train position is selected as the primary random variable, using this variable we can derive the power demand of the train.

Among few studies, Burger et al. in [2] investigate the amount of required reserve for the Swiss electric railway power system based on a static probabilistic method. This method is relying on the probability of power plant outages and load forecast error to find the required reserve for satisfying an accepted level of deficit (load shedding). To the best knowledge of the author of this thesis, the problem of energy and reserve scheduling for an ERC to minimize the cost of providing energy and reserve considering the security of supply is not reported in the literature.

A literature review on methods for operating reserve provision is presented in 3.1.2. In summary, deterministic and probabilistic techniques can be both used to establish reserve requirements. The deterministic approaches set the amount of the required reserve in the scheduling problem to a predefined amount equal to the largest online generator, some fraction of the peak load or any combination of both of these. Although these techniques can be understood and implemented easily, they do not explicitly and accurately reflect the actual system risk. Probabilistic techniques, however, can provide a comprehensive and realistic evaluation of the risk by incorporating the stochastic nature of system components and load behavior [35].

Both deterministic and stochastic optimization approaches are widely used for energy and reserve scheduling. The authors in [72] solve the energy and reserve self-scheduling problem for a joint hydro and pumped-storage plants using a deterministic approach. Galiana et al. in [57] applied scenario based stochastic optimization for an electricity market which, schedule energy and reserve to balance power during primary, secondary and tertiary regulation intervals.

References [58, 57, 56] employ a two-stage stochastic optimization technique to provide the required reserve services explicitly. In the explicit reserve services provision model, the reserve requirements are taken into account considering possible realization of different scenarios. Each scenario can include the size and location of a unit outage, demand fluctuation or any other possible disturbance. However, the main drawback of this method is that the obtained solutions only provide probabilistic guarantees to the system security. Moreover, for the purpose of scenario generation, the probability distribution function of the uncertain parameter has to be known in advance.

Robust optimization is an alternative framework to stochastic optimization for solving problems dealing with uncertainty. In recent years, this uncertainty management approach has been received lots of attention in power system [3, 4]. In robust optimization the uncertainty model is not stochastic, but rather deterministic and set-based. The decision-maker constructs a solution that is not only feasible for all realizations of the uncertain parameters within the uncertainty set (e.g. confidence intervals) but also optimal for the worst realization of such uncertain parameters [59].

Authors in [73] propose an energy management algorithm that allows the cluster of demands to buy, store and sell energy at suitable times. A framework for computing the worst-case robust profit and optimizing the self-schedules of price-taker generators in energy market is presented in [74]. Adaptive or adjustable robust optimization technique is also used for security constrained unit commitment [3], energy and reserve scheduling under security criterion [4].

In this chapter, the energy and reserve scheduling for an electric railway company is formulated in two stages. The first (dispatching) stage deals with day-ahead decision variables considering the forecast of energy demand of railway substations. For each generator and interconnecting converter, day-ahead decision variables includes the hourly output power set point, part of provided reserve to be used for ERC's frequency control scheme and part of provided reserve to be sold in the reserve market.

Since, in real-time, the energy demand (load) of electric railway substations is not equal to its forecast value, the second (balancing) stage is required to ensure the security of supply. In the second stage, the provided reserves (from first stage) are activated in order to maintain the power balance in the system.

The load forecast error is an important uncertain parameter in the problem. In this study, a short term load forecast method based on Auto-Regressive Integrated Moving Average (ARIMA) time series is applied to find the load forecast of ERPS substations. Moreover, this load forecast technique is applied to capture the temporal and spatial correlations between the loads of ERPS substations.

Afterward, an adaptive robust optimization method is proposed for dealing with energy demand uncertainty in the scheduling problem. Building an appropriate uncertainty set, which covers the most significant characteristics of uncertainty, is crucial for the effectiveness of the proposed robust method. In this respect, the proposed uncertainty set in this chapter, consider the temporal and spatial correlation between energy demand forecast error of the ERC substations. Moreover it provides the control parameters to control the level of robustness of the obtained solution against the variation of real energy demand from the forecast value. This robustness is desirable for electric railway power systems where the penalty associated with the infeasible solution is very high. Hence, the concept of robust optimization is consistent with the risk-averse fashion in which the electric railway power systems are operated.

The main drawback of this approach caused by its solution algorithm. In fact, the second stage problem should be linear in order to obtain its dual problem. Otherwise the adaptive robust problem is not solvable.

Next a two-stage stochastic optimization method is proposed for dealing with the problem uncertainties. Here, in addition to the energy demand forecast error, the availability of the ERC generators and the interconnecting converters are subject to uncertainty. Monte Carlo simulation is used to generate scenarios for representing the realization of uncertain parameters. Since computation requirements for solving scenario-based optimization models depends on the number of scenarios, a scenario reduction technique based on k-medoids clustering algorithm [6] is adapted for a trade off between solution accuracy and computation burden.

The main advantage of this method is that there is no limitation on the second stage modeling. Hence, in this approach we have proposed an enhanced two stages scheduling that considers more detailed technical aspects such as the efficiency of the converters and energy imbalance aggregation over all converters.

Finally to demonstrate the effectiveness of the proposed robust and stochastic methods, a realistic case study based on the characteristic of an ERC in the western part of Switzerland is presented. Moreover a discussion on the advantages and disadvantages of each method considering the characteristics of ERC is provided.

Given the above context, the main contributions of this chapter are:

1. to model the multi-period self-scheduling problem of an ERC in two stages (day ahead dispatching and real time balancing) considering cascaded hydro plants, interconnecting converters and internal transmission network constraints in a linear way;
2. to apply a short term load forecast technique based on time-series to obtain the uncertainty characteristics of energy demand forecast error of the ERC substations;
3. to propose an adaptive robust optimization technique to solve the above two stages (1) scheduling problem considering the spatial and temporal correlations between energy demand forecast error uncertainty of the ERC substations;
4. to propose an enhanced two stages self scheduling problem formulation that considers detailed technical considerations in addition to (1) using binary variables;
5. to propose a two stages stochastic optimization technique to solve above (4) two stage scheduling problem considering energy demand forecast error uncertainty and the availability of the generators and interconnecting converters.

### 4.1.2 Chapter Organization

The rest of the chapter is organized as follow: section 4.2 describes a short term load forecast method based on ARIMA time series to find the ERC load forecast characteristics. The deterministic two stages self-scheduling problem of the ERC is presented in section 4.3. In section 4.4, the adaptive robust optimization technique is introduced to solve the self-scheduling problem dealing with the uncertainties. The stochastic optimization method is presented in section 4.5. Section 4.6 discusses the advantages and drawbacks of the proposed methods. Finally, the conclusion and summary are presented in section 4.7.

## 4.2 Energy Demand Forecast for ERPS

In this section a short term load forecast method based on ARIMA time-series is used to find the load forecast of the ERC. The time step of load forecasting here is 15 minutes and one hour while the measured quantity is the consumed energy (demand) in those periods. The first objective of this short term load forecast is to provide a load prediction for energy and reserve self scheduling of the ERC. The second aim is to find an appropriate uncertainty set to cover the uncertainties on the error of load forecast. The uncertainty set should also cover the temporal and spatial correlations on the energy demand at substations. In this respect the load forecast is performed for each substation and for the whole system separately. This uncertainty set is used in section 4.4 to find a robust energy and reserve schedule against the variations of energy demands at ERC's substations. More details on the results are provided in case study section 4.2.2.

### 4.2.1 Time-Series Methods

Time-series methods are among the most popular approaches that have been applied and are still being applied to short time load forecast. Using the time-series approach, a model is first developed based on the previous data, then future load is predicted based on this model [75]. In this section we describe the general formulation of time-series methods from Auto-Regressive (AR) to Auto-Regresive Moving Average (ARMA) and ARIMA.

If the load is assumed to be a linear combination of previous loads, then the AR model can be used to model the load profile, which is given by [75] as:

$$\hat{y}_t = -\sum_{i=1}^{m} \alpha_{it} y_{t-i} + w_t \tag{4.1}$$

where $\hat{y}_t$ is the predicted load at time $t$, $w_t$ is a rndom load disturbance, $\alpha_{it}$ are unknown [U+0081] coefficients. (4.1) is the AR model of order $m$ while the unknown coefficients [U+0081] in (4.1) can be tuned on-line using the well-known Least Mean Square (LMS) algorithm [76].

In the ARMA model, the current value of the time series $y(t)$ is expressed linearly in terms of its values at previous periods $[y(t-1), y(t-2), \ldots]$ and in terms of previous values of a white noise $[a(t-1), a(t-2), \dots]$. For an ARMA of order $(p, q)$, the model can be written as:

$$y(t) = \phi_1 y(t-1) + \cdots + \phi_p y(t-p) + a(t) - \theta_1 a(t-1) - \cdots - \theta_q a(t-q) \tag{4.2}$$

The parameter identification for a general ARMA model can be done by a recursive scheme, or using a maximum-likelihood approach, which is basically a non-linear regression algorithm. By defining the lag operator $B^i y(t) = y(t-i)$, the following lag operator polynomials can be defined to condense the notation and solve linear difference equations.

$$\phi(B) = 1 - \phi_1 B - \phi_2 B^2 - \cdots - \phi_p B^p \tag{4.3a}$$

$$\theta(B) = 1 + \theta_1 B + \theta_2 B^2 + \cdots + \theta_q B^q \tag{4.3b}$$

Therefore, the condensed ARMA formulation is as 4.4.

$$\phi(B) y(t) = \theta(B) a(t) \tag{4.4}$$

If the process is non-stationary, then transformation of the series to the stationary form has to be done first. This transformation can be performed by the differencing process. Let us define the $\nabla$ operator as $\nabla y(t) = (1-B) y(t)$. For a series, with AR and MA orders equal to $p$ and $q$, that needs to be [U+0080] differentiated $d$ times, i.e. ARIMA$(p, d, q)$, the model can be written as:

$$\phi(B) \nabla^d y(t) = \theta(B) a(t) \tag{4.5}$$

So far we have restricted our attention to non-seasonal data and non-seasonal ARIMA models. However, ARIMA models are also capable of modeling a wide range of seasonal data. A seasonal ARIMA model is formed by including additional seasonal terms in the ARIMA models we have seen so far. It can be written as ARIMA$(p, d, q)(p_s, d_s, q_s)_s$, where $s$ is the number of periods per season. Note that the seasonal terms of the model are similar to non-seasonal terms, but they involve backshifts of the seasonal period [77]. Therefore, the general formulation of ARIMA model, which includes differencing, multiplicative seasonality and seasonal differencing is:

$$\phi(B) \nabla^d \Phi(B) \nabla^{d_s} y(t) = \theta(B) \Theta(B) a(t) \tag{4.6}$$

where the seasonal lag operator are defined as:

$$\Phi(B) = 1 - \Phi_1 B^s - \Phi_2 B^{2s} - \cdots - \Phi_{p_s} B^{p_s s} \tag{4.7a}$$

$$\Theta(B) = 1 + \Theta_1 B^s + \Theta_2 B^{2s} + \cdots + \Theta_{q_s} B^{q_s s} \tag{4.7b}$$

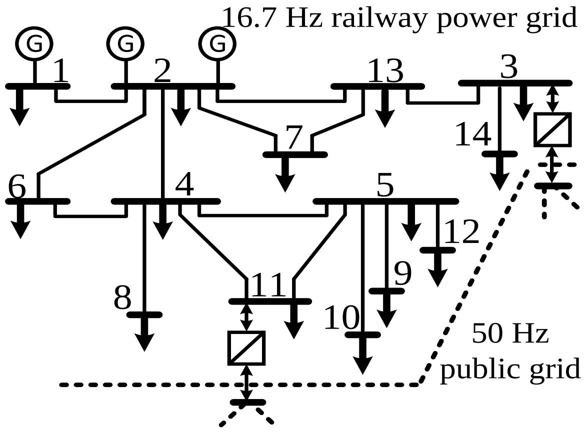


Figure 4.1 – Transmission network of ERPS including 14 substations

The ARIMA model can be enhanced by considering the external time series, such as the weather condition (temperature) [78]. However in this study we use the basic ARIMA model as formulated in equation 4.6.

### 4.2.2 Case Study

The ARIMA model in (4.6) has been applied to predict the energy demand of Swiss electric railway system in the western part of Switzerland that includes 14 substations. The configuration of substations is presented in figure 4.1. Both nodal and total load forecast have been done considering time step of 15 minutes and one hour energy consumptions. Two days (12 and 19, October, 2013) have been selected to perform the ARIMA forecast method. The hourly and 15 minutes energy demand data used to forecast these two days are from 7 to 18, October, 2013. Note that the forecast results for the second day (19, October, 2013) will also be used in the case study sections 4.4.3 and 4.5.2 to show the effectiveness of adaptive robust optimization and stochastic optimization techniques for dealing with energy demand uncertainties in ERPS.

#### Hourly total energy demand (HT)

The results of forecasting the total hourly energy demand of the whole system (indexed by "HT") are depicted in figure 4.2. The average of hourly errors in comparison with the real data over 24 hours (MDE: Mean Day Error) can be calculated as:

$$MDE^{\mathrm{HT}} = \frac{1}{24}\sum_{t}\left|\frac{L_t^{\mathrm{HT}} - \tilde{L}_t^{\mathrm{HT}}}{L_t^{\mathrm{HT}}}\right| \tag{4.8}$$

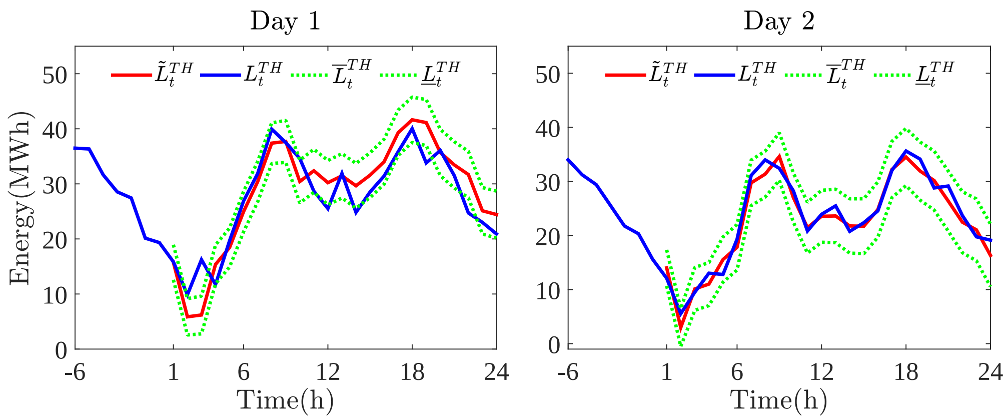


Figure 4.2 – Hourly total energy demand forecast results

where $L_t^{\mathrm{HT}}$ and $\tilde{L}_t^{\mathrm{HT}}$ are the real and forecast values of total hourly energy demand of the whole system during time period $t$ ($t = 1, \ldots, 24$). MDE for the first and the second day are 14.1% and 8.6%, respectively.

An index for uncertainty in any of the forecast model is the variability of what is still unexplained after fitting the model. It can be measured through the variance of the error term. The smaller the variance, the more precise the prediction of energy demand is. Note that, the value of variance is unknown, therefore an estimation can be used. The square mean error of the conditional forecast $\tilde{L}_t^{\mathrm{HT}}$ can be used as such an estimate. Let us name it ${\sigma^2}_t^{\mathrm{HT}}$, for the hourly energy demand of the whole system. Using $\sigma_t^{\mathrm{HT}}$, the confidence interval for the obtained forecast values can be derived. Assuming that the error of the forecast follows a normal distribution, we define the uncertainty index $\xi_t^{\mathrm{HT}} = z\sigma_t^{\mathrm{HT}}$ as an estimation of the level of variation of the real load from the forecast values at each time period. Here, $z = \Phi^{-1}(\alpha)$ and $\alpha$ is the level of confidence. Finally, the upper and lower bounds of the confidence interval $(\overline{L}_t^{\mathrm{HT}}, \underline{L}_t^{\mathrm{HT}})$ can be calculated as:

$$\begin{aligned} \overline{L}_t^{\mathrm{HT}} &= \tilde{L}_t^{\mathrm{HT}} + \xi_t^{\mathrm{HT}} \\ \underline{L}_t^{\mathrm{HT}} &= \tilde{L}_t^{\mathrm{HT}} - \xi_t^{\mathrm{HT}} \end{aligned} \tag{4.9}$$

The upper and lower bounds of the 95% confidence interval ($\alpha = 0.95 \Rightarrow z = 1.64$) is depicted by the green dashed line in figure 4.2. In other words with the confidence level of 0.95%, the real energy demands will be in the interval bounded by the green dashed lines.

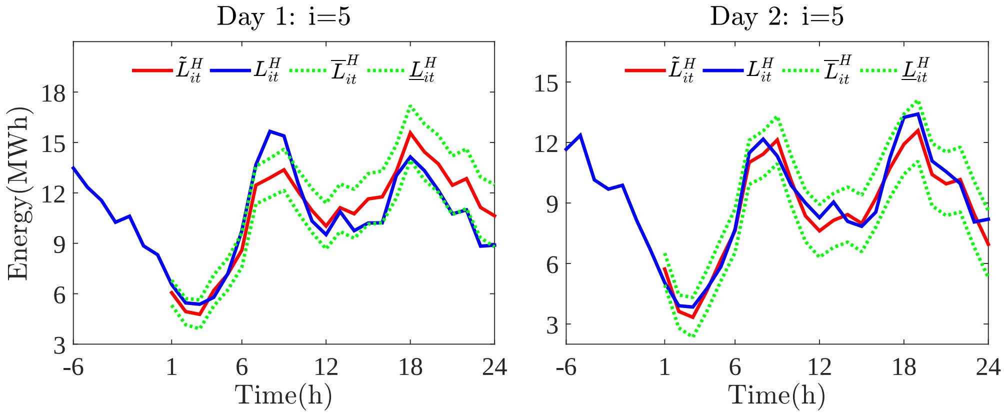


Figure 4.3 – Hourly nodal energy demand forecast results for bus 5

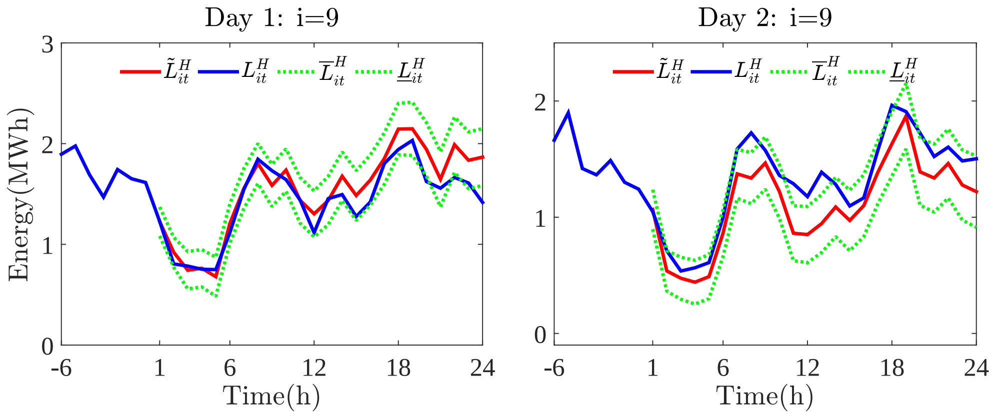


Figure 4.4 – Hourly nodal energy demand forecast results for bus 9

**Hourly nodal energy demands (H)**

To consider the power network constraints in energy and reserve scheduling problem, the load forecast for each substation of the system is needed. In this respect, the same ARIMA model is applied for the time series based on the load data of each substation separately. Figures 4.3-4.4 show the forecast results (indexed by "H") for the selected substations 5 and 9, receptively. For illustrative purpose, these buses are selected based on the level of energy demand. From geographical point of view, bus 5 is located in the heart of the railway network with high energy demand while bus 9 with low demand is located far from the traffic connections in the center.

Similar to the total energy demand forecast, the mean day error for each bus ($MDE_i^{\mathrm{H}}$) can be calculated by replacing the nodal hourly energy demand $L_{it}^{\mathrm{H}}$ and its forecast $\tilde{L}_{it}^{\mathrm{H}}$ in equation (4.8). The numerical results for all buses, are presented in table 4.1. Note that bus 2 has no load during the study period.

Table 4.1 – Mean day error for hourly nodal energy demand forecast

| Bus | 1 | 2 | 3 | 4 | 5 | 6 | 7 | 8 | 9 | 10 | 11 | 12 | 13 | 14 |
|---|---|---|---|---|---|---|---|---|---|---|---|---|---|---|
| Day1 | 0.24 | 0 | 0.24 | 0.71 | 0.11 | 0.15 | 0.04 | 0.06 | 0.17 | 0.15 | 0.3 | 0.2 | 0.32 | 0.27 |
| Day2 | 0.11 | 0 | 0.14 | 0.05 | 0.01 | 0.3 | 0.02 | 0.02 | 0.07 | 0.2 | 0.1 | 0.09 | 0.08 | 0.05 |

For uncertainty index, similar to $\xi_t^{\mathrm{HT}}$, we can define $\xi_{it}^{\mathrm{H}}$ which provides an estimation of the level of variation of the real load at bus $i$ from the forecast value during time period $t$. Figure 4.5 shows the calculated values of $\xi_{it}^{\mathrm{H}}$ for all buses as well as the values of $\xi_t^{\mathrm{HT}}$. From this numerical results two points can be observed.

First, the estimated level of variation of the energy demand (for both nodal and total forecasts) is a monotonous increasing function over time as formulated in 4.10. The reason is that the forecasts for the earlier times is relying more on the real data from the day before, while the forecast for the later times is relying more on the forecast of the earlier times which is less accurate in comparison to the real data.

$$\xi_{t_1}^{\mathrm{HT}} \leq \xi_{t_2}^{\mathrm{HT}} \Leftrightarrow t_1 \leq t_2 \tag{4.10a}$$

$$\xi_{it_1}^{\mathrm{H}} \leq \xi_{it_2}^{\mathrm{H}} \Leftrightarrow t_1 \leq t_2, \quad \forall i \tag{4.10b}$$

Second, for each time period $t$, the sum of the estimated level of error for each bus over all buses ($\sum_i \xi_{it}^{\mathrm{H}}$) is higher than the estimated level of error for the total energy demand forecast $\xi_t^{\mathrm{HT}}$ as formulated in 4.11. This is due to the fact that it is not expected to have the variation of energy demand for all buses in the same direction (all higher/lower than the forecast) at the same time. Note that the main source of the nodal energy demand variation is the change in the train movements program. The number of trains that are connected to the system during an hour is not changing significantly. Therefore, a higher demand in comparison to the forecast at a bus, which comes from the higher number of connected trains to that substation, leads to a lower demand in another bus.

$$\sum_i \xi_{it}^{\mathrm{H}} \geq \xi_t^{\mathrm{HT}}, \quad \forall t \tag{4.11}$$

**15 minutes total energy demands (QT)**

In this section the 15 minutes total energy demand forecast is investigated. The results of this load forecast analysis will be used in the construction of load uncertainty set considering

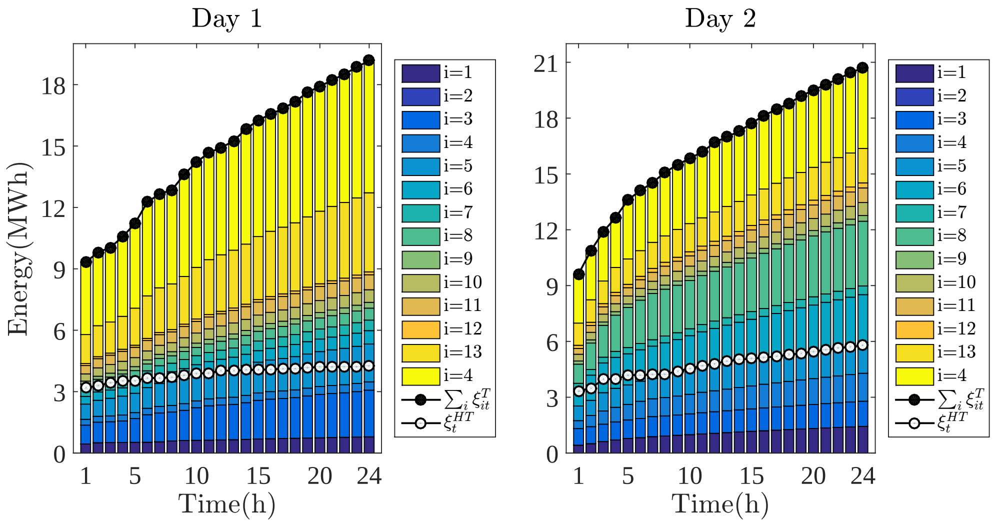


Figure 4.5 – Estimated level of error for nodal (bus1-bus14) and total hourly energy demand

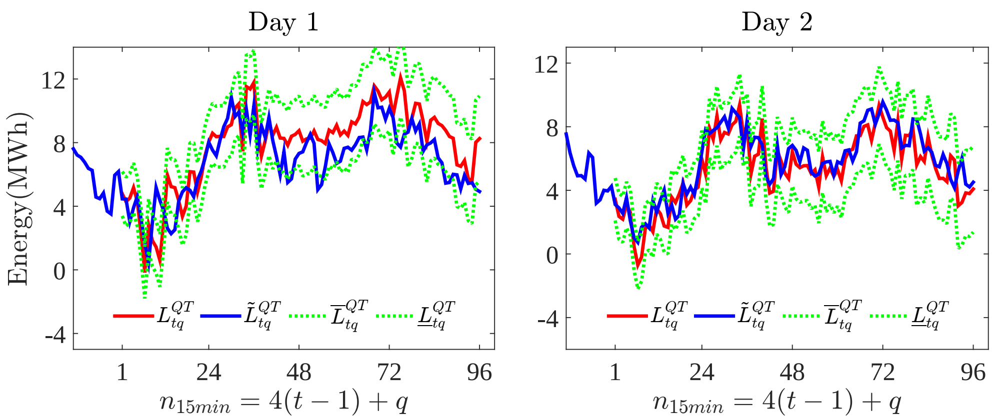


Figure 4.6 – 15 minutes total energy demand forecast results

the 15 minutes time step for the balancing stage. The forecast results (indexed by "QT") are provided in figure 4.6 where $L_{tq}^{QT}$ is the total energy demand during quarter $q^{\text{th}}$ ($q = 1,\ldots 4$) of time interval $t$ ($t = 1,\ldots 24$). Similar to the hourly total energy demand forecast, here $\tilde{L}_{tq}^{QT}$, $\overline{L}_{tq}^{QT}$ and $\underline{L}_{tq}^{QT}$ are the forecast value and upper and lower bounds of forecast confidence interval. Note that the forecast results are obtained based on a load time series with 15 minutes resolution. Therefore the x axis in figure 4.6 is labeled by the element number of this time series ($n_{15min}$). For each 15 minutes time interval ($q^{\text{th}}$ quarter of time $t$), the corresponding time series element number is $n_{15min} = 4(t-1)+q$.

The mean day error based on 15 minutes forecast data can be calculated in two ways. The first formulation is based on summing up the relative forecast error for each 15 minutes element as presented in (4.12a). The second formulation (4.12b) is based on first summing up the

Table 4.2 – Mean day error for 15 minutes total energy demand forecast

| | $MDE^{\text{QT(1)}}$ | $MDE^{\text{QT(2)}}$ |
|---|---|---|
| Day 1 | 31.0% | 20.7% |
| Day 2 | 18.8% | 11.4% |

forecast values during each hour to calculate the hourly energy demand and then summing up the relative error of hourly energy demand forecast over 24 hours as formulated in (4.12b). The obtained mean daily error using equations (4.12a) and (4.12a) are provided in table 4.2.

$$MDE^{\text{QT(1)}} = \frac{1}{96}\sum_t\sum_q \left|\frac{L^{\text{HQ}}_{tq} - \tilde{L}^{\text{HQ}}_{tq}}{L^{\text{HQ}}_{tq}}\right| \tag{4.12a}$$

$$MDE^{\text{QT(2)}} = \frac{1}{24}\sum_t \left|\frac{L^{\text{HT}}_{t} - \sum_q \tilde{L}^{\text{HQ}}_{t}}{L^{\text{HT}}_{t}}\right| \tag{4.12b}$$

Next, we investigate the 15 minutes forecast error uncertainty index ($\xi^{\text{QT}}_{tq}$). Similar to the hourly forecast error index, $\xi^{\text{QT}}_{tq}$ is an estimation of the level of variation of the real load during quarter $q^{\text{th}}$ of time interval $t$. Figure 4.7 shows the calculated values of $\xi^{\text{QT}}_{tq}$ for each 15 minutes period as well as the values of $\xi^{\text{HT}}_{t}$ for each hour.

From this numerical results it can be observed that for each time period $t$, the sum of the estimated level of error for each intra 15 minutes period ($\sum_q \xi^{\text{QT}}_{tq}$) is higher than the estimated level of error for the hourly total energy demand forecast $\xi^{\text{HT}}_{t}$ as formulated in (4.13). This is due to the fact that it is not expected to have the variation of energy demand for all 15 minutes period inside an hour in the same direction. The main source of 15 minutes energy demand variation is the unexpected delays in the train movement programs. Therefore an increment in a 15 minute period energy demand leads to a decrement in the next 15 minute period energy demand.

$$\sum_q \xi^{\text{QT}}_{tq} \geq \xi^{\text{HT}}_{t}, \quad \forall t \tag{4.13}$$

### 15 minutes nodal energy demands (Q)

In this section an ARIMA model based on 15 minutes time series is applied to forecast the 15 minutes energy demand of each substation. Forecast results (Indexed by "Q") are shown

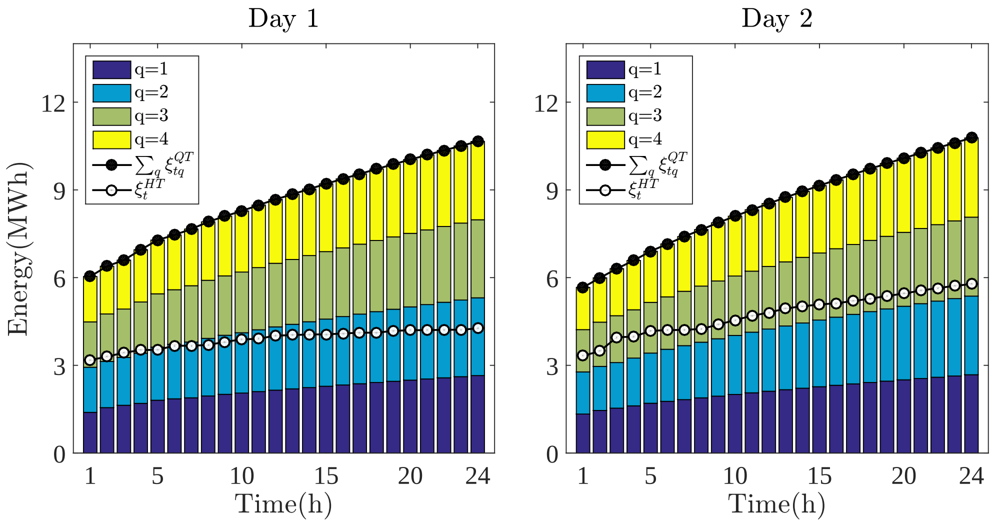


Figure 4.7 – Estimated level of error for 15 minutes and hourly total energy demands

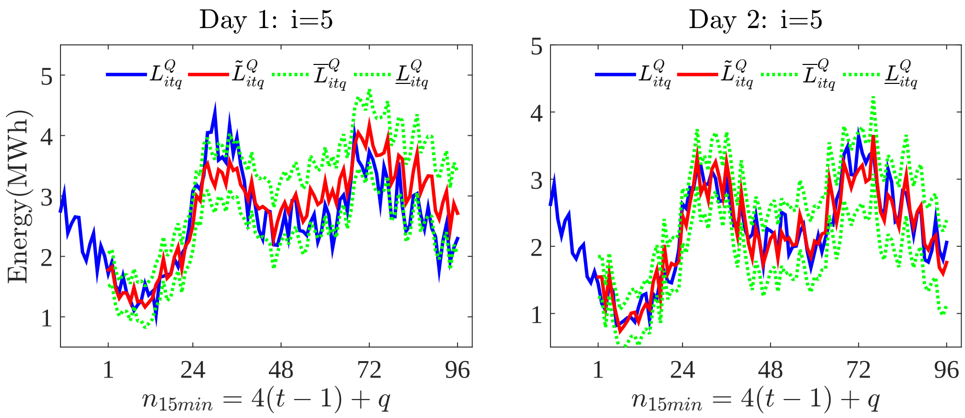


Figure 4.8 – 15 minutes nodal energy demand forecast results for bus 5

in figures 4.8-4.9 for the selected buses 5 and 9. The uncertainty index $\xi_{itq}^{\mathrm{Q}}$ which is an estimation of the level of variation of the real load at bus $i$ from the forecast value during quarter $q^{\mathrm{th}}$ of time interval $t$ can be analyzed from two aspects, namely, spatial and temporal aspects. From spatial aspect, the sum of the $\xi_{itq}^{\mathrm{Q}}$ over all buses is higher than the uncertainty index for the 15 minutes total energy demand ($\xi_{tq}^{\mathrm{QT}}$) as formulated in (4.14a) and depicted in figure 4.10 for all time periods. From temporal aspect, the sum of $\xi_{itq}^{\mathrm{Q}}$ over all 15 minutes period of each hour, for each bus is higher than uncertainty index for hourly energy demand of that bus ($\xi_{it}^{\mathrm{QH}}$) as formulated in (4.14b). This temporal error correlation which is valid for all buses, is depicted in figures 4.11-4.12 for the selected buses 5 and 9, respectively.

$$\sum_i \xi_{itq}^{\mathrm{Q}} \geq \xi_{tq}^{\mathrm{QT}}, \quad \forall q, \forall t \tag{4.14a}$$

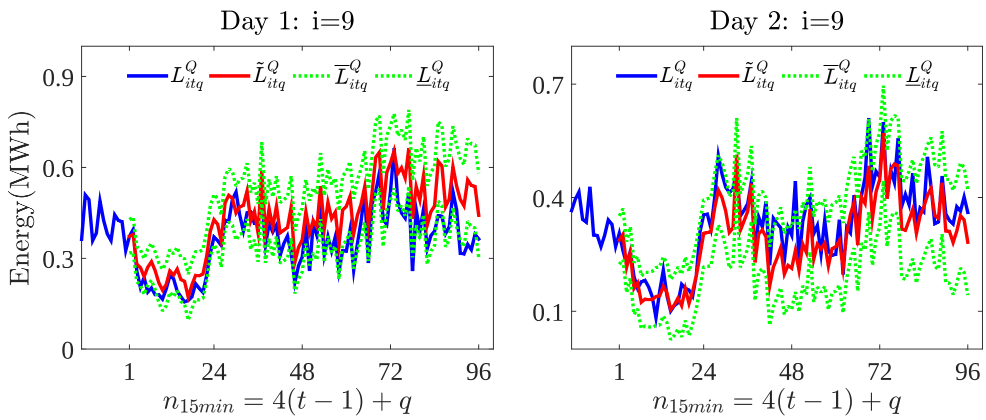


Figure 4.9 – 15 minutes nodal energy demand forecast results for bus 9

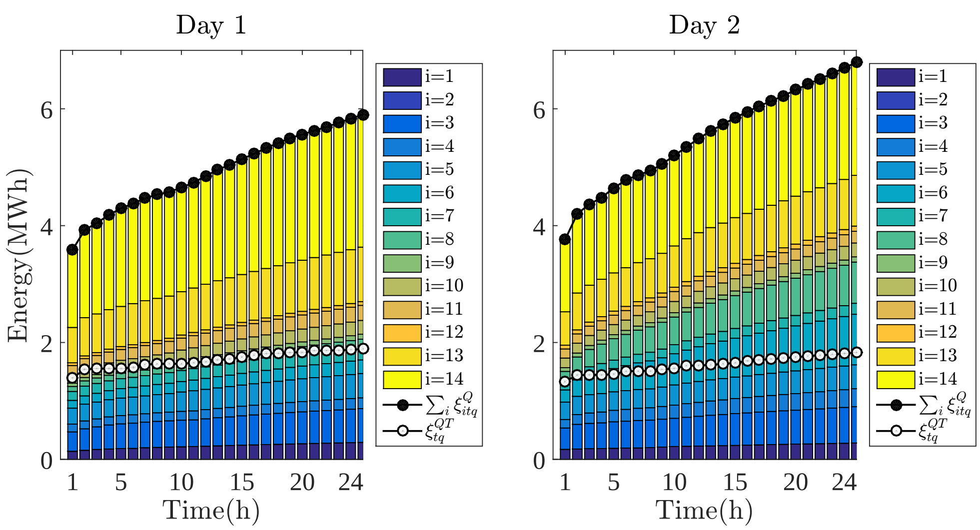


Figure 4.10 – Estimated level of error for nodal (bus1-bus14) and total 15 minutes energy demand

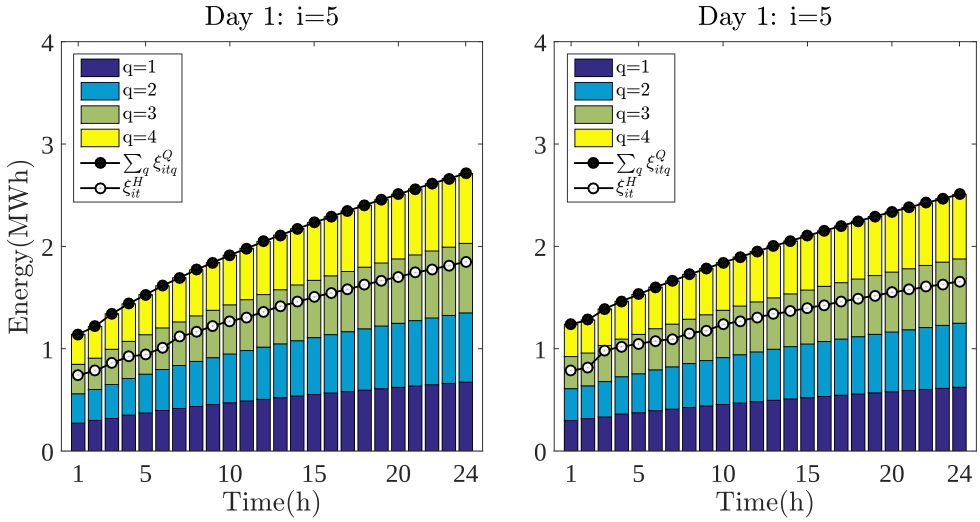


Figure 4.11 – Estimated level of error for 15 minutes and hourly nodal energy demand for bus 5

$$\sum_q \xi^{\mathrm{Q}}_{itq} \geq \xi^{\mathrm{H}}_{it}, \quad \forall i, \forall t \tag{4.14b}$$

## 4.3 Two-stage Scheduling Problem Formulation

In this section, we propose the mathematical formulation dealing with the energy and reserve scheduling for the ERC. The proposed formulation follows the energy and reserve provision framework which is presented in chapter 3. In this respect, a two stage optimization model is introduced.

The first (dispatching) stage deals with day-ahead decision variables. For each generator and interconnecting converter, day-ahead decision variables includes the hourly output power set point, part of provided reserve to be used for the ERC's frequency control system and part of provided reserve to be sold in the reserve market. The time step for the decision variables at this stage is one hour.

The second (balancing) stage, deals with the real time decision variables. For each generator and interconnecting converter, real time decision variables includes the activation of the provided reserve in the both upward and downward directions. These decision variables make the ERC operator enable to manage the energy demand variations from the forecast values. Moreover, a set of load shedding variables are introduced in this stage to ensure the feasibility of the second stage problem in case of strong demand fluctuations. Following the energy balancing structure as described in section 3.2, the time step for balancing stage decision

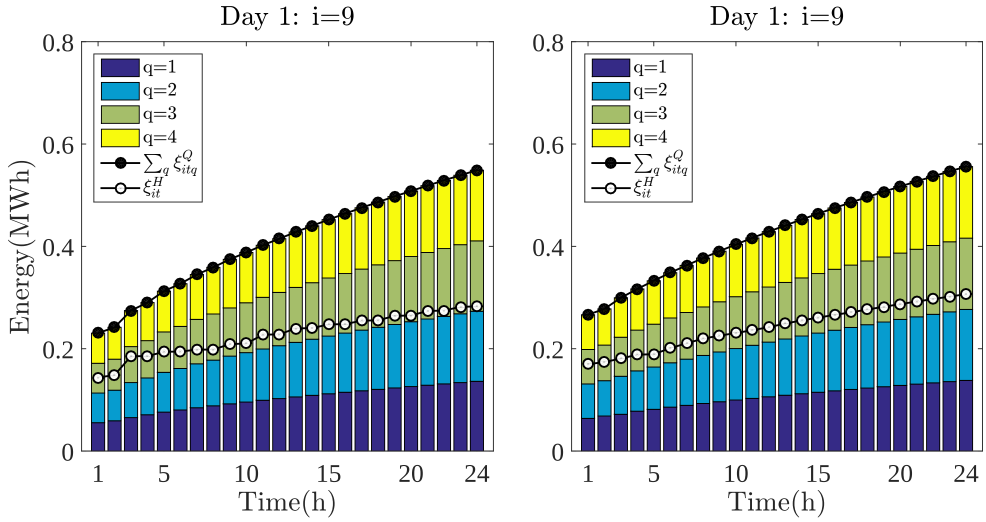


Figure 4.12 – Estimated level of error for 15 minutes and hourly nodal energy demand for bus 9

variables is 15 minutes.

It should be noted that the problem is modeled in a way to have only continuous variables with linear constraints in the second stage problem. Hence, the adaptive robust optimization problem derived from this two stage problem can be effectively solved.

### 4.3.1 First Stage (Dispatching) Formulation

The first stage (dispatching) cost minimization problem can be formulated as the following MILP problem (4.15).

$$\min_{\mathbf{x}} \sum_t \sum_h (c^{SU}_{ht} + C_h p_{ht} + C^+_h r^+_{ht} + C^-_h r^-_{ht}) - \sum_t (\pi^+_t r^{\text{sell}^+}_t + \pi^-_t r^{\text{sell}^-}_t) - \sum_t \sum_k \pi^{\text{p}}_t p^{\text{c}}_{kt} \tag{4.15a}$$

$$\text{s.t.} \quad \sum_{h\in\mathcal{G}_i} p_{ht} - \sum_{k\in\mathcal{C}_i} p^{\text{c}}_{kt} = L_{it} + \sum_{j\in\mathcal{N}_i} B_{ij}(\delta^0_{jt} - \delta^0_{it}), \quad \forall i, \forall t \tag{4.15b}$$

$$c^{SU}_{ht} \geq C^{SU}_h (u_{ht} - u_{h,t-1}), \quad \forall h, \forall t \geq 1 \tag{4.15c}$$

$$c^{SU}_{h,1} \geq C^{SU} u_{h,1}, \quad \forall h \tag{4.15d}$$

$$c^{SU}_{ht} \geq 0, \quad \forall h, \forall t \tag{4.15e}$$

$$|B_{ij}(\delta^0_i - \delta^0_{jt})| \leq T^{\max}_{ij}, \quad \forall (i,j), \forall t \tag{4.15f}$$

$$\delta^0_{1,t} = 0, \quad \forall t \tag{4.15g}$$

$$p_{ht}, r^+_{ht}, r^-_{ht} \geq 0, \quad \forall h, \forall t \tag{4.15h}$$

$$p_{ht} + r^+_{ht} \leq P^{\max}_h u_{ht}, \quad \forall h, \forall t \tag{4.15i}$$

$$p_{ht} - r^-_{ht} \geq P^{\min}_h u_{ht}, \quad \forall h, \forall t \tag{4.15j}$$

$$-R_h^{\text{down}} \le p_{ht} - p_{h,t-1} \le R_h^{\text{up}}, \quad \forall h, \forall t \ge 1 \tag{4.15k}$$

$$r_{kt}^{\text{c}^+}, r_{kt}^{\text{c}^-} \ge 0, \quad \forall k, \forall t \tag{4.15l}$$

$$p_{kt}^{\text{c}} + r_{kt}^{\text{c}^+} \le P_k^{\text{c}^{\max}}, \quad \forall k, \forall t \tag{4.15m}$$

$$p_{kt}^{\text{c}} - r_{kt}^{\text{c}^-} \ge -P_k^{\text{c}^{\max}}, \quad \forall k, \forall t \tag{4.15n}$$

$$0 \le r_t^{\text{sell}^+} \le \min\left\{ \sum_{k\in C_i} (r_{kt}^{\text{c}^+} - r_{kt}^{\text{dc}^+}), \sum_{h\in G_i} (r_{ht}^{+} - r_{ht}^{\text{d}+}) \right\}, \quad \forall t \tag{4.15o}$$

$$0 \le r_t^{\text{sell}^-} \le \min\left\{ \sum_{k\in C_i} (r_{kt}^{\text{c}^-} - r_{kt}^{\text{dc}^-}), \sum_{h\in G_i} (r_{ht}^{-} - r_{ht}^{\text{d}-}) \right\}, \quad \forall t \tag{4.15p}$$

$$v_{mt} = v_{m,t-1} + \xi_{mt} + \sum_{h\in H_m^{\text{in}}} (w_{ht}^{\text{d}} + w_{ht}^{\text{s}}) - \sum_{h\in H_m^{\text{out}}} (w_{ht}^{\text{d}} + w_{ht}^{\text{s}}), \quad \forall m, \forall t \tag{4.15q}$$

$$v_{m,0} = V_m^0, \quad \forall m, \forall t \tag{4.15r}$$

$$V_m^{\min} \le v_{mt} \le V_m^{\max}, \quad \forall m, \forall t \tag{4.15s}$$

$$w_{ht}^{\text{d}} + w_{ht}^{\text{s}} \le W_h^{\max}, \quad \forall m, \forall t \tag{4.15t}$$

$$w_{ht}^{\text{d}}, w_{ht}^{\text{s}} \ge 0, \quad \forall m, \forall t \tag{4.15u}$$

$$p_{ht} = \eta_h w_{ht}^{\text{d}} - P_h^{\text{fix}} u_{ht} \ge 0, \quad \forall m, \forall t \tag{4.15v}$$

The optimization variables of the problem are defined as:

$$\mathbf{x} = \{u_{ht}, p_{ht}, r_{ht}^{+}, r_{ht}^{-}, r_{ht}^{\text{d}+}, r_{ht}^{\text{d}-}, c_{ht}^{SU}, p_{kt}^{\text{c}}, r_{kt}^{\text{c}^+}, r_{kt}^{\text{c}^-}, r_{kt}^{\text{dc}^+}, r_{kt}^{\text{dc}^-}, r_t^{\text{sell}^+}, r_t^{\text{sell}^-}, \delta_{it}, w_{ht}^{\text{d}}, w_{ht}^{\text{s}}, v_{mt}\}$$

This set of variables includes the energy and reserve schedule of all the generators and interconnecting converters, the state (voltage angle) of the transmission network buses as well as water flow and reservoir water level variables for the cascaded hydroelectric power plants.

The objective function (4.15a) is to minimize the cost of the ERC over the scheduling period. It includes the operational cost of the ERC's generators (first term) minus the revenue from selling upward and downward tertiary reserves in the reserve market (second term) plus/minus the cost/revenue of buying/selling energy from/to the energy market through the converters (third term)[1]. Here, the positive or negative sign of $p_{kt}^{\text{c}}$ denotes that ERC sells or buys energy through converter $k$ at time $t$, respectively. The operational cost of hydro power plants includes the start up cost plus the linearised cost of energy and reserve provision.

The set of constraints (4.15b)-(4.15v) are binding the objective function (4.15a). Constraints (4.15c)-(4.15e) models the start up cost of the hydroelectric power plants. The constraints (4.15b) enforce the power balance for all buses of the ERC transmission system. The power

[1]It is assumed that the price of selling and buying energy are identical. In practice, there could be different prices for buying and selling energy considering the transmission grid tariff on the public grid side.

flow in the transmission line is simply modeled using the voltage angle of terminal buses of the line (DC load flow model), so constraints (4.15f) represent the transmission lines flow limits. Moreover, the constraint (4.15g) considers bus number 1 as the reference for the angle of the voltage. The set of constraints (4.15h)-(4.15j) model the generator operating point limits as well as the upward and downward ramp rate limits. The constraints (4.15l)-(4.15n) set the limits on the operating point of the converters.

The amount of the tertiary reserve that the ERC can sell to the reserve market is not only limited by the sum of the available capacity in the interconnecting converters minus the part of reserve capacity that would be used for the internal frequency control but also limited by the reserve provision of the ERC's generators minus the internal reserve demand of the ERC (4.15o)-(4.15p).

The set of constraints (4.15q)-(4.15v) models the cascaded hydro power plants. The constraints (4.15q) set the water level of the reservoirs at the end of time interval $t$ equal to the water inflow/outflow during time interval $t$ plus the water level of the reservoir at the end of time interval $t-1$. In this equation, it is assumed that the time required for the water discharged from one reservoir to reach its direct down stream reservoir, is negligible in comparison with the time step of the problem (one hour). The constraint (4.15r) set the initial value for the variables of water level of the reservoirs. The constraints (4.15s) set the maximum and minimum allowable volume of water in the reservoirs during the scheduling period. The constraints (4.15t)-(4.15u) limit the water discharge and water spillage variables. Finally, equality constraint (4.15v) connect the hydroelectric power generation variables to the turbined water flow variables. In this equation the parameter of the water flow to power conversion rate ($\eta_h$) is the product of the efficiency of the hydro turbine, the height of the dam and the specific weight of water.

In summary, the first stage dispatching problem can be formulated in a matrix form as presented in (4.16).

$$\min_{\mathbf{x}} \mathbf{c_x x} \tag{4.16a}$$

$$\text{s.t.} \quad \mathbf{Ax} = \mathbf{L} \tag{4.16b}$$

$$\mathbf{Gx} \leq \mathbf{g} \tag{4.16c}$$

where $\mathbf{c_x}$ is the matrix of cost coefficients in the objective function (4.15a). Constraints (4.16b) represents the nodal power balance equations (4.15b). Note that $\mathbf{L}$ is the vector of forecast energy demand at substations ($\mathbf{L} = \{L_{it} : \forall i, \forall t, \forall q,\}$). Finally, the set of technical constraints (4.15c)-(4.15v) are represented by the inequality constraint (4.16c).

### 4.3.2 Second Stage (Balancing) Formulation

The second stage (balancing or redispatching) problem can be formulated as (4.17).

$$\min_{\mathbf{y}} \sum_{t,q}\sum_{h} C_h(p^{+}_{htq} - p^{-}_{htq}) + \sum_{i,t,q} C^{\mathrm{sh}} l^{\mathrm{sh}}_{itq} + \sum_{t,q}\sum_{k}(\pi^{\mathrm{long}}_{t} p^{\mathrm{c}^{+}}_{ktq} + \pi^{\mathrm{short}}_{t} p^{\mathrm{c}^{-}}_{ktq}) \tag{4.17a}$$

$$\text{s.t.} \quad \sum_{h\in G_i}(p^{+}_{htq} - p^{-}_{htq}) + \sum_{k\in C_i}(p^{\mathrm{c}^{+}}_{ktq} - p^{\mathrm{c}^{-}}_{ktq}) + l^{\mathrm{LS}}_{itq} - \sum_{j\in N_i} B_{ij}(\delta_{itq} - \delta^{0}_{it} - \delta_{jtq} + \delta^{0}_{jtq}) = \Delta l_{itq}, \quad \forall i, \forall t, \forall q \tag{4.17b}$$

$$|B_{ij}(\delta_{itq} - \delta_{jtq})| \le T^{\max}_{ij}, \quad \forall (i,j), \forall t, \forall q \tag{4.17c}$$

$$\delta_{1,tq} = 0, \quad \forall t, \forall q \tag{4.17d}$$

$$p^{+}_{htq}, p^{-}_{htq}, p^{\mathrm{c}^{+}}_{kt}, p^{\mathrm{c}^{-}}_{kt} \ge 0, \quad \forall h, \forall t, \forall q \tag{4.17e}$$

$$p^{+}_{htq} \le \overline{p}^{+}_{ht}, \quad \forall h, \forall t, \forall q \tag{4.17f}$$

$$p^{-}_{htq} \le \overline{p}^{-}_{ht}, \quad \forall h, \forall t, \forall q \tag{4.17g}$$

$$p^{\mathrm{c}^{+}}_{ktq} \le \overline{p}^{\mathrm{c}^{+}}_{kt}, \quad \forall k, \forall t, \forall q \tag{4.17h}$$

$$p^{\mathrm{c}^{-}}_{ktq} \le \overline{p}^{\mathrm{c}^{+}}_{kt}, \quad \forall k, \forall t, \forall q \tag{4.17i}$$

The optimization variables of the problem are defined as $\mathbf{y} = \{p^{+}_{htq}, p^{-}_{htq}, p^{\mathrm{c}^{+}}_{ktq}, p^{\mathrm{c}^{-}}_{ktq}, \delta_{itq}, l^{\mathrm{LS}}_{itq}\}$. This set of variables includes the energy redispatch of all the generators and interconnecting converters as well as the state of the transmission network buses in the second stage (balancing).

The objective function (4.17a) is to minimize the cost of energy balancing. It includes the cost of redispatching ERC's generators plus the the cost of imbalances through the converters (second term). Here, the aim of balancing is to follow the energy demand variation during each quarter of hour ($\Delta l_{itq}$) as presented in the set of constraints (4.17b). Moreover the set of constraints (4.17b) -(4.17d) are modeling the DC power flow and the transmission flow limits in the balancing stage. The energy redispatching variables ($p^{+}_{ht}, p^{-}_{ht}, p^{\mathrm{c}^{+}}_{kt}, p^{\mathrm{c}^{-}}_{kt}$) are limited by the first stage decisions on the internal reserve provision ($r^{\mathrm{d}+}_{ht}, r^{\mathrm{d}-}_{ht}, r^{\mathrm{dc}^{+}}_{kt}, r^{\mathrm{dc}^{-}}_{kt}$) as presented in (4.17f) -(4.17i). Note that the amount of upper bound of upward/downward energy redispatch for generators and converters ($\overline{p}^{+}_{ht}, \overline{p}^{-}_{ht}, \overline{p}^{\mathrm{c}^{+}}_{kt}, \overline{p}^{\mathrm{c}^{-}}_{kt}$) depend on the amount of corresponding provided reserves in the first stage problem. For instance, for the hydro power unit $h$, the provided upward reserve for ERC internal frequency control is equal to $r^{\mathrm{d}+}_{ht}$. Therefore, the maximum available upward redispatching energy for this generator for each 15 minutes period $q$ during time interval $t$ is:

$$\overline{p}^{+}_{ht}(\mathrm{MWh}) = r^{\mathrm{d}+}_{ht}(\mathrm{MW}) \times 15(\mathrm{min}) = \frac{r^{\mathrm{d}+}_{ht}}{4}\mathrm{MWh} \quad \forall \mathrm{t}, \forall \mathrm{q} \tag{4.18}$$

The upper bounds of upward and downward redispatch energy for all generators and interconnecting converters follow similar formulation as below:

$$\overline{p}^{+}_{ht}(\text{MWh}) = \frac{r^{\text{d}+}_{ht}}{4}(\text{MWh}) \quad \forall h, \forall t, \forall q \tag{4.19a}$$

$$\overline{p}^{-}_{ht}(\text{MWh}) = \frac{r^{\text{d}-}_{ht}}{4}(\text{MWh}) \quad \forall h, \forall t, \forall q \tag{4.19b}$$

$$\overline{p}^{\text{c}^+}_{kt}(\text{MWh}) = \frac{r^{\text{dc}^+}_{kt}}{4}(\text{MWh}) \quad \forall k, \forall t, \forall q \tag{4.19c}$$

$$\overline{p}^{\text{c}^-}_{kt}(\text{MWh}) = \frac{r^{\text{dc}^-}_{kt}}{4}(\text{MWh}) \quad \forall k, \forall t, \forall q \tag{4.19d}$$

Finally, similar to the first stage problem, the second stage balancing problem can be formulated in a matrix form as (4.20).

$$\min_{\mathbf{y}} \mathbf{c_y y} \tag{4.20a}$$

$$\text{s.t.} \quad \mathbf{Py} + \mathbf{Qx} = \Delta\mathbf{L} \tag{4.20b}$$

$$\mathbf{Ny} + \mathbf{Mx} \leq \mathbf{d} \tag{4.20c}$$

where $\mathbf{c_y}$ is the matrix of cost coefficients in the objective function (4.17a). Constraints (4.20b) represents the nodal power balance equations (4.17b). Note that $\Delta\mathbf{L}$ is the vector of the variations of energy demand of substations from the forecast vaslues ($\Delta\mathbf{L} = \{\Delta l_{itq} : \forall i, \forall t, \forall q,\}$). Finally the set of technical constraints (4.17c)-(4.17i) are represented by the inequality constraint (4.20c).

Note that in the second stage problem, the values of the first stage decision variables $\mathbf{x}$ are given. In fact, the first and the second stage problems are meaningful while each problem consider the other one. In the next sections of this chapter, we propose adaptive robust optimization and stochastic optimization approaches for dealing with uncertainties on the presented two stage scheduling problem.

## 4.4 Adaptive Robust Optimization Approach

Robust optimization (RO) has recently gained lots of attention in power system as a modeling framework for optimization under uncertainty. The RO models require only moderate information about the underlying uncertainty, such as the mean and the range of the uncertain data. Moreover, the robust model construct an optimal solution that is immune against all realization of the uncertain data within the deterministic uncertainty set. This robustness is desirable for electric railway power systems where the penalty associated with the infeasible solution is very high. Hence the concept of robust optimization is consistent with the risk-averse fashion in which the electric railway power systems are operated.

In this section we first propose an appropriate uncertainty set, which is a key building block of the robust model. Then the adaptive robust optimization formulation is proposed in section 4.4.2 to model the two stage scheduling problem under uncertainties. To obtain the robust solution, in the second stage problem, we are looking for the minimum re-dispatching (balancing) cost while the energy demand variation at each bus is varying within the uncertainty set in a way to maximally affect the objective function. The solution methods based on dual and primal cutting plane algorithms are discussed in Appendix A. Finally, a realistic case study is presented in section 4.4.3 to demonstrate the effectiveness of the proposed adaptive robust optimization method.

### 4.4.1 Uncertainty Set

In robust optimization, uncertainty is modeled through uncertainty sets, which are the building blocks of a robust optimization model and have direct impact on its performance. A well constructed uncertainty set should 1) capture the most significant aspects of the underlying uncertainty, 2) balance robustness and conservativeness of the robust solution, and 3) be computationally tractable[79].

A simple uncertainty set to cover uncertainties in the 15 minutes energy demand forecast error can be constructed based on the confidence interval of the 15 minutes nodal energy demand forecast error as presented in (4.21).

$$-\xi^{\mathrm{Q}}_{itq} \leq \Delta l_{itq} \leq \xi^{\mathrm{Q}}_{itq}, \quad \forall i, \forall t, \forall q \tag{4.21}$$

Here the variation of the 15 minutes energy demand of bus $i$ during quarter $q$ of time interval $t$ ($\Delta l_{itq}$)can vary with in $[-\xi^{\mathrm{Q}}_{itq}, \xi^{\mathrm{Q}}_{itq}]$. Assume that $\xi^{\mathrm{Q}}_{itq}$ is obtained based on 95% confidence interval, the uncertainty set (4.21) covers all the variation of real energy demand from the forecast value with 95% level of confidence.

To control the level of robustness of the solution against this 15 minutes nodal load variation, we introduce the control parameter $\Gamma^{\mathrm{Q}}$ ($0 \leq \Gamma^{\mathrm{Q}} \leq 1$) as presented in (4.22), where the higher value of $\Gamma^{\mathrm{Q}}$ corresponds to more robust solution.

$$-\Gamma^{\mathrm{Q}}\xi^{\mathrm{Q}}_{itq} \leq \Delta l_{itq} \leq \Gamma^{\mathrm{Q}}\xi^{\mathrm{Q}}_{itq}, \quad \forall i, \forall t, \forall q \tag{4.22}$$

Referring to load forecast error analysis presented in section 4.2, we can say that the above uncertainty set (4.22) is too conservative. In fact, it is not expected that all the error of 15 minutes energy demand forecasts are realized in the same direction over the time and for all buses of the system. Therefore, to consider both the temporal and spatial correlation between 15 minutes nodal energy demand forecast error at the ERC substations, we propose the following uncertainty set (eq: uncertainty set).

$$-\Gamma^{\mathrm{Q}}\xi^{\mathrm{Q}}_{itq} \leq \Delta l_{itq} \leq \Gamma^{\mathrm{Q}}\xi^{\mathrm{Q}}_{itq}, \quad \forall i, \forall t, \forall q \tag{4.23a}$$

$$-\Gamma^{\mathrm{H}}\xi^{\mathrm{H}}_{it} \leq \sum_{q} \Delta l_{itq} \leq \Gamma^{\mathrm{H}}\xi^{\mathrm{H}}_{it}, \quad \forall i, \forall t \tag{4.23b}$$

$$-\Gamma^{\mathrm{QT}}\xi^{\mathrm{T}}_{tq} \leq \sum_{i} \Delta l_{itq} \leq \Gamma^{\mathrm{QT}}\xi^{\mathrm{QT}}_{tq}, \quad \forall t, \forall q \tag{4.23c}$$

The above uncertainty set (4.23) includes all the three characteristic of an appropriate uncertainty set. First, the parameter $\Gamma^{\mathrm{Q}}$ controls the level of robustness of the solution against the variation of energy demand at each substation during 15 minutes periods. Then, equation (4.23b) captures the temporal correlation in the energy demand variations. Here, the uncertainty index $\xi^{\mathrm{H}}_{it}$ based on confidence interval for the error of the hourly nodal energy demand forecast at bus $i$ as described in section 4.2. Note that the "one hour" summation period is chosen based on the hourly periodical characteristic of train time tables. Finally equation (4.23c) captures the spatial correlation between energy demand variations in different buses where $\xi^{\mathrm{TQ}}_{tq}$ is obtained based on the confidence interval of the 15 minute total energy demand forecast error.

In other words, the parameters $\Gamma^{\mathrm{H}}$ and $\Gamma^{\mathrm{TQ}}$ controls the level of robustness against the total energy demand variations during each 15 minutes period and hourly energy demand variations at each bus, receptively. The uncertainty set can be presented in a general matrix form, as below, for the purpose of incorporation in the adoptive optimization formulation.

$$\mathbf{B}\boldsymbol{\Delta}\mathbf{L} \leq \mathbf{b} \tag{4.24}$$

### 4.4.2 Problem Formulation

To obtain the robust solution, in the second stage problem we are looking for the minimum re-dispatching (balancing) cost while the energy demand variation of each bus is varying, within the above uncertainty set, in a way to maximally affect the objective function. The compact form of the adoptive robust problem can be formulated as (4.25).

$$\min_{\mathbf{x}} \mathbf{c_x x} + \max_{\boldsymbol{\Delta}\mathbf{L}} \; \min_{\mathbf{y}} \mathbf{c_y y} \tag{4.25a}$$

$$\text{s.t.} \quad \mathbf{Py} + \mathbf{Qx} = \Delta\mathbf{L} \qquad : \boldsymbol{\lambda} \tag{4.25b}$$

$$\mathbf{Ny} + \mathbf{Mx} \leq \mathbf{d} \qquad : \boldsymbol{\mu} \tag{4.25c}$$

$$\text{s.t.} \quad \mathbf{B\Delta L} \leq \mathbf{b} \tag{4.25d}$$

$$\text{s.t.} \quad \mathbf{Ax} = \mathbf{L} \tag{4.25e}$$

$$\mathbf{Gx} \leq \mathbf{g} \tag{4.25f}$$

Since the min-max-min problem cannot be immediately employed in practice, we should convert the inner problem from max-min structure to max-max structure. In this respect, we substitute the right hand side minimization problem (second stage problem (4.20)) with its dual. The reformulated problem is presented in (4.26).

$$\min_{\mathbf{x}} \mathbf{c_x x} + \max_{\mathbf{\Delta L}} \ \max_{\boldsymbol{\lambda},\boldsymbol{\mu}} \boldsymbol{\lambda}^{\mathrm{T}}(\mathbf{\Delta L} - \mathbf{Qx}) + \boldsymbol{\mu}^{\mathrm{T}}(\mathbf{d} - \mathbf{Mx}) \tag{4.26a}$$

$$\text{s.t.} \quad \mathbf{P}^{\mathrm{T}}\boldsymbol{\lambda} + \mathbf{N}^{\mathrm{T}}\boldsymbol{\mu} = \mathbf{c}_{\mathbf{y}}^{\mathrm{T}} \tag{4.26b}$$

$$\mu \leq \mathbf{0} \tag{4.26c}$$

$$\text{s.t.} \quad \mathbf{B\Delta L} \leq \mathbf{b} \tag{4.26d}$$

$$\text{s.t.} \quad \mathbf{Ax} = \mathbf{L} \tag{4.26e}$$

$$\mathbf{Gx} \leq \mathbf{g} \tag{4.26f}$$

By merging the right hand and mid maximization problems, we could obtain the solvable problem (4.27).

$$\min_{\mathbf{x}} \mathbf{c_x x} + \max_{\mathbf{\Delta L},\boldsymbol{\lambda},\boldsymbol{\mu}} \boldsymbol{\lambda}^{\mathrm{T}}(\mathbf{\Delta L} - \mathbf{Qx}) + \boldsymbol{\mu}^{\mathrm{T}}(\mathbf{d} - \mathbf{Mx}) \tag{4.27a}$$

$$\text{s.t.} \quad \mathbf{P}^{\mathrm{T}}\boldsymbol{\lambda} + \mathbf{N}^{\mathrm{T}}\boldsymbol{\mu} = \mathbf{c}_{\mathbf{y}}^{\mathrm{T}} \tag{4.27b}$$

$$\mu \leq \mathbf{0} \tag{4.27c}$$

$$\mathbf{B\Delta L} \leq \mathbf{b} \tag{4.27d}$$

$$\text{s.t.} \quad \mathbf{Ax} = \mathbf{L} \tag{4.27e}$$

$$\mathbf{Gx} \leq \mathbf{g} \tag{4.27f}$$

It should be noted that here the right hand maximization problem, is a bilinear problem since it includes the cross product of the optimization variables $\boldsymbol{\lambda}$ and $\mathbf{\Delta L}$.

Referring to the min-max problem (4.27), it can be observed that:

1. The right hand maximization problem is bilinear and defined over a polyhedral set. As a result, the optimal solution of this maximization problem is on one of the vertixes of this set.

2. The day ahead decision variables **x** only appears in the objective function and not in the constraints. Therefore, the feasible polyhedron of the inner maximization problem is independent of the day ahead decisions and consequently has a finite number of vertexes.

Note that problem (4.27) is computationally solvable. Several solution algorithms such as bender decomposition techniques and primal cut algorithm are proposed in the literature to solve a general min-max problem. Two solution algorithm, namely, the dual- bender cutting-plane algorithm and the primal cut algorithm are presented in Appendix A. A discussion on the tractability of these solution algorithms is also provided in Appendix A. In short, the dual-bender cutting-plane algorithm is more appropriate for solving the min-max problem (4.27) considering a huge number of vertexes derived from the uncertainty set (4.23).

### 4.4.3 Case Study

To demonstrate the effectiveness of the proposed method, a case study based on the characteristic of the Swiss ERPS in the western part of Switzerland is addressed.

The transmission system of the ERC has 14 substations (132 KV) which are connected through 16 transmission lines as depicted in Fig. 4.1. The ERC has three cascaded hydro power plants, whose their water reservoirs are connected to each other through one connecting river. The hydro power plants and reservoirs data are presented in table 4.3 and table 4.4, respectively. Two bidirectional static frequency converters connect ERPS to the public power grid at bus 3 and 11. The rated power of the converters ($P_k^{c^{max}}$) are 16 MW and 24 MW, respectively.

The load data of the system are obtained from load forecast analysis presented in section 4.2.2 for the second day (October 19, 2013). The day ahead and energy imbalance prices as well as the reserve market prices are presented in 4.13. To find the day ahead energy and reserve schedule, problem (4.27) is solved using the benders-dual cutting-plane algorithm presented in Appendix A.2. The algorithm is implemented under GAMS[2] [80] environment and it took 19.3s on a 3.4 GHz Windows machine to solve the problem.

[2]GAMS: General Algebraic Modeling System

Table 4.3 – Hydro Power Plants Data

| $h$ | $P_h^{\max}$ | $P_h^{\min}$ | $C_h^{\mathrm{P}}$ | $C_h^{+}$ | $C_h^{-}$ | $C_h^{\mathrm{SU}}$ | $W_h^{\max}$ | $\eta_h$ |
|---|---|---|---|---|---|---|---|---|
| 1 | 36 | 5 | 5.7 | 0.5 | - | 450 | 6.4 | 0.57 |
| 2 | 3.2 | - | 1.2 | - | - | - | 2 | 0.9 |
| 3 | 48 | 9 | 5.7 | - | - | 550 | 6.8 | 0.72 |

Table 4.4 – Cascaded Reservoirs data

| Reservoir $m$ | $V_m^{\max}$ ($\mathrm{m}^3 \times 10^3$) | $h \in H_m^{\mathrm{in}}$ | $h \in H_m^{\mathrm{out}}$ | $\xi_m$ ($\mathrm{m}^3/\mathrm{s}$) |
|---|---|---|---|---|
| 1 | 100000 | - | 1 | 2.4 |
| 2 | 81.6 | 1 | 2 | 1.2 |
| 3 | 27.2 | 2 | 3 | - |

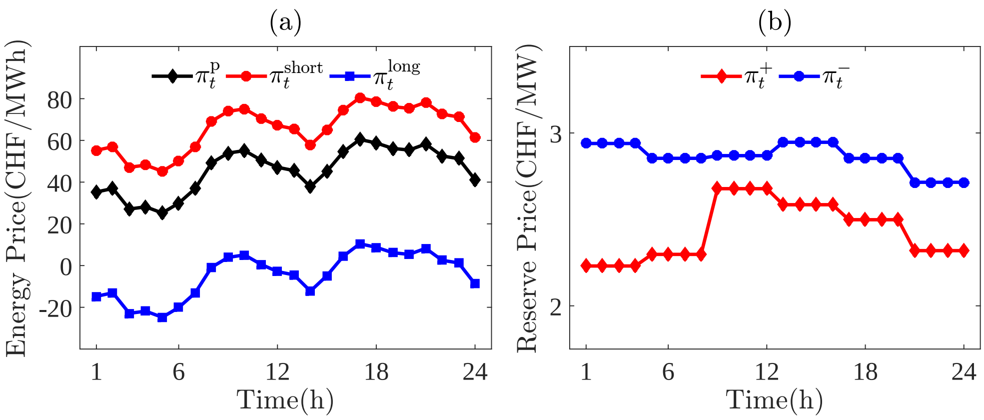


Figure 4.13 – (a) Day-ahead and imbalance energy prices (b) Upward and downward reserve prices

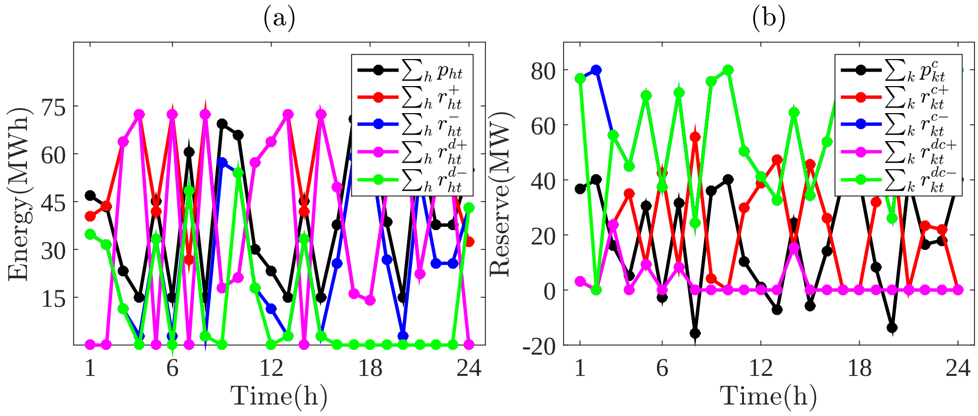


Figure 4.14 – (a) Generators aggregated schedule (b) Converters aggregated schedule

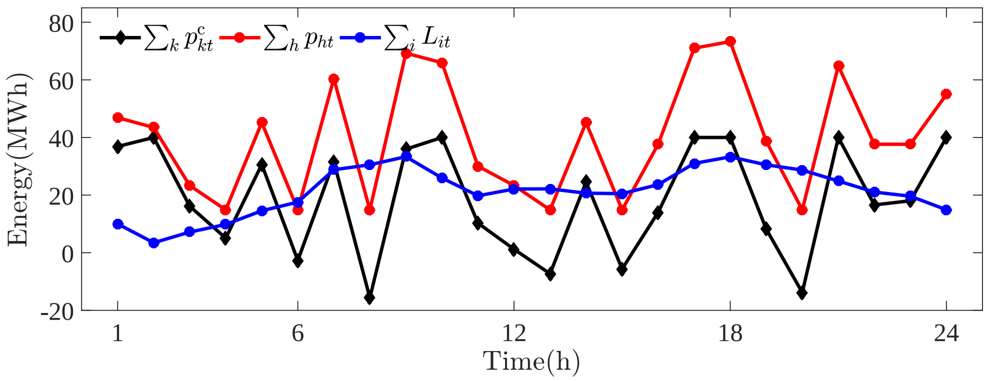


Figure 4.15 – Day-ahead energy schedule of the generators and the interconnecting converters vs the total load forecast

The aggregated schedule of the generators and the interconnecting converters are presented in figure 4.14. Moreover, figure 4.15 shows the quantity of scheduled sold and bought energy, energy schedule of generators and hourly total load forecast during 24 h scheduling period on 19, October, 2013.

The total day-ahead dispatching cost is -14362 CHF, that is composed of the operational cost of providing energy and reserve through the hydro power generators (6149 CHF) minus the revenue from selling energy (28746 CHF), plus the cost of buying energy (8235 CHF). Moreover, the second stage balancing cost considering the worst realization of uncertain energy demand at substations within the uncertainty set (4.23) is 621 CHF. Note that the control parameters $\Gamma^{Q}$, $\Gamma^{H}$ and $\Gamma^{QT}$ are assumed to be 1, which leads to the most conservative solution.

## 4.5 Stochastic Optimization Approach

Stochastic programming is a mathematical framework for dealing with problems under uncertainties [81, 82]. In this section, two-stage stochastic optimization is used to handle the uncertainties in the joint energy and reserve provision problem.

The first (dispatching) stage deals with the day-ahead decision variables. For each generator and interconnecting converter, day-ahead decision variables includes the hourly output power set point, part of provided reserve to be used for the ERC's frequency control system and part of provided reserve to be sold in the reserve market.

In the second (balancing) stage, Monte Carlo approach is used to generate scenarios including the energy demand of railway substations and the availability of generators and interconnecting converters.

Energy demand scenarios are generated using normal distribution for the energy demand forecast error at each substation. In fact, the quantity of energy demand at each substation depends on the position and the speed of trains that are electrically connected to that substation. Hence the uncertain energy demand of the ERC substations are temporally and spatially correlated. The historical data also shows both the temporal and spatial correlations in the energy demand of railway substations. In this work, both the temporal and spatial correlation derived from the historical data has been considered in scenario generation to obtain a realistic representation of energy demand uncertainties.

Scenarios for the availability of generator and converter units are generated using sequential Monte Carlo simulation based on exponential distributions. A two-state continuous-time Markov chain model is applied to represent available and unavailable states of each unit [5]. The parameters of the exponential distributions for the available and unavailable periods are derived from the Mean Time To Failure (MTTF) and the Mean Time To Repair (MTTR) values of each unit, respectively.

Since computation requirements for solving scenario-based optimization models depends on the number of scenarios, a scenario reduction technique based on k-medoids clustering algorithm [6] is adapted for a trade off between solution accuracy and computation burden. The clustering technique aims to group the similar scenarios into groups and represents this group by a single scenario, usually called representative scenario [83]. The k-medoids algorithm returns the representative scenarios which are from the original generated scenario set. This allows us to use the algorithm in the situations where the binary data are included in the original scenario set.

Unlike the adaptive robust optimization approach, the solution of stochastic optimization approach is not immune against any realization of uncertain parameter. However, to guarantee a desirable level of security of supply, we use the expected load not served (ELNS) as a probabilistic measure of the risk to find the quantity of required reserve.

Finally, for the reduced set of scenarios ($s \in \mathscr{S}$), the optimization problem can be formulated in a general form as follows:

$$\min_{\mathbf{x},\mathbf{y}^s} \mathbf{c_x x} + \sum_{s \in \mathscr{S}} \rho^s \mathbf{c_y y}^s \tag{4.28a}$$

$$\text{s.t.} \quad \mathbf{Ax} = \mathbf{L} \tag{4.28b}$$

$$\mathbf{Gx} \leq \mathbf{g} \tag{4.28c}$$

$$\mathbf{Py}^s + \mathbf{Qx} = \mathbf{L}^s \tag{4.28d}$$

$$\mathbf{Ny}^s + \mathbf{Mx} \leq \mathbf{d}^s \tag{4.28e}$$

Where $\mathbf{x}$ and $\mathbf{y}^s$ are the vectors of the first and the second stage variables. $\mathbf{A}, \mathbf{L}, \mathbf{G}, \mathbf{g}, \mathbf{P}, \mathbf{Q}, \mathbf{L^s}, \mathbf{d}, \mathbf{M}$ and $\mathbf{N}$ are the corresponding vectors and matrices to model the constraints. The overall objective function includes the first stage costs ($\mathbf{c_x x}$) plus the expectation of the second stage costs using the probability of the realization of each scenario ($\rho^s$). The constraint (4.28b) represents the first stage equality constraint including load balance and network flow based on the hourly load forecast ($\mathbf{L}$) for all substations. The inequality constraints (4.28c) represent the technical constraints of the generators, the interconnecting converters and the cascaded hydro power plants in the first stage. The second stage equality constraint (4.28d) represents the load balance taking into account the realization of load scenarios $\mathbf{L^s}$ ($\mathbf{L^s} = \{L^s_{itq} : \forall i, \forall t, \forall q, \forall s \in \mathscr{S}\}$) during each 15 minutes time step for each scenario. Finally, the second stage inequality constraints (4.28e) represent the constraints over redispatching the output power of available generators and interconnecting converters based on the part of provided reserve in the first stage that is allocated for ERC frequency control system. Beside, the ELNS limitation is modeled as a second stage inequality constraint. The first and the second stage problem formulations are explained in section 4.5.1 in details.

### 4.5.1 Enhanced Two-Stage Scheduling Formulation

#### First Stage(Dispatching) Formulation

In this section, we extend the first stage formulation considering the losses of the interconnecting converters. Note that due to the converter losses, the imported or exported energy through the converter in the two sides are different. Let us define $p^{\mathrm{ER}}_{kt}$ as a bidirectional variable representing energy schedule of the converter on the electric railway side. If $p_{kt}^{\mathrm{ER}} \geq 0$, ERC is selling energy through converter $k$ during time period $t$. Otherwise, if $p_{kt}^{\mathrm{ER}} \leq 0$, it is buying energy during this period. Hence, the converter loss can be modeled by considering equation (4.29) in the optimization problem.

$$p_{kt}^{\mathrm{ER}} = \frac{p_{kt}^{\mathrm{sell}}}{\eta_k} - \eta_k p_{kt}^{\mathrm{buy}}, \quad \forall k, \forall t \tag{4.29}$$

where $p_{kt}^{\mathrm{sell}}$ and $p_{kt}^{\mathrm{buy}}$ are positive variable that represent the energy schedule (selling or buying) of the converter on the public grid side and $\eta_k$ is the efficiency of the converter.

The extended set of first stage optimization variables is defined as $\mathbf{x} = \{u_{ht}, p_{ht}, r_{ht}^{+}, r_{ht}^{-}, r_{ht}^{d+}, r_{ht}^{d-}, c_{ht}^{\mathrm{SU}}, p_{kt}^{\mathrm{buy}}, p_{kt}^{\mathrm{sell}}, p_{kt}^{\mathrm{ER}}, r_{kt}^{\mathrm{c}^{+}}, r_{kt}^{\mathrm{c}^{-}}, r_{kt}^{\mathrm{dc}^{+}}, r_{kt}^{\mathrm{dc}^{-}}, q_t^{+}, q_t^{-}, \delta_{it}^{0}, w_{ht}^{\mathrm{d}}, w_{ht}^{\mathrm{sp}}, v_{mt}\}$.

Using the extended set of first stage variables, the first stage problem can be formulated as follows:

$$\min_{\mathbf{x}} \sum_t \sum_h (c_{ht}^{SU} + C_h p_{ht} + C_h^{+} r_{ht}^{+} + C_h^{-} r_{ht}^{-}) - \sum_t (\pi_t^{+} r_t^{\mathrm{sell}^{+}} + \pi_t^{-} r_t^{\mathrm{sell}^{-}}) - \sum_t \sum_{k \in C_i} \pi_t^{\mathrm{p}} (p_{kt}^{\mathrm{sell}} - p_{kt}^{\mathrm{buy}}) \tag{4.30a}$$

$$\text{s.t.} \quad \sum_{h \in \mathcal{G}_i} p_{ht} - \sum_{k \in \mathcal{C}_i} p_{kt}^{\mathrm{ER}} = L_{it} + \sum_{j \in \mathcal{N}_i} B_{ij} (\delta_{jt}^{0} - \delta_{it}^{0}), \quad \forall i, \forall t \tag{4.30b}$$

$$p_{kt}^{\mathrm{ER}} = \frac{p_{kt}^{\mathrm{sell}}}{\eta_k} - \eta_k p_{kt}^{\mathrm{buy}}, \quad \forall k, \forall t \tag{4.30c}$$

$$p_{kt}^{\mathrm{sell}}, p_{kt}^{\mathrm{buy}} \geq 0, \quad \forall k, \forall t \tag{4.30d}$$

$$p_{kt}^{\mathrm{ER}} + r_{kt}^{\mathrm{c}^{+}} \leq P_k^{\mathrm{c}^{\max}}, \quad \forall k, \forall t \tag{4.30e}$$

$$p_{kt}^{\mathrm{ER}} - r_{kt}^{\mathrm{c}^{-}} \geq -P_k^{\mathrm{c}^{\max}}, \quad \forall k, \forall t \tag{4.30f}$$

$$\text{Constraints (4.15c)-(4.15l) and (4.15o)-(4.15v)} \tag{4.30g}$$

In the third term of the objective function, the cost/revenue of buying/selling energy from/to the energy market through the converters are considered from public power gird side. After considering the loss of interconnecting converters, the rest of this first stage formulation is similar to the formulation presented in section 4.3.1.

**Second Stage(balancing) Formulation**

The optimization variables of the second stage problem are defined as $\mathbf{y}^s = \{p_{htq}, p_{ktq}^{\mathrm{in}}, p_{ktq}^{\mathrm{out}}, p_{ktq}^{\mathrm{ER}}, \delta_{itq}, l_{itq}^{\mathrm{sh}}, p_{tq}^{\mathrm{im}}, p_{tq}^{\mathrm{short}}, p_{tq}^{\mathrm{long}}\}^s$. This set of variables includes the energy redispatch of all the generators and interconnecting converters (in both of the public grid and electric railway sides) as well as the state of the transmission network buses in the redispatch stage and the load shedding variable at each bus and the short and long imbalance energy variables. Note that this set of variables are defined for the realization of scenario $s$, during e $q$ quarter of time period $t$.

The cost function of the second stage (balancing) for the realization of each scenario can be formulated as follows:

$$\begin{aligned} \mathbf{c_y y}^s = \sum_{h\in\mathscr{G}^s} C_h(\sum_{t,q} p^s_{htq} - \sum_t p_{ht}) - \sum_{h\notin\mathscr{G}^s}\sum_t C_h p_{ht} \\ + \sum_{t,q}\sum_i C^{\text{sh}} {l^{\text{sh}}_{itq}}^s + \sum_{t,q}(\pi^{\text{short}}_t {p^{\text{short}}_{tq}}^s + \pi^{\text{long}}_t {p^{\text{long}}_{tq}}^s) \qquad \forall s \in \mathscr{S} \end{aligned} \tag{4.31}$$

The cost function (4.31) includes the cost of redispatching available ERC's generators (first term); minus the cost of energy dispatching for the unavailable generators which are not providing energy in the balancing stage (second term); plus the cost of load shedding (third term) and the cost of energy imbalances through the interconnecting converters (forth term). Note that $\mathscr{G}^s$ is set of available generators following the realization of scenario $s$. In this study, the cost of imbalances are calculated based on the price of short and long imbalances following balancing policy of the TSO as presented in [65]. In general the short and long imbalances prices are considerably higher than and lower than the day ahead prices, receptively.

The aim of the balancing stage, after realization of scenario $s$ in the set of reduced scenarios ($\mathscr{S}$), is to follow the energy demand during each quarter of hour ($L^s_{itq}$) considering the available generators and converters. In this respect, the nodal power balance can be formulated as follows:

$$\sum_{h\in\mathscr{G}_i\cap\mathscr{G}^s} {p_{htq}}^s - \sum_{k\in\mathscr{C}_i\cap\mathscr{C}^s} {p^{\text{ER}}_{ktq}}^s + {l^{\text{LS}}_{tq}}^s = \sum_{j\in N_i} B_{ij}({\delta_{jtq}}^s - {\delta_{itq}}^s) + {L_{itq}}^s, \quad \forall i, \forall t, \forall q, \forall s \in \mathscr{S} \tag{4.32}$$

where

$$ {p^{\text{ER}}_{ktq}}^s = \frac{{p^{\text{out}}_{ktq}}^s}{\eta_k} - \eta_k {p^{\text{in}}_{ktq}}^s, \quad \forall k \in \mathscr{C}^s, \forall t, \forall q, \forall s \in \mathscr{S} \tag{4.33a}$$

$$ {p^{\text{ER}}_{ktq}}^s = 0, \quad \forall k \notin \mathscr{C}^s, \forall t, \forall q, \forall s \in \mathscr{S} \tag{4.33b}$$

Here, $\mathscr{C}^s$ is the set of available interconnecting converters following the realization of scenario $s$. Moreover, the positive variables ${p^{\text{in}}_{ktq}}^s$ and ${p^{\text{out}}_{ktq}}^s$ represent the real quantity of imported and exported energy through the interconnecting converter after realization of scenario $s$, respectively.

As mentioned earlier, the second stage inequality constraints (4.28e) are also binding the overall objective function (4.28a). In this respect, equation (4.34) represents the transmission flow limits in the balancing stage.

$$|B_{ij}(\delta^s_{itq} - \delta^s_{jtq})| \leq T^{\max}_{ij}, \quad \forall (i,j), \forall t, \forall q, \forall s \in \mathscr{S} \tag{4.34}$$

Moreover the energy redispatching variables for each scenario, $\{p_{htq}, p^{\text{in}}_{ktq}, p^{\text{out}}_{ktq}, p^{\text{ER}}_{ktq}\}^s$ are limited by the first stage decisions on the part of reserve that is provided by the ERC's generators and interconnecting converters for the operation of ERC frequency control system $\{r^{\text{d+}}_{ht}, r^{\text{d−}}_{ht}, r^{\text{dc}^+}_{kt}, r^{\text{dc}^-}_{kt}\}$.

$$p_{htq}{}^s, p^{\text{in}\,s}_{kt}, p^{\text{out}\,s}_{kt} \geq 0, \quad \forall h, \forall h, \forall t, \forall q, \forall s \in \mathscr{S} \tag{4.35}$$

$$p^s_{htq} \leq (p_{ht} + r^{d+}_{ht}) \times \frac{15\text{min}}{60\text{min}}, \quad \forall h, \forall t, \forall q, \forall s \in \mathscr{S} \tag{4.36}$$

$$p^s_{htq} \geq (p_{ht} - r^{d-}_{ht}) \times \frac{15\text{min}}{60\text{min}}, \quad \forall h, \forall t, \forall q, \forall s \in \mathscr{S} \tag{4.37}$$

$$p^{\text{ER}\ s}_{ktq} \leq (p^{\text{ER}}_{kt} + r^{\text{dc}^+}_{kt}) \times \frac{15\text{min}}{60\text{min}}, \quad \forall k, \forall t, \forall q, \forall s \in \mathscr{S} \tag{4.38}$$

$$p^{\text{ER}\ s}_{ktq} \geq (p^{\text{ER}}_{kt} - r^{\text{dc}^+}_{kt}) \times \frac{15\text{min}}{60\text{min}}, \quad \forall k, \forall t, \forall q, \forall s \in \mathscr{S} \tag{4.39}$$

The quantity of energy imbalance is the sum of imbalances for all interconnecting converters during each 15 minute time step. It can be formulated as:

$$p^{\text{im}\,s}_{tq} = \sum_{k \in \mathscr{C}^s} (p^{\text{ER}}_{kt} \times \frac{15\text{min}}{60\text{min}} - p^{\text{ER}\ s}_{ktq}) + \sum_{k \notin \mathscr{C}^s} p^{\text{ER}}_{kt} \times \frac{15\text{min}}{60\text{min}} \quad \forall t, \forall q, \forall s \in \mathscr{S} \tag{4.40}$$

In equationn (4.40), the first and the second terms represent the energy imbalances due to the redispatching of the available converters and the day ahead energy schedule for the converters which are not available in the balancing stage, respectively. The energy imbalance variable

$p_{tq}^{\mathrm{im}^s}$ can take both of positive and negative values, which corresponds to the short and long imbalances, respectively. Hence, the corresponding short and long imbalance variables that are used in the second stage cost function (4.31), take value depending on the sign of the imbalance power as formulated below.

$$p_{tq}^{\mathrm{short}^s} = \max\{0, p_{tq}^{\mathrm{im}^s}\}, \quad \forall t, \forall q, \forall s \in \mathscr{S} \tag{4.41}$$

$$p_{tq}^{\mathrm{long}^s} = \min\{0, p_{tq}^{\mathrm{im}^s}\}, \quad \forall t, \forall q, \forall s \in \mathscr{S} \tag{4.42}$$

Note that the above equations (4.41)-(4.42) can be simply linearized using auxiliary binary variables.

Finally, the ELNS can be calculated using the load shedding variables. To ensure that the risk level of the obtained energy and reserve schedule is desirable, the ELNS should be limited as follows.

$$\sum_{s \in \mathscr{S}} \sum_{i,t,q} \rho^s l_{itq}^{\mathrm{sh}\ s} \leq \mathrm{ELNS}^{\max} \tag{4.43}$$

Referring to all the above mentioned formulations, the improved second stage problem considers constraints (4.32)-(4.43).

### 4.5.2 Case Study

To demonstrate the effectiveness of the proposed method, a case study based on the characteristic of the Swiss railway company in the western part of Switzerland is addressed. The network structure and price data are similar to the case study presented in section 4.4.3. The MTTF and MTTR for the generators are 147 h and 3 h, which corresponds to 0.02 forced outage rate for the generators. The MTTF and MTTR for the generators are 198 h and 2 h, which corresponds to 0.01 forced outage rate for the converters. Moreover, the efficiency of the interconnecting converters connected to buses 3 and 11 are 0.85 and 0.95, respectively.

The total hourly energy demand forecast for all buses as well as the load scenarios are shown in Fig. 4.16(a). This load data corresponds to the the load forecast of the system on 19, October, 2013. The original number of load and availability scenarios is 1000. Each scenario at each time step is a vector including the per unit ([0,1]) realization of load forecast error of 14 substations and the availability (0 or 1) of three generators and two converters. The number of scenarios

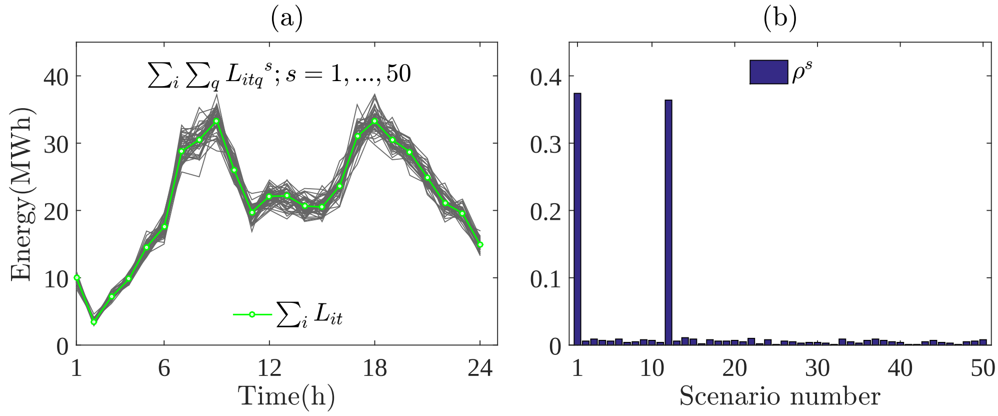


Figure 4.16 – (a) Energy demand forecast and scenarios (b) Probability of reduced scenarios

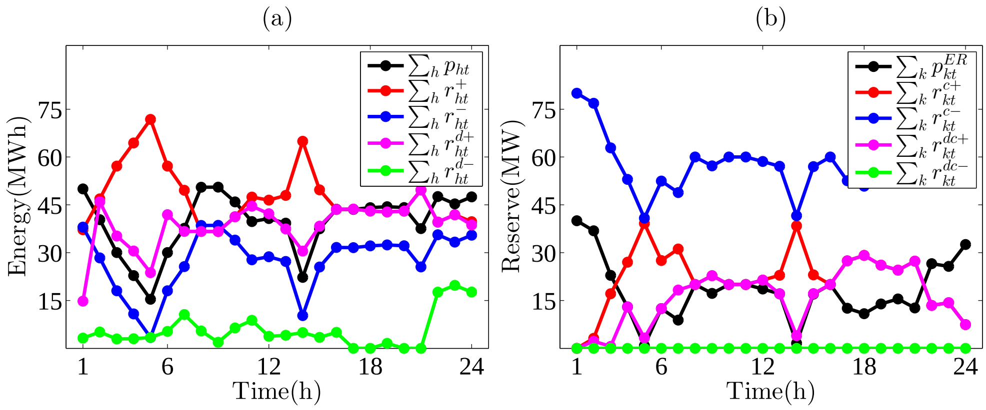


Figure 4.17 – (a) Generators aggregated schedule (b) Converters aggregated schedule

are reduced to 50 using the k-medoid clustering algorithm. The main criteria of the clustering algorithm is to minimize the distances between original and reduced scenarios. The result of the scenario clustering algorithm which is the probability of the reduced number of scenarios is shown in figure 4.16(b). The given energy and reserve market prices as well as the price of short and long imbalances are depicted in figure 4.13.

To find the optimal energy and reserve schedule for the ERC, the two-stages stochastic optimization problem is solved using CPLEX tool under GAMS [80]. The solution took 158$s$ on a 3.4 GHz windows machine. The aggregated day-ahead energy and reserve schedule of the generators and interconnecting converters are shown in figure 4.17. Moreover, the quantity of sold energy, upward and downward reserve for each hour is depicted in figure 4.18. The results also show that the ERC does not buy energy from day ahead market during the scheduling period based on the given price of energy and reserve.

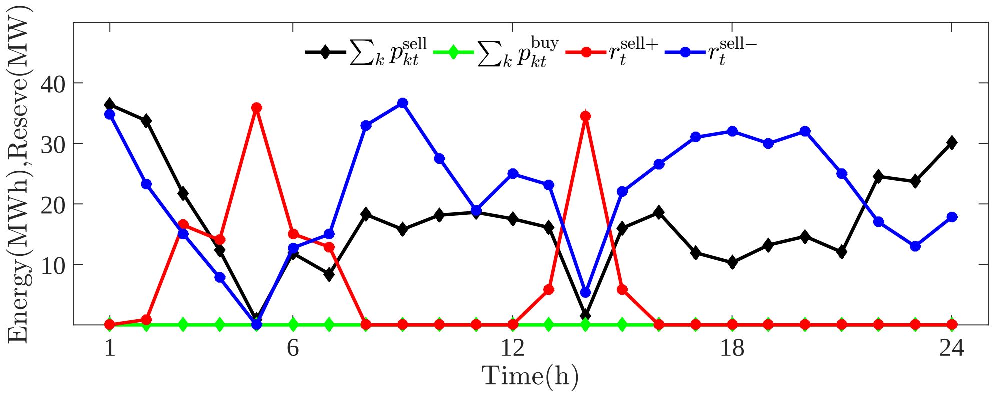


Figure 4.18 – Day-ahead energy and reserve transactions through the interconnecting converters

Table 4.5 – Total cost and the second stage cost components

| Cost/Revenue | Mean | SD | s=1 | s=16 |
|---|---|---|---|---|
| Total cost(CHF) | -14057 | 115 | -15555 | -12466 |
| Second stage cost(CHF) | -13 | 115 | -1511 | 1578 |
| Generators redispatching cost(CHF) | 19 | 69 | 993 | 809 |
| Short imbalances cost(CHF) | 36 | 241 | 0 | 1825 |
| Long imbalances cost(CHF) | -48 | 178 | -2505 | -2066 |
| Load shedding cost(CHF) | 0.58 | 1.96 | 0 | 1010 |

The total day-ahead scheduling cost is -14044 CHF, that is composed of the operational cost of providing energy and reserve through the hydro power generators (6107 CHF) minus the revenue from selling energy (18516 CHF), minus the revenues from selling upward (336 CHF) and downward (1299 CHF) reserves. The total cost as well as the second stage cost depends on the realization of scenarios. The expected total cost and the components of the second stage cost as well as the standard deviations that are obtained based on the reduced set of scenarios are presented in Table 4.5. Moreover, the costs related to a high probable scenario ($s = 1, \rho^1 = 0.374$) and a low probable scenario ($s = 16, \rho^{16} = 0.002$) are presented in this table. The VOLL ($C^{\text{sh}}$) is assumed to be 2000 CHF/MWh and the ELNS$^{\text{max}}$ is 0.1% of the total energy demand forecast. As it can be seen in this table, in average, the imbalance and load shedding costs in the second stage is negligible in comparison with the first stage cost. It means that the proposed energy and reserve scheduling can provide an appropriate schedule that can effectively follow the load variations and the unforced outages of generators and converters in the balancing stage. In other words, the part of reserve provision of generators that is kept for the internal frequency control scheme, is effectively used in the balancing stage.

## 4.6 Methods Comparison

In the previous sections, we have proposed and investigated two alternative approaches, namely, Adaptive robust optimization (ARO) and two-stage stochastic optimization (SO) for dealing with uncertainties in the energy and reserve provision problem. In this section we summarize the advantages and drawbacks of these methods considering different criteria such as uncertainty and risk management approach, required information from the uncertain parameter, the obtained total cost, solution computation time and modeling limitations derived from computation tractability.

In terms of modeling limitations, stochastic optimization approach is more flexible in the sense that both of the first and second stage formulation can contains binary variables. As a results, some detailed technical considerations such as interconnecting converter losses and the aggregation of energy imbalances over all converters can be simply included in the problem formulation. In contrast, the computation tractability of ARO approach imposes that the second stage problem has to be linear including only continuous variables. Otherwise, the dual problem of the second stage problem cannot be obtained and consequently the ARO problem cannot be effectively solved.

To compare these approaches considering the obtained total cost, we have solved the stochastic problem while the efficiency of converters are assumed to be 1 and all the generators and converters are available. The day ahead scheduling cost obtained from the solution of SO problem is -16296 CHF, which is 11% lower than the one obtained from solution of ARO problem (-14362 CHF). Note that these results depend on the value of $ELNS^{\max}$ (maximum allowable expected load not served) and VOLL (value of lost load).

The uncertainty and risk management using ARO approach is more conservative and risk averse. In fact, the obtained schedule guarantees that the balancing problem is feasible for any realization and optimal for the worst realization of the uncertain energy demand at the substations within the uncertainty set. Since the uncertainty set is obtained considering the nodal load forecast error, the obtained schedule can guarantee the security of supply with a very high level of confidence. In contrast, the uncertainty management using SO approach is based on a probabilistic representation of the uncertain parameters. Here, the level of the security of the system depends on the values of $ELNS^{\max}$ and VOLL.

In general, the ARO approach needs only few information about the uncertain parameter (i.e. the mean and the range). For uncertainties associated with energy demand at substations, these information can be simply provided using forecast techniques. On the contrary, the SO approach requires an accurate estimation of Probability Distribution Function (PDF) of

Table 4.6 – Methods Comparison

| | Adaptive Robust Optimization | Stochastic Optimization |
|---|---|---|
| Uncertainty Management | Conservative and risk averse<br>Optimal for the worst case | Probabilistic guarantee<br>Cost vs Security |
| Required information from the uncertain parameters | Few information (mean and range) | Estimation of PDF |
| Solution computation time | Moderate (Low) | High |
| Modeling flexibility | Low | High |

the uncertain parameter to ensure the accuracy of the results derived from the generated scenarios. Note that, in general, the estimation of probability distribution function is more difficult than the estimation of the mean or the range of an uncertain parameter.

The solution computation time of the SO problem increases by increasing the number of scenarios. In general, the SO problem should be solved considering a large number of scenarios to guarantee the solution accuracy. The solution computation time of the ARO problem depends on the number of iterations required by the iterative solution algorithm. In general, solution computation time of the ARO problem is considerably lower than the one of the SO problem.

Finally, table 4.6 provides a summary of the methods comparison considering the above mentioned criteria.

## 4.7 Summary and Conclusion

In this chapter the problem of joint energy and reserve scheduling in an ERPS has been addressed. In this problem, the variation of energy demand at each substation from its forecast value is an uncertain parameter. To investigate the characteristics of this uncertain parameter, a short term load forecast method based on ARIMA time series is applied using realistic data from Swiss ERPS . The results of this study, show the spatial and the temporal correlations among the energy demand of ERPS substations.

Next, joint energy and reserve scheduling problem has been formulated as a two stages optimization problem including first (day ahead) and second (balancing) stages. Two mathematical approaches, namely, adaptive robust optimization (ARO) and stochastic optimization (SO) are proposed for dealing with uncertainties in this scheduling problem.

The uncertainty and risk management using ARO approach is more conservative and risk averse. This method, effectively considers the temporal and spatial correlation between energy demand forecast error of the ERC substations. In fact, the day-ahead obtained schedule (solution) guarantees that the balancing problem is feasible for any realization and optimal for the worst realization of the uncertain energy demand at substations within the uncertainty set. Since the uncertainty set is obtained considering the nodal load forecast error, the obtained schedule can guarantee the security of supply with a very high level of confidence. In contrast, the uncertainty management using SO approach is based on a probabilistic representation of the uncertain parameters. Here, the level of the security of the system depends on the values of $ELNS^{\max}$ and VOLL (value of lost load).

Moreover, the proposed ARO approach provides the control parameters to control the level of robustness of the obtained solution against the energy demand variations. This robustness is desirable for ERCs where security of supply is the first objective. However, the main drawback of this approach is that the computation tractability imposes that the second stage problem has to be linear including only continuous variables.

On the contrary, the proposed two stages stochastic optimization method is more flexible in the sense that both of the first and second stage formulation can contains binary variables. Here, the two stage problem formulation is improved to include some detailed technical considerations such as interconnecting converter losses and the aggregation of energy imbalances over all converters. Moreover, the proposed method covers the uncertainties associated with the availability of generators and interconnecting converters in the balancing stage.

The numerical results show that ERC can effectively utilize the interconnecting converters for energy trading and selling reserve without threatening it security of supply.

Finally, these two approaches have been compared considering different criteria considering different criteria such as uncertainty and risk management approach, required information from the uncertain parameter, the obtained total cost, solution computation time and modeling limitations derived from computation tractability. A summary of this comparison is presented in table 4.6.

# 5 Offering Strategy methods for Participating in Energy and Reserve Markets

## Chapter Overview

*This chapter proposes appropriate offering strategy methods for an ERC to participate in energy and reserve markets. In this respect, first the problem of energy and reserve scheduling for ERC is modeled in based on a single-stage formulation. Next, a discrete robust optimization technique is used to solve the problem taking into account the uncertain energy and reserve prices as well as the uncertain hourly energy demand of ERC's substations. Afterward, a reserve offering curve construction algorithm based on the solution of robust energy and reserve scheduling is proposed. This algorithm takes into account the correlation between upward and downward reserve prices. Moreover, an appropriate energy offering curve construction algorithm is presented. Finally, to show the effectiveness of the proposed methods, a realistic case study based on the characteristic of an ERC in Switzerland is presented.*

## 5.1 Introduction

### 5.1.1 Motivation and Aims

Most of the interconnecting converters (specially in central European countries) can be used to exchange energy in both directions from 50 Hz to 16.7 Hz system, and vice versa. The bidirectional capability of converters allows ERCs to buy/sell energy (depending on the price of energy and their own demand) from/to the energy market.

Moreover, with the advent of the liberalization of the electricity sector, new markets have emerged including markets for frequency control reserves. The purpose of reserve markets is to provide reserves for the system operator to ensure the security of supply in case of imbalances in public power grid. ERCs are interested to participate in the reserve markets as they see an opportunity to make profits by selling reserves.

Generally the electric railway installations (i.e., generators, converters, etc.) are over sized to reduce the risk of power shortage in case of strong fluctuations in electric railway power demand. Moreover, fast interconnecting converters along with fast hydroelectric power plants allow ERCs to adjust the energy exchanges through the converters to reduce the imbalances in the public power grid.

It should be noted that the main objective of an ERC is to ensure the security of supply of its own demand. Afterward, ERC is interested to maximize its profit from participating in energy and reserve markets. Therefore ERC is looking for a robust offering strategy to participate in the markets, in the sense that uncertainties in energy demand of its own substations would not threaten its security of supply.

In this chapter we follow the European electricity markets structure where the reserve market is cleared before the energy market is clearing. Hence, the day ahead energy market prices are not known when ERC has to submit the upward and downward reserve offering curves to the reserve market. For instance, in Switzerland the reserve market is cleared in two days ahead basis. Note that the variations of day ahead energy prices from the forecast values can move the solution of the energy and reserve scheduling problem from an optimal point (minimum total cost) to any suboptimal point. Therefore, besides the security of supply, the reserve offering strategy of ERC should be robust against the uncertainty in the upcoming day ahead energy market prices.

Within the above context, the aim of this chapter is: 1) to propose an appropriate offering strategy method for an ERC to participate in reserve markets and 2) to find optimal energy offering curve taking into account the outputs (accepted reserve offers) of the reserve market.

Both of the proposed energy and reserve offering strategies are using the solutions of a robust energy and reserve scheduling of ERC generators and converters.

### 5.1.2 Literature Review and Contributions

Most of researches in low frequency electric railway power systems has focused more on technical problems (i.e. stability [8], converter control [9]-[10], system simulation and modeling [11], etc.) than economic and market issues. Among few studies, in the 1990s, Ollofsson et al. in [12] and [13] solve the load flow and optimal power flow problems for the Swedish electric railway system considering controlled and uncontrolled interconnecting converters. To the best knowledge of the author of this thesis, the problem of energy and reserve scheduling for an ERC for participating in energy and reserve markets has not been reported in the literature.

On the other hand, the problem of optimal bidding strategy in energy markets has been deeply investigated in power system literature. A state of the art review on modeling and methods could be found in [84]. In this respect, a stochastic mixed-integer optimization formulation is established in [85] to deal with the price uncertainties, bidding risk management, and self-scheduling requirements for a hydrothermal system considering its own energy and reserve demand. The authors in [86] provides a bidding strategy for a price-taker under price uncertainty using an appropriate probability description of hourly market prices. A risk-constrained bidding strategy for energy and reserve markets by modeling price uncertainties with scenarios is presented in [87]. The authors in [88] provide a model for determining optimal bidding strategies for hydro power producer, taking day ahead power market price uncertainty into account. In particular, market price scenarios are generated and a stochastic mixed-integer linear programming model is developed. A two-stage stochastic programming approach is also proposed in [89] to model the real decision making process of a wind park operators in a spot-market framework under uncertainty.

To find the offering strategy for ERC in reserve markets; first, we solve the joint energy and reserve self-scheduling problem of ERC. Solving this scheduling problem, we obtain the optimum quantity of reserve that ERC can offer to the reserve market for the given energy and reserve prices. Then, we could construct the hourly reserve offering curves based on the solutions of the self-scheduling problems for different levels of reserve price.

The multi period self-scheduling problem for an ERC considering generators, interconnecting converters and network constraints is a mixed integer linear programming (MILP) problem. In this optimization problem, both of the cost coefficients (energy and reserve prices) and the data involved in the constraints (energy demands of substations) are subject to uncertainty. Referring to these uncertainties, the previous study (presented in section 1.2.1 and chapter 4), is mainly dedicated to consider uncertainties in the constraints and hence, a sophisticated two-stages problem formulation is proposed. In contrast, the study presented in this section, is mainly dedicated to consider uncertainties in the cost coefficients. Therefore, a more simple single-stage formulation is proposed in this study.

Robust optimization is an alternative framework to stochastic programming for solving problems dealing with uncertainty. In recent years, this uncertainty management approach has been received lots of attention in power system [3, 4]. In robust optimization the uncertainty model is not stochastic, but rather deterministic and set-based. The decision-maker constructs a solution that is not only feasible for all realizations of the uncertain parameters within the uncertainty set (e.g. confidence intervals) but also optimal for the worst realization of such uncertain parameters [59]. In [90], the authors propose an energy offering strategy considering the day ahead energy price uncertainties via robust optimization. The proposed method efficiently improves the profit of offering in energy market by using nested energy price intervals instead of energy price forecast in the energy offering curve construction.

In this chapter, a discrete (mixed integer) robust optimization technique, relying on [7], is applied to solve the robust self-scheduling problem of ERC taking into account uncertainties in the energy and reserve prices as well as uncertainties in the energy demand of railway substations. This proposed robust energy and reserve scheduling model allows controlling the degree of conservatism of the solution and moreover it is computationally tractable.

Afterward, we propose an effective algorithm for constructing the upward reserve offering curve by iteratively solving the above mentioned robust energy and reserve scheduling problem for different levels of upward reserve price. For each level of upward reserve price, the robust scheduling problem is solved, taking into account the energy price and downward reserve price uncertainties as well as energy demand uncertainties.

Note that the proposed reserve offering algorithm, in this chapter, does not definitely maximize the revenue of ERC in the reserve market. However, as mentioned earlier, ERC has to participate in energy market after determination of awarded reserve offers by the reserve market. Here the proposed reserve offering strategy leads to the reduction of the total cost of ERC in both reserve and energy markets. This total cost includes the cost of energy trading (positive for buying energy and negative for selling energy), plus operational cost of ERC's generators, minus the revenue from selling reserves to the reserve market.

Finally, we present an energy offering curve construction algorithm taking into account some fixed amount of reserve that ERC has to sell into the reserve market. This algorithms also relying on the solution of energy and reserve self scheduling problem while the set of energy prices is the only uncertain parameter in the objective function.

Given the above context, the main contributions of this chapter are fourfold:

1. to propose a discrete robust optimization technique to solve a single stage scheduling problem considering price and demand uncertainties (uncertain parameters in objective function and constraints);

2. to propose offering curve construction algorithm for participating in reserve market based on the robust energy and reserve self-scheduling considering the correlation between upward and downward reserve prices;

3. to present energy offering curve construction algorithms for participating in energy markets considering the awarded reserve offers from the output of the reserve market.

### 5.1.3 Chapter Organization

The rest of the chapter is organized as follow: section 5.2 describes the position of ERC in self-scheduled energy and reserve markets. The single-stage scheduling problem of ERC is presented in section 5.3. In section 5.4, the discrete robust optimization technique is introduced to solve the self-scheduling problem dealing with the uncertainties. Next, the offering strategy for reserve market is presented in section 5.5 and section 5.6 discusses energy offering curve construction algorithms. To show the effectiveness of the presented methods, Section 5.7 gives numerical results for a realistic case study in Switzerland. Finally, the conclusion and summary are presented in section 5.8.

## 5.2 ERC in Self-scheduled Energy and Reserve Markets

The energy market structure in this work, follows European energy exchange market (EPEX) rules [91]. Here, an ERC is a price-taker in the market where the prices do not change by any action of any participant. EPEX accepts demand or generation offers (a price and quantity pair) from the market participants including ERC, and determines the market-clearing price (MCP) at which energy is bought and sold in a day ahead.

In most of central European countries, reserve markets are separately being coordinated by the transmission system operators (TSOs). The aim of the reserve markets is to provide primary, secondary and tertiary control reserves as defined in [92] for the TSO to remove any imbalances in the public power grid. Without loosing generality, in this work we consider the Swiss reserve market structure [65] where the TSO is the only buyer in the reserve market

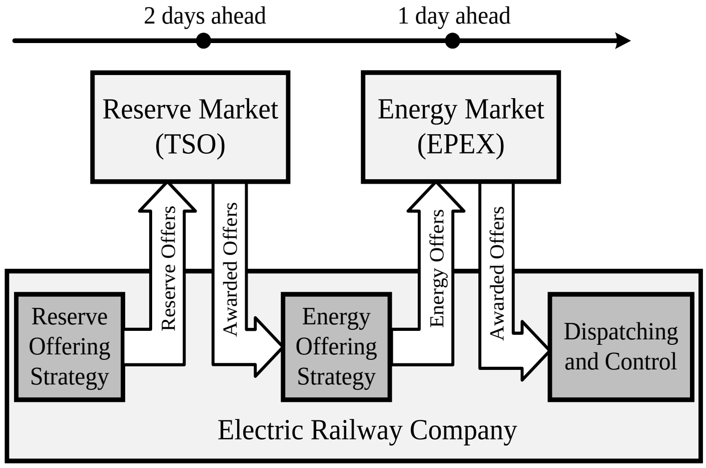


Figure 5.1 – ERC in energy and reserve market structure

and ERC like any other generation company can only offer to sell reserves in the market. As mentioned earlier, the provided primary and secondary reserves by ERC's generators are required for its internal frequency control mechanism. However, ERC is interested to offer the tertiary reserve (upward and downward) to the market from the remaining capacity of its own generators.

The TSO accepts offers for providing upward and downward tertiary reserves separately from the market participants in two days ahead. Then the TSO constructs the reserve supply curve by sorting the offers from the lowest price offer to the highest price offer. Afterward, the awarded offers are determined by intersecting the TSO reserve demand curve with the reserve supply curve. Here the price of the most expensive awarded offer is considered as the reserve market price. It is important to stress that only the provision of reserves is addressed in this work, not its deployment (delivered energy).

From chronological point of view, first ERC has to send the reserve offers two days ahead, then the TSO clear the reserve market and send back the awarded offers to ERC. Afterward ERC has to find the optimal energy offering taking into account the fixed reserve provision as imposed by the awarded reserve offers. Finally EPEX clear the energy market and send the awarded energy offers back to ERC. For illustrative purposes, Figure 5.1 shows ERC interaction with energy and reserve markets.

## 5.3 Deterministic Single-Stage Energy and Reserve Scheduling for ERC

### 5.3.1 Problem Assumptions

In this section the multi period self scheduling problem for an ERC is modeled as a single stage cost minimization problem considering the following assumptions.

1. The scheduling time step is one hour.
2. The end user of the system are the electric railway substations (132/15 kV transformers).
3. The hourly energy demand of the railway substations are known in advance ($L_{it}$).
4. The price of energy and upward/downward reserves are known in advance ($\pi_t^p, \pi_t^+, \pi_t^-$).
5. The generators are installed in hydroelectric power plants where the water reservoirs can be cascaded via connecting rivers or water channels.
6. The internal high power transmission network is loss less and modeled by DC load flow equations.
7. For the purpose of internal primary and secondary frequency control, ERC has to provide both upward and downward reserve from its own generators. The quantity of this internal reserve demand ($R_t^+, R_t^-$) is varying along the hour of the day and is determined in a deterministic way as a portion of energy demand of the system for the given hour.

The aim of this deterministic single-stage scheduling problem is to find the optimum quantity of reserve that ERC can offer to the reserve market for a given known energy and reserve prices ($\pi_t^p, \pi_t^+, \pi_t^-$).

### 5.3.2 Problem Formulation

The above mentioned cost minimization problem can be formulated as the following MILP problem:

$$\min_{\Psi} \sum_t \sum_h (c_h^{SU} + C_h p_{ht} + C_h^+ r_{ht}^+ + C_h^- r_{ht}^-) - \sum_t (\pi_t^+ q_t^+ + \pi_t^- q_t^-) - \sum_t \sum_k \pi_t^{\mathrm{p}} p_{kt}^{\mathrm{c}} \tag{5.1a}$$

$$\text{s.t.} \quad - \sum_{h \in G_i} p_{ht} + \sum_{k \in C_i} p_{kt}^{\mathrm{c}} + L_{it} + \sum_{j \in N_i} B_{ij}(\delta_{it} - \delta_{jt}) = 0, \quad \forall i, \forall t \tag{5.1b}$$

$$c_{ht}^{SU} \geq C^{SU}(u_{ht} - u_{h,t-1}), \quad \forall h, \forall t \geq 1 \tag{5.1c}$$

$$c_{h,1}^{SU} \geq C^{SU} u_{h,1}, \quad \forall h \tag{5.1d}$$

$$c_{ht}^{SU} \geq 0, \quad \forall h, \forall t \tag{5.1e}$$

$$|B_{ij}(\delta_{it} - \delta_{jt})| \leq T_{ij}^{\max}, \quad \forall (i,j), \forall t \tag{5.1f}$$

$$\delta_{1,t} = 0, \quad \forall t \tag{5.1g}$$

$$p_{ht}, r_{ht}^{+}, r_{ht}^{-} \geq 0, \quad \forall h, \forall t \tag{5.1h}$$

$$p_{ht} + r_{ht}^{+} \leq P_h^{\max} u_{ht}, \quad \forall h, \forall t \tag{5.1i}$$

$$p_{ht} - r_{ht}^{-} \geq P_h^{\min} u_{ht}, \quad \forall h, \forall t \tag{5.1j}$$

$$-R_h^{\text{down}} \leq p_{ht} - p_{h,t-1} \leq R_h^{\text{up}}, \quad \forall h, \forall t \geq 1 \tag{5.1k}$$

$$r_{kt}^{\text{c}^+}, r_{kt}^{\text{c}^-} \geq 0, \quad \forall k, \forall t \tag{5.1l}$$

$$p_{kt}^{\text{c}} + r_{kt}^{\text{c}^+} \leq P_k^{\text{c}^{\max}}, \quad \forall k, \forall t \tag{5.1m}$$

$$p_{kt}^{\text{c}} - r_{kt}^{\text{c}^-} \geq -P_k^{\text{c}^{\max}}, \quad \forall k, \forall t \tag{5.1n}$$

$$Q_t^{+^{\min}} \leq q_t^{+} \leq \min\left\{ \sum_{k \in C_i} r_{kt}^{\text{c}+}, \sum_{h \in G_i} r_{ht}^{+} - R_t^{+} \right\}, \quad \forall t \tag{5.1o}$$

$$Q_t^{-^{\min}} \leq q_t^{-} \leq \min\left\{ \sum_{k \in C_i} r_{kt}^{\text{c}-}, \sum_{h \in G_i} r_{ht}^{-} - R_t^{-} \right\}, \quad \forall t \tag{5.1p}$$

$$v_{mt} = v_{m,t-1} + \xi_{mt} + \sum_{h \in H_m^{\text{in}}} (w_{ht}^{\text{d}} + w_{ht}^{\text{s}}) - \sum_{h \in H_m^{\text{out}}} (w_{ht}^{\text{d}} + w_{ht}^{\text{s}}), \quad \forall m, \forall t \tag{5.1q}$$

$$v_{m,0} = V_m^0, \quad \forall m, \forall t \tag{5.1r}$$

$$V_m^{\min} \leq v_{mt} \leq V_m^{\max}, \quad \forall m, \forall t \tag{5.1s}$$

$$w_{ht}^{\text{d}} + w_{ht}^{\text{s}} \leq W_h^{\max}, \quad \forall m, \forall t \tag{5.1t}$$

$$w_{ht}^{\text{d}}, w_{ht}^{\text{s}} \geq 0, \quad \forall m, \forall t \tag{5.1u}$$

$$p_{ht} = \eta_h w_{ht}^{\text{d}} - P_h^{\text{fix}} u_{ht} \geq 0, \quad \forall m, \forall t \tag{5.1v}$$

The optimization variables of the problem are defined as $\Psi = \{q_t^{+}, q_t^{-}, p_{ht}, r_{ht}^{+}, r_{ht}^{-}, c_{ht}^{SU}, p_{kt}^{\text{c}}, r_{kt}^{\text{c}^+}, r_{kt}^{\text{c}^-}, \delta_{it}, w_{ht}^{\text{d}}, w_{ht}^{\text{s}}, u_{ht}, v_{mt}\}$. This set of variables includes the energy and reserve schedule of all the generators and interconnecting converters, the state of the transmission network buses as well as water flow and reservoir water level variables for the cascaded hydroelectric power plants.

The objective function (5.1a) is to minimize the cost of ERC over the scheduling period. It includes the operational cost of ERC's generators (first term) minus the revenue from selling upward and downward tertiary reserves in the reserve market (second term) plus/minus the cost/revenue of buying/selling energy from/to the energy market through the converters (third term). Note that, since the interconnecting converters are bidirectional, $p_{kt}^{c}$ can take positive or negative values. Negative/positive value for $p^c_{kt}$ means that ERC buys/sells energy from/to the energy market through the converter $k$ during time interval $t$. Furthermore, the operational cost of the hydro power plants includes the start up cost plus the linearized cost of energy and reserve provision.

The set of constraints (5.1b)-(5.1v) are binding the objective function (5.1a). Constraints (5.1c)-(5.1e) model the start up cost of the hydroelectric power plants. The constraints (5.1b) enforce the power balance for all buses of the system. The power flow in the transmission line is simply modeled using the voltage angle of the terminal buses of the line; so constraints (5.1f) represent the transmission lines flow limits. Moreover, the constraint (5.1g) considers bus number 1 as the reference for the angle of the voltages. The set of constraints (5.1h)-(5.1j) model the generator operating point limits as well as the upward and downward ramp rate limits. The constraints (5.1l)-(5.1n) set the limits on the operating point of the converters. Note that the amount of reserved capacity for each converter depends on the maximum capacity of the converter and the energy schedule of the converter.

The amount of the tertiary reserve that ERC can sell to the reserve market is not only limited by the sum of the available capacity of the interconnecting converters ($q^+_t \leq \sum_{k\in C_i} r^{c+}_{kt}$) but also limited by the reserve provision of ERC's generators minus the internal reserve demand of ERC ($q^+_t \leq \sum_{h\in G_i} r^+_{ht} - R^+_t$). These limits for both upward and downward reserve are presented in the right side inequality of (5.1o)-(5.1p). Moreover, since $q^+_t$ and $q^-_t$ are positive variables, the left side inequality of constraints (5.1o) and (5.1p) ensure that the upward and downward reserve provision of ERC's generators are higher than its internal reserve demand ($R^+_t, R^-_t$). Note that the minimum allowable quantity for reserve offers ($Q^{+^{\min}}_t, Q^{-^{\min}}_t$) are positive parameters. These parameters are used in the offering curve construction algorithm in section V to ensure that the reserve offering curves are monotonously increasing.

The set of constraints (5.1q)-(5.1v) model the cascaded hydro power plants. The constraints (5.1q) set the water level of the reservoirs at the end of time interval $t$ equal to the water inflow/outflow during time interval $t$ plus the water level of the reservoir at the end of time interval $t-1$. In this equation, it is assumed that the time required for the water discharged from one reservoir to reach its direct down stream reservoir is negligible comparing with the time step of the problem (one hour). The constraint (5.1r) set the initial value for the variables of water level of the reservoirs. The constraints (5.1s) set the maximum and minimum allowable volume of water in the reservoirs during the scheduling period. The constraints (5.1t)-(5.1u) limit the water discharge and water spillage variables.

Finally, equality constraint (5.1v) connect the hydroelectric power generation variables to the turbined water flow variables. In this equation, the parameter of the water flow to power conversion rate ($\eta_h$) is the product of the efficiency of the hydro turbine, the height of the dam and the specific weight of water.

Note that the cost function and the technical constraints related to the other types of power plants (e.g. thermal units), can be easily incorporated in the the proposed model.

## 5.4 Uncertainty Management via Robust Optimization

### 5.4.1 Uncertainty Sets

In this section we first, present a general uncertainty set to consider the variation of price coefficients in the deterministic objective function (5.1a) as follows:

$$\begin{aligned} \Pi := \Big\{ &\pi_t^{\mathrm{p}} \in [\underline{\pi}_t^{\mathrm{p}}, \overline{\pi}_t^{\mathrm{p}}]; \forall t \in J_0^{\mathrm{p}} \\ &\pi_t^{+} \in [\underline{\pi}_t^{+}, \overline{\pi}_t^{+}]; \forall t \in J_0^{+} \\ &\pi_t^{-} \in [\underline{\pi}_t^{-}, \overline{\pi}_t^{-}]; \forall t \in J_0^{-} \Big\}. \end{aligned} \tag{5.2}$$

The parameters with over line and underline represent the upper bound and lower bound of the uncertainty set. The values of these parameters can be obtained from the confidence interval of price forecasts. Note that the presented uncertainty set $\Pi$ is a general comprehensive set that can include all price uncertainties in the objective function (5.1a). We use the control parameter $\Gamma_0$ to choose the number of uncertain parameters in the proposed robust optimization formulation. Moreover, the selection of upper bound and lower bound values in $\Pi$, depends also on the application and the desired level of robustness of the robust scheduling problem. For instance, in the proposed algorithm for construction of upward reserve offering curves in section 5.5, at each iteration, we fix the upward reserve price ($\underline{\pi}_t^{+} = \pi_t^{+}; \overline{\pi}_t^{+} = \pi_t^{+}$). Moreover, due to the negative correlation between upward and downward reserve prices, at each step of the proposed algorithm, the value of upper bound of downward reserve price is considered as a linear function of the value of the fixed upward reserve price.

To model energy demand uncertainties, the hourly energy demand of each railway substation is simply considered as a symmetric random variable that can take values in the following interval:

$$\Lambda := \Big\{ L_{it} \in [\tilde{L}_{it} - \hat{L}_{it}, \tilde{L}_{it} + \hat{L}_{it}]; \forall t \in J_{it}^{L} \Big\}. \tag{5.3}$$

where $\tilde{L}_{it}$ and $\hat{L}_{it}$ are respectively the forecast energy demand and the half of the length of the corresponding forecast confidence interval for bus $i$ during period $t$. To control the level of robustness, we introduce the protection factor ($\Gamma^{\mathrm{L}}_{it}, \forall i, t$) varying between [0,1] to control the level of robustness of the problem against energy demand variations. Note that, the temporal and spatial correlations between load forecast errors of substations for the sake of simplicity in the robust problem formulation is neglected.

### 5.4.2 Robust Optimization Formulation

The robust optimization method constructs solutions that are deterministically immune to any realizations of prices and demands in the uncertainty sets $\Pi$ and $\Lambda$, respectively. To control the level of robustness against the variation of energy and reserve prices, we use the integer control parameter $\Gamma_0$, which takes values in $[0, |J_0|]$. $|J_0|$ is the sum of number of unknown energy, upward or downward reserve prices during the optimization schedule ($|J_0| = \left|J_0^+\right| + \left|J_0^-\right| + \left|J_0^{\mathrm{p}}\right|$). In other words, we are looking for an optimal solution over all price realizations in $\Pi$ where a number $\Gamma_0$ of price coefficients can vary in such a way to maximally influence the objective function. If $\Gamma_0 = 0$, we completely ignore the influence of the price deviations, while if $\Gamma_0 = \left|J_0^+\right| + \left|J_0^-\right| + \left|J_0^{\mathrm{p}}\right|$ we are considering all possible price deviations, which is indeed most conservative. In general a higher value of $\Gamma_0$ increases the level of robustness at the expense of higher cost.

It is worth to mention that the worst realization of price uncertainties is not known in advance. ERC can sell or buy energy to/from the market at any hours, therefore the maximum or minimum prices for all times does not definitely lead to the worst case.

At each bus $i$ for each time $t$, we use a continuous number $\Gamma^L_{it}$ which takes values in the interval $[0, 1]$ to adjust the level of robustness of the proposed method in the nodal power bus constraint. Since the only uncertain parameter in constraint (5.1b) is the energy demand of the substation ($L_{it}$), $\Gamma^L_{it}$ cannot be an integer number (unlike $\Gamma_0$). Moreover, we have to replace equality in the original nodal balance (5.1b) by "lower than or equal", for dealing with uncertainty in the energy demand of the railway substations. The main consequence of this replacement is that the obtained solution could be less minimized in the case that real energy demand is very close to the forecast energy demand. However, since the main objective of ERC is the security of its own supply, the obtained robust and conservative solution is desirable in this case.

Considering the above mentioned uncertainty management approach, the proposed robust counterpart of the original deterministic problem (5.1a)-(5.1v) can be formulated as (5.4).

$$\min_{\Psi} c(\Psi) + \max_{\{S_0|S_0\subseteq J_0,|S_0|\leq\Gamma_0\}} \left\{ \sum_t \sum_k (\overline{\pi}^{\mathrm{p}}_t - \underline{\pi}^{\mathrm{p}}_t)|p^{\mathrm{c}}_{kt}| + \sum_t (\overline{\pi}^{+}_t - \underline{\pi}^{+}_t)|q^{+}_t| + \sum_t (\overline{\pi}^{-}_t - \underline{\pi}^{-}_t)|q^{-}_t| \right\} \tag{5.4a}$$

$$\text{s.t.} \quad -\sum_{h\in G_i} p_{ht} + \sum_{k\in C_i} p^{\mathrm{c}}_{kt} + \sum_{j\in N_i} B_{ij}(\delta_{it}-\delta_{jt}) + \tilde{L}_{it} l_{it} + \max_{l_{it}}\{\hat{L}_{it}\Gamma^{\mathrm{L}}_{it}|l_{it}|\} \leq 0, \quad \forall i, \forall t \tag{5.4b}$$

$$1 \leq l_{it} \leq 1 \tag{5.4c}$$

$$\text{Contraints}(5.1\text{c}) - (5.1\text{v}) \tag{5.4d}$$

Note that in the robust objective function (5.4a), $c(\Psi)$ represents the deterministic objective function (5.1a). Moreover, the auxiliary variable $l_{it}$ is introduced to convert the uncertain parameter ($L_{it}$) from right hand side to the left hand side coefficients, for the sake of clarification in the mathematical formulation.

### 5.4.3 Linear Counterpart of the Robust Formulation

In this section we present the linear counterpart of the robust problem (5.4), based on the mathematical approach introduced in [7]. Considering the given vector of variables that are affected by uncertain parameters in the objective function ($\mathbf{x}^* = \{p^{\mathrm{c}^*}_{kt}, q^{+^*}_t, q^{-^*}_t\}$), let us define $\beta_0(\mathbf{x}^*)$:

$$\beta_0(\mathbf{x}^*) = \max_{\{S_0|S_0\subseteq J_0,|S_0|\leq\Gamma_0\}} \left\{ \sum_t \sum_k (\overline{\pi}^{\mathrm{p}}_t - \underline{\pi}^{\mathrm{p}}_t)|p^{\mathrm{c}^*}_{kt}| + \sum_t (\overline{\pi}^{+}_t - \underline{\pi}^{+}_t)|q^{+^*}_t| + \sum_t (\overline{\pi}^{-}_t - \underline{\pi}^{-}_t)|q^{-^*}_t| \right\} \tag{5.5}$$

This is identical to:

$$\begin{aligned}\beta_0(\mathbf{x}^*) = \max \Bigg\{ & \sum_t \sum_k (\overline{\pi}^{\mathrm{p}}_t - \underline{\pi}^{\mathrm{p}}_t)|p^{\mathrm{c}^*}_{kt}| z^{\mathrm{p}}_t + \sum_t (\overline{\pi}^{+}_t - \underline{\pi}^{+}_t)|q^{+^*}_t| z^{+}_t + \sum_t (\overline{\pi}^{-}_t - \underline{\pi}^{-}_t)|q^{-^*}_t| z^{-}_t : \\ & \sum_t (z^{\mathrm{p}}_t + z^{+}_t + z^{-}_t) \leq \Gamma_0, 0 \leq z^{\mathrm{p}}_t, z^{+}_t, z^{-}_t \leq 1, \forall t \Bigg\}\end{aligned} \tag{5.6}$$

Similarly for the robust constraint (5.4b), we have:

$$\beta_{it}(l^*_{it}) = \max_{l^*_{it}}\{\hat{L}_{it}\Gamma^{\mathrm{L}}_{it}|l^*_{it}|\} \quad \forall i, \forall t \tag{5.7}$$

This is identical to:

$$\beta_{it}(l^*_{it}) = \max\left\{\hat{L}_{it}|l^*_{it}|z^{\mathrm{L}}_{it} : z^{\mathrm{L}}_{it} \leq \Gamma^{\mathrm{L}}_{it}, 0 \leq z^{\mathrm{L}}_{it} \leq 1\right\} \quad \forall i, \forall t \tag{5.8}$$

Since the maximization problems (5.6) and (5.8) are feasible and bounded, by strong duality we can replace their dual minimization problems into the robust problem (5.4a)-(5.4d). Consequently the Robust Mixed Integer Linear Programming (RMILP) counterpart problem of the original MILP problem (5.1a)-(5.1v) considering uncertainty sets $\Pi$ and $\Lambda$ can be formulated as (5.9).

$$\begin{aligned}
\min_{\Psi,\Phi} \sum_t \sum_h (c^{SU}_h + C_h p_{ht} + C^+_h r^+_{ht} + C^-_h r^-_{ht}) - \sum_t (\overline{\pi}^+_t q^+_t + \overline{\pi}^-_t q^-_t) - \sum_t \sum_k \overline{\pi}^{\mathrm{p}}_t p^{\mathrm{c}}_{kt} & \qquad (5.9\mathrm{a})\\
+ \Gamma_0 z_0 + \sum_t (\rho^+_t + \rho^-_t + \rho^{\mathrm{p}}_t) &\\
\text{s.t.} \quad z_0 + \rho^+_t \geq (\overline{\pi}^+_t - \underline{\pi}^+_t) y^+_t, \forall t \in J^+_0 & \qquad (5.9\mathrm{b})\\
z_0 + \rho^-_t \geq (\overline{\pi}^-_t - \underline{\pi}^+_t) y^-_t, \forall t \in J^-_0 & \qquad (5.9\mathrm{c})\\
z_0 + \rho^{\mathrm{p}}_t \geq (\overline{\pi}^-_t - \underline{\pi}^+_t) y^{\mathrm{p}}_t, \forall t \in J^{\mathrm{p}}_0 & \qquad (5.9\mathrm{d})\\
z_0, \rho^{\mathrm{p}}_t, \rho^+_t, \rho^-_t, y^{\mathrm{p}}_t, y^+_t, y^-_t \geq 0, \forall t & \qquad (5.9\mathrm{e})\\
q^+_t \leq y^+_t, \forall t & \qquad (5.9\mathrm{f})\\
q^-_t \leq y^-_t, \forall t & \qquad (5.9\mathrm{g})\\
\sum_{k \in C_i} p^{\mathrm{c}+}_{kt} \leq y^{\mathrm{p}}_t, \forall t & \qquad (5.9\mathrm{h})\\
-\sum_{h \in G_i} p_{ht} + \sum_{k \in C_i} p^{\mathrm{c}}_{kt} + \sum_{j \in N_i} B_{ij}(\delta_{it} - \delta_{jt}) + \tilde{L}_{it} l_{it} + \Gamma^L_{it} z^L_{it} + \rho^L_{it} \leq 0, \quad \forall i, \forall t & \qquad (5.9\mathrm{i})\\
z^L_{it} + \rho^L_{it} \geq \hat{L}_{it} y^L_{it}, \quad \forall i, \forall t & \qquad (5.9\mathrm{j})\\
l_{it} \leq y^L_{it}, \quad \forall i, \forall t & \qquad (5.9\mathrm{k})\\
z^L_{it}, \rho^L_{it} \geq 0, \quad \forall i, \forall t & \qquad (5.9\mathrm{l})\\
\text{Contraints(5.1c)} - \text{(5.1v)and(5.4c)} & \qquad (5.9\mathrm{m})
\end{aligned}$$

From mathematical point of view, the above RMILP problem (5.9a)-(5.9m) is obtained using duality properties of the original problem. In addition to the original optimization variables $\Psi$, a set of dual variables $\Phi = \{z_0, z^L_{it}, \rho^{\mathrm{p}}_t, \rho^+_t, \rho^-_t, \rho^L_{it}, y^{\mathrm{p}}_t, y^+_t, y^-_t, y^L_{it}\}$ is used to formulate the robust problem. In the objective function (5.9a), $z_0, \rho^{\mathrm{p}}_t, \rho^+_t, \rho^-_t, y^{\mathrm{p}}_t, y^+_t, y^-_t$ are the dual variables of the maximization problem (5.6) used to consider the price variation in the uncertainty set $\Pi$. Similarly $z^{\mathrm{L}}_{it}, y^{\mathrm{L}}_{it}, \rho^{\mathrm{L}}_{it}$ are the dual variables of maximization problem (5.8) used to consider the nodal energy demand variation in the uncertainty set $\Lambda$.

## 5.5 Reserve Offering Strategy

As mentioned earlier, the daily tertiary reserve market is cleared in two days-ahead basis while the energy market (EPEX) is cleared in a day-ahead basis. Therefore ERC has to submit the upward and downward tertiary reserve offers before submitting the energy offers. In this section, an algorithm to construct the hourly offering curves for the upward tertiary reserve is proposed. The algorithm relies on the solution of the proposed robust energy and reserve scheduling in section 5.4.

### 5.5.1 Desired uncertainty set

Before solving the robust scheduling problem, first we should specify the values of the upper bounds and lower bounds in the general uncertainty set $\Pi$. We assume that energy prices in the day ahead market are independent uncertain parameters from the reserve prices. The upper bound and lower bound of energy price are obtained based on the confidence interval of the energy price forecast. An example for such values considering 95% confidence intervals (with 95% confidence level, the actual energy price is inside the interval) is presented in figure 5.7.

The statistical data of the Swiss reserve market [65] shows that the upward and downward reserve prices are correlated uncertain parameters. As historical price data shows in Figure 5.2, by increasing the price of upward reserve, the downward reserve is decreasing. This negative correlation between upward and downward reserve prices are also presented in Table 5.1 for different hours. Therefore at each step, when we set a price to construct the offering curve for the upward reserve, we should update the interval for the downward reserve price. In this respect, the total uncertainty set for the reserve prices is modeled by a triangular region as depicted in Figure 5.3. Note that $\pi_t^{+\max}, \pi_t^{+\min}$ and $\pi_t^{-\max}, \pi_t^{-\min}$ are also obtained based on the confidence intervals of the upward reserve price and downward reserve price forecast. Examples are provided in Figs. (5.8)-(5.9)

Referring to the above description of the price uncertainties and fixing the upward reserve price at each step of offering curve construction, the uncertainty set can be formulated as

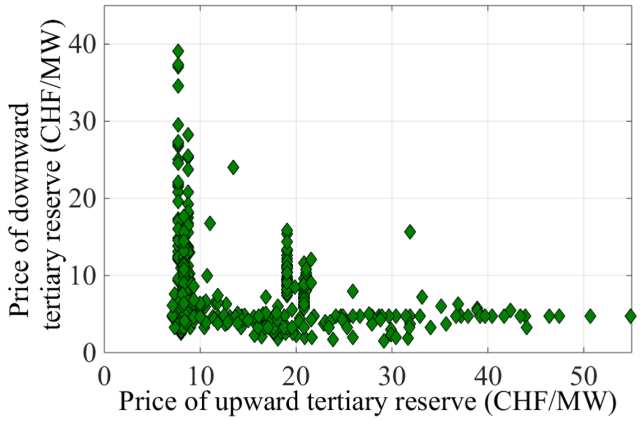


Figure 5.2 – Upward and downward reserve price samples from Swiss reserve market data from January, 6, 2014 to July, 13, 2014

Table 5.1 – Correlation between upward and downward reserve prices in Swiss reserve market

| Time(h) | 1-4 | 5-8 | 9-12 | 13-16 | 17-20 | 21-24 |
|---|---|---|---|---|---|---|
| | -0.20 | -0.24 | -0.29 | -0.23 | -0.23 | -0.17 |

(5.10).

$$\Pi(\pi_t^+) := \Big\{ \pi_t^{\mathrm{p}} \in [\pi_t^{\max}, \pi_t^{\min}]; \forall t \\ \pi_t^- \in [\pi_t^{-\min}, \overline{\pi}_t^-(\pi_t^+)]; \forall t \Big\}. \tag{5.10}$$

where the upper bound of the downward reserve price as presented in figure 5.2 can be linearly formulated as (5.11).

$$\overline{\pi}_t^- = \pi_t^{+\min} + \left(\pi_t^{+\max} - \pi_t^+\right) \frac{\pi_t^{-\max} - \pi_t^{-\min}}{\pi_t^{+\max} - \pi_t^{+\min}}; \forall t \tag{5.11}$$

In the above uncertainty set $\Pi(\pi_t^+)$, we choose the control parameter $\Gamma_0$ equal to 48 to consider all the possible variation of energy and reserve prices during the scheduling period.

### 5.5.2 Upward Reserve Offering Curve Construction Algorithm

The following algorithm is proposed to construct the upward reserve offering curves.

1. Find the upper bound and the lower bound of the price confidence intervals $(\pi_t^{\max}, \pi_t^{\min}, \pi_t^{+\max}, \pi_t^{+\min}, \pi_t^{-\max}, \pi_t^{-\min})$, based on the confidence intervals of the energy

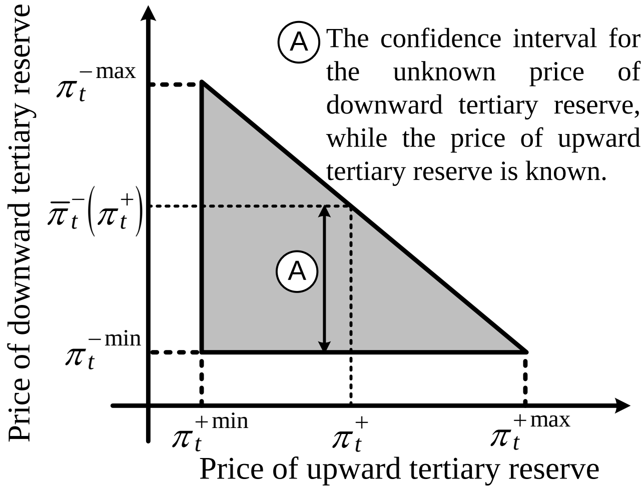


Figure 5.3 – The upper bound of uncertain downward reserve price for a given fixed upward reserve price

and reserve price forecasts.

2. Set the upward reserve prices $\pi_t^+ = \pi_t^{+\min}; \forall t$ (initial values).

3. Set the initial values for minimum quantity of upward reserve offers ($Q_t^{+^{\min}} = 0$; No limitation at the beginning of the algorithm)

4. Update the uncertainty set $\Pi(\pi_t^+)$ based on the given price of upward reserve in step 7.

5. Solve robust optimization problem (5.9a)-(5.9m) to obtain the hourly quantity of upward reserve that ERC can offer at iteration $m$, $q_t^{+m}$.

6. Update the minimum quantity of upward reserve offers for the next iteration with the obtained solution at this iteration ($Q_t^{+(m+1)^{\min}} = q_t^{+m}$) to ensure that the offering curve is monotonously increasing.

7. Increase the upward tertiary reserve price with the increment step $\sigma \geq 0$ ($\pi_t^{+(\mathrm{m}+1)} = \pi_t^{+\mathrm{m}} + \sigma; \forall t$). Repeat iteratively (indexed by $m$) steps 4-7 covering the whole range of upward tertiary reserve prices. The stop criteria is when $\pi_t^+ = \pi_t^{+\max}$.

8. Construct the hourly offering curves using the obtained results. Each iteration $m$ provides a price and a reserve quantity for each time ($\pi_t^{+\mathrm{m}}, q_t^{+\mathrm{m}}; \forall t$). For each time $t$, the pairs of prices and quantities in all iterations ($\pi_t^{+\mathrm{m}}, q_t^{+\mathrm{m}}$); $\forall m$ result in the offering curve for that time. Examples of such offering curves are provided in the case study section.

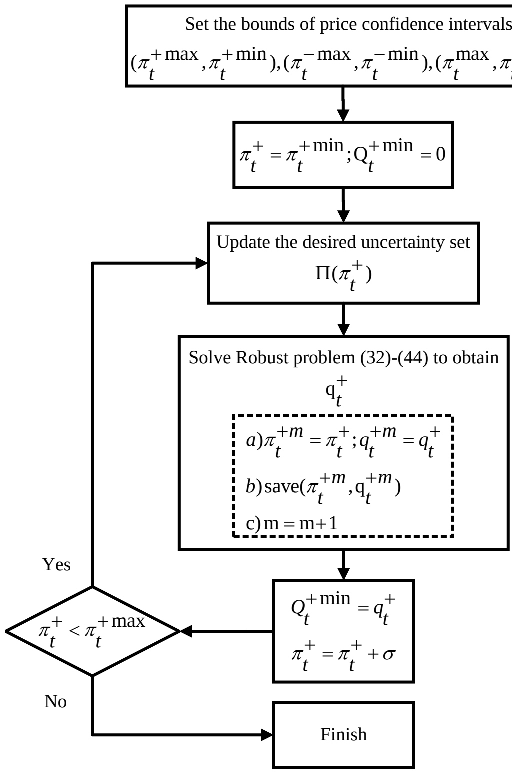


Figure 5.4 – Flowchart of the reserve offering algorithm

To clarify the proposed reserve offering algorithm, the corresponding flowchart is also presented in Figure 5.4.

It should be noted that the proposed algorithm is relying on the fact that the upward reserve prices for different hours of a day are positively correlated to each other. In other words, it is not likely that there turn out to be high prices (upward reserve) at hour 1 and low prices at hour $T$. The statistical analysis as presented in table 5.2 shows that there is a high positive correlation between the prices of upward reserve of different hours of a day. The correlation values are obtained based on a six month period from January 2014 to July 2014. Therefore, the presented offering strategy is effective in most of the cases, the numerical results presented in section 5.7 shows the effectiveness of the proposed algorithm.

To construct the downward reserve offering curves, the same algorithm can be used by replacing the variables and the parameters of upward reserve with the variables and the parameters of downward reserve accordingly.

Table 5.2 – Correlation between upward reserve prices at different hours of day in Swiss reserve market

| Time(h) | 1-4 | 5-8 | 9-12 | 13-16 | 17-20 | 21-24 |
|---|---|---|---|---|---|---|
| 1-4 | 1 | 0.69 | 0.61 | 0.68 | 0.48 | 0.70 |
| 5-8 | 0.69 | 1 | 0.91 | 0.93 | 0.85 | 0.87 |
| 9-12 | 0.61 | 0.91 | 1 | 0.90 | 0.90 | 0.95 |
| 13-16 | 0.68 | 0.93 | 0.90 | 1 | 0.84 | 0.92 |
| 17-20 | 0.48 | 0.85 | 0.90 | 0.84 | 1 | 0.84 |
| 21-24 | 0.70 | 0.87 | 0.95 | 0.92 | 0.84 | 1 |

Finally, it should be noted that in the cases where there is no meaningful correlation between upward and downward reserve prices, the presented algorithm can also be used by fixing the upper bound of downward reserve price equal to $\pi_t^{+\max}$ for all iterations (removing step (4)).

## 5.6 Energy Offering Strategy

As already mentioned, the energy offering curves can be submitted to the energy market after the reserve market is cleared and the awarded reserve offers are determined. Therefore, any energy offering curve construction algorithm should take into account the amount of reserve that ERC has sold in the reserve market in advance. In this respect, the proposed energy and reserve scheduling models 5.1 and 5.9, can be applied for obtaining energy offering curves by fixing the value of the variables $q_t^+$ and $q_t^-$ with the quantity of awarded reserve offers $Q_t^{+^{\text{win}}}$ and $Q_t^{-^{\text{win}}}$, respectively.

The energy offering curve at each hour $t$ consists of a set of price-quantity pairs. The quantity can be obtained by the optimal solution of self-scheduled problem ($\sum_k p_{kt}^{c^*}$) considering a given energy price ($\pi_t^{\text{p}}$).

The problem of optimal energy offering curve construction algorithm is deeply investigated in power system literature. Several deterministic and stochastic [84] and a robust [90] energy offering strategy are reported in recent years. Next in this section, we extend a classical deterministic offering strategy proposed by Conejo et al. in [86] to find the optimal energy offering curves for an ERC. The main difference according to [86] is considering the possibility for ERC to offer both the positive and negative energy quantities into the energy market.

Let us assume that $\pi_t^{\text{p}}$ is the energy market price forecast and $\pi_t^{\min}$ and $\pi_t^{\min}$ are the upper bound and the lower bound of the corresponding confidence interval with the confidence level $\alpha$ (e.g. $\alpha = 99\%$). Note that these values can differ from the energy forecast values used for reserve offering strategy since ERC has the possibility to update its energy price forecast after the reserve market is cleared. To obtain the value of the optimal solution $\sum_k p_{kt}^{c^*}$, we should solve the deterministic self-scheduling model (5.1) considering $q_t^+ = Q_t^{+^{\text{win}}}$ and $q_t^- = Q_t^{-^{\text{win}}}$. As a result, constraints (5.1o) and (5.1p) that control the reserve offering variables will be ineffective. Moreover, the second term of the objective function (5.1a), i.e., the revenue from selling upward and downward reserves has no effect on the optimal solution any more.

Regarding the value of the optimal solution $\sum_k p_{kt}^{c^*}$, the following cases are possible.

**case 1:** $0 \leq \sum_k p_{kt}^{c^*} \leq Q_t^{\text{p}max}$ The energy offering curve consists of the following two blocks of energy and corresponding price $(\sum_k p_{kt}^{c^*}, \pi_t^{\min})$ and $(Q_t^{\text{p}max} - \sum_k p_{kt}^{c^*}, \pi_t^{\max})$.

**case 2:** $Q_t^{\text{p}min} \geq \sum_k p_{kt}^{c^*} \leq 0$ The energy offering curve consists of the following two blocks of energy and corresponding price $(\sum_k p_{kt}^{c^*}, \pi_t^{\max})$ and $(Q_t^{\text{p}min} - \sum_k p_{kt}^{c^*}, \pi_t^{\min})$.

where the maximum and minimum allowable quantities for energy offering ($Q_t^{\text{pmax}}$ and $Q_t^{\text{pmin}}$) can be calculated as (5.12)-(5.13).

$$Q_t^{\text{pmax}} = \sum_k P_k^{\text{c}^{\max}} - Q_t^{+^{\text{win}}}, \quad \forall t \tag{5.12}$$

$$Q_t^{\text{pmin}} = -\sum_k P_k^{\text{c}^{\max}} + Q_t^{-^{\text{win}}}, \quad \forall t \tag{5.13}$$

Note that this offering curve algorithm guarantees with a level of confidence of $\alpha$ that the accepted (awarded) energy offer in the market is $\sum_k p_{kt}^{c^*}$, which is the optimal solution.

## 5.7 Case study

To show the effectiveness of the proposed method, a case study based on the characteristic of an ERC in the western part of Switzerland, is presented in this section.

### 5.7.1 Data

The transmission system of ERC has 14 substations (132 KV) which are connected by 16 transmission lines as depicted in Figure 5.5. ERC has three cascaded hydroelectric power plants, which their water reservoirs are connected to each other through one connecting river. The first power plant is connected to bus 1, while the second and the third power plants are connected to bus 2. Table 5.3 shows the technical characteristics as well as the cost coefficients

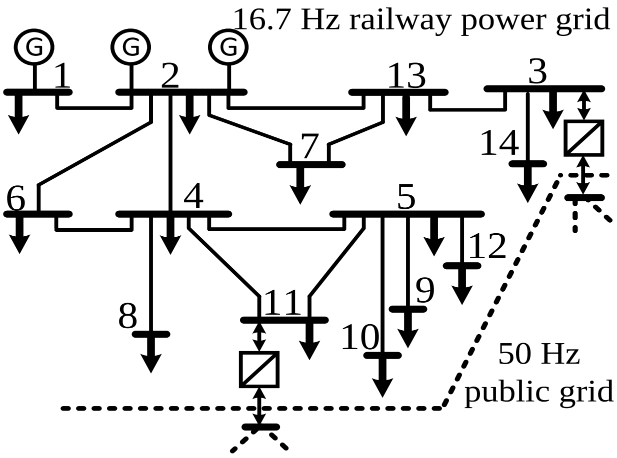


Figure 5.5 – Transmission network of ERC

Table 5.3 – Hydro Power Plants Data

| $h$ | $P_h^{\max}$ | $P_h^{\min}$ | $C_h^{\mathrm{P}}$ | $C_h^{+}$ | $C_h^{-}$ | $C_h^{\mathrm{SU}}$ | $W_h^{\max}$ | $\eta_h$ |
|---|---|---|---|---|---|---|---|---|
| 1 | 92.6 | 10 | 5.7 | 0.5 | 0.1 | 450 | 16 | 0.57 |
| 2 | 8 | - | 1.2 | - | - | - | 8 | 0.9 |
| 3 | 107 | 10 | 6.2 | 0.5 | 0.1 | 550 | 17 | 0.72 |

of the hydroelectric power plants. Moreover, the characteristics of the cascaded reservoirs are presented in Table 5.4. Two bidirectional static frequency converters connect ERC to the public power grid at bus 3 and 11. The rated power of the converters are 40 MW and 60 MW, respectively.

The energy demand estimation for each bus and the total energy demand estimation of ERC is shown in Figure 5.6. The peak of the estimated energy demand is 163 MWh between 8 am and 9 am. The length of the confidence interval for energy demand estimation at each bus ($2\hat{L}_{it}$) is considered to be 10 percent of the estimated energy demand ($\tilde{L}_{it}$). The amount of internal

Table 5.4 – Cascaded Reservoirs data

| Reservoir $m$ | $V_m^{\max}$ ($\mathrm{m}^3 \times 10^3$) | $h \in H_m^{\mathrm{in}}$ | $h \in H_m^{\mathrm{out}}$ | $\xi_m$ ($\mathrm{m}^3/\mathrm{s}$) |
|---|---|---|---|---|
| 1 | 250000 | - | 1 | 6 |
| 2 | 204 | 1 | 2 | 3 |
| 3 | 68 | 2 | 3 | - |

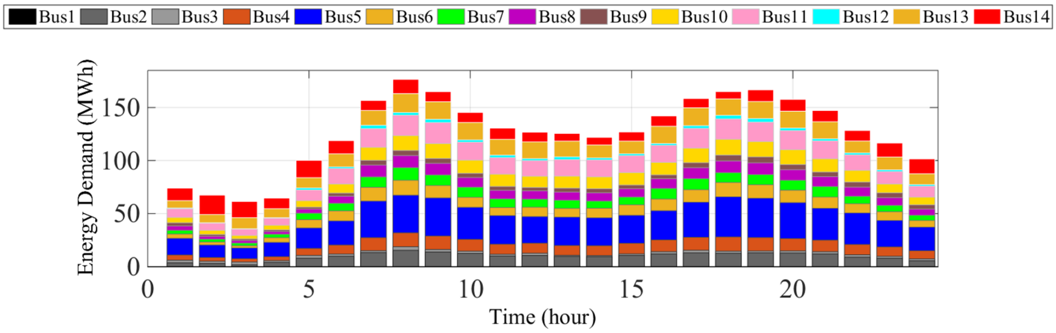


Figure 5.6 – Forecasted energy demand of the railway substations

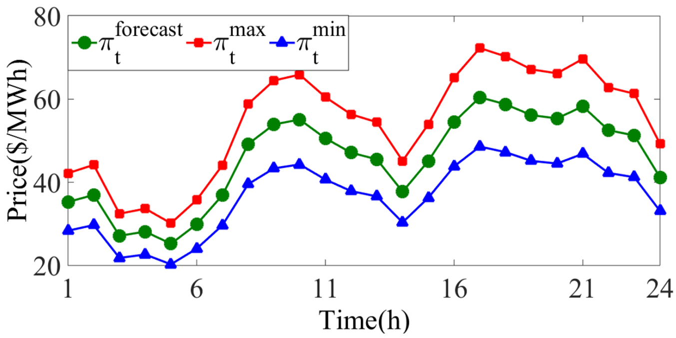


Figure 5.7 – Energy price confidence interval

reserve demand of ERC is 9% of its estimated total energy demand at each hour.

The upward and downward reserve price confidence intervals as well as the estimated prices are plotted in Figure 5.8 and Figure 5.9, respectively. These intervals are derived based on 95% confidence intervals for the error of the reserve price forecast. The energy price forecast and its corresponding confidence interval (95%) based on EPEX day ahead market data for Switzerland (SWISSIX) are also depicted in Figure 5.7.

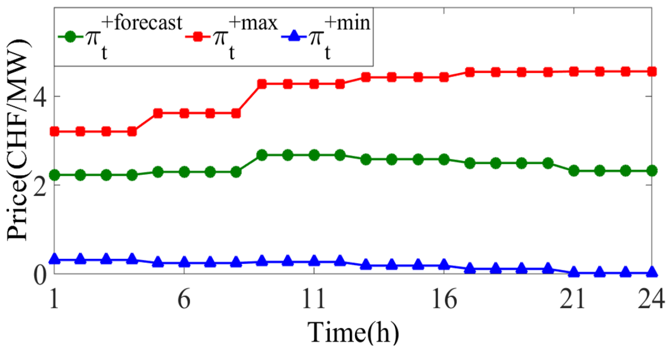


Figure 5.8 – Upward reserve price confidence interval

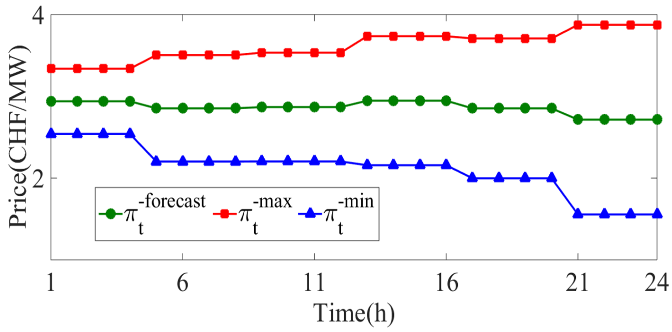


Figure 5.9 – Downward reserve price confidence interval

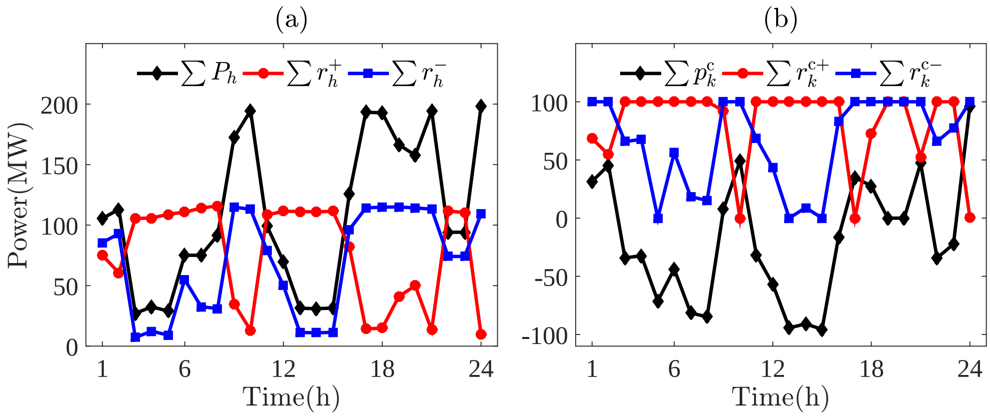


Figure 5.10 – Total hourly energy and reserve schedule for (a) ERC generators and (b) interconnecting converters

### 5.7.2 Results

First the deterministic scheduling problem (5.1a)-(5.1v) is solved while the energy, upward and downward reserve prices are known in advance. The energy, upward and downward reserve prices at each hour are equal to the forecast prices as depicted in Figures 5.7-5.9, respectively. The total hourly energy and reserve schedule of ERC generators and converters are depicted in figure 5.10. The total cost of ERC for the given day is 25564 CHF, including cost of energy and reserve provision (16825 CHF) plus the net cost of energy trading through the converters (15890 CHF) minus the revenue from selling upward and downward reserves (7156 CHF). Note that the net cost of energy trading trough the converters is the cost of buying (32272 CHF) minus the cost of selling energy (16378 CHF). As it can be seen, ERC can compensate more than one fourth of its total cost from participating in the reserve market.

Next, we investigate the effect of uncertainties in the energy demand estimation of the railway substations. As mentioned earlier, the role of parameter $\Gamma_{it}$ is to control the level of robustness

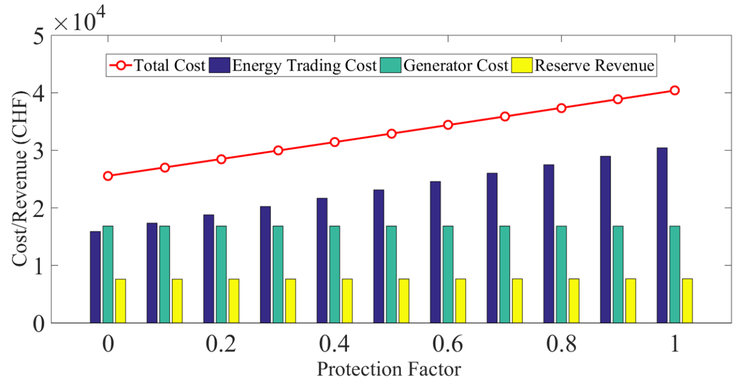


Figure 5.11 – Effect of the protection factor on the costs and the revenues of ERC.

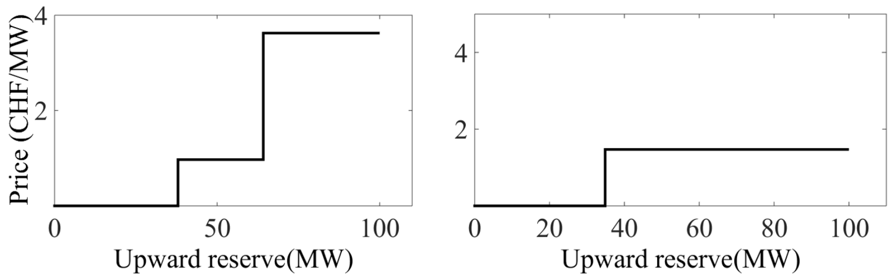


Figure 5.12 – Offering curves for upward tertiary reserve from 8 am to 9 am (left) and from 4 pm to 5 pm (right)

of the solution against the variation in the energy demand of bus $i$ at time $t$. Let us name this value "protection factor", since the higher value of $\Gamma_{it}(\forall i, \forall t)$ means the higher level of protection against uncertainties in the energy demand of the railway substations. The results in Figure 5.11 show that by increasing the level of protection factor, the net cost of trading energy through the converters is increasing while the cost of energy and reserve provision of ERC generators and revenue from selling reserves are not changing significantly. The revenue from selling reserves is slightly reduced from (7156 CHF) to (6861 CHF) while the protection factor is moving from 0 to 1. Therefore, the effect of selling reserves on the security of supply of ERCs demand is negligible. However regarding the increase of the total cost, the trade-off between profitability and robustness of the solution can be seen in Figure 5.11.

To obtain the offering curves for the upward tertiary reserves, problem (5.9a)-(5.9m) is solved for 10 iterations based on the proposed algorithm in section 5.5.2. The problem is solved using CPLEX under GAMS on a Windows based system with four 3.4 GHz processors. The 10 problems (iterations) are solved in 0.3 s. The selected offering curves are shown in Figure. 5.12. Each curve provides pairs of quantity and price for offering. The reserve offering curves provides essential information for ERC to participate in the reserve market.

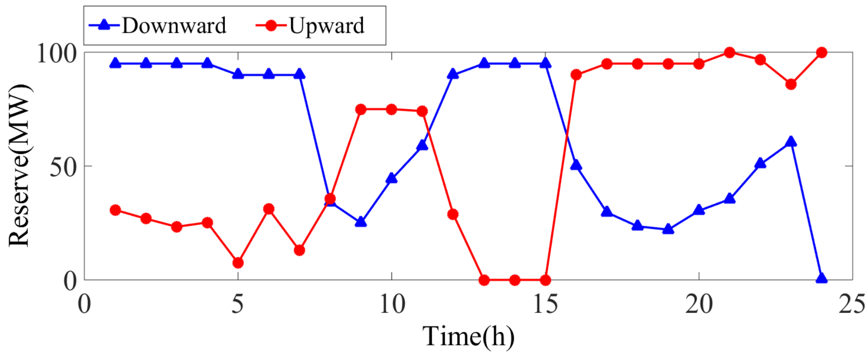


Figure 5.13 – Mean of the hourly awarded offers for randomly generated reserve market price scenarios

To demonstrate the results of the reserve offering, first we have to simulate the reserve and energy market framework as described in section 5.2 (ERC in self-scheduled energy and reserve markets). For this purpose the following simulation has been performed.

1. Run the reserve offering curve algorithm
2. Simulate the reserve market prices and find the awarded reserve offers
3. Run an energy offering curve algorithm considering the fixed amount of provided reserve that are imposed by the awarded reserve offers in 2)
4. Simulate the energy market prices and find the total cost and revenues

From chronological point of view, the above simulation is compatible with the energy and reserve structure as presented in Figure 5.1.

The scenarios associated with price of energy, upward and downward reserves are generated using normal distribution. To build the normal distributions, ARIMA model is used based on historical time series data as proposed in [93]. The mean of normal distribution is the forecast price and the variance is the mean square error of forecasts. Note that this is a realistic price sampling where the upward and downward reserve price scenarios are independently generated based on their corresponding forecasts. The mean of quantity of awarded upward and downward reserve offers is depicted in Figure 5.13.

Next, we compare the proposed reserve offering strategy based on robust energy and reserve scheduling with a deterministic reserve offering. For this purpose, the deterministic offering technique reported in [86] is adopted, based on the solution of the deterministic ERC energy and reserve self-scheduling problem, to find the optimal deterministic reserve offering curve.

Table 5.5 – Comparing of the offering methods

| | Deterministic offering | | Proposed offering | |
|---|---|---|---|---|
| Cost/Revenue (CHF) | Mean | SD | Mean | SD |
| Total Cost | 24231 | 2049 | 20612 | 2636 |
| Energy Trading | 19964 | 2696 | 15503 | 1791 |
| Operation Cost | 9378 | 1481 | 11955 | 1965 |
| Reserve Revenue | 5197 | 940 | 6846 | 728 |

The offering technique uses the estimated prices from ARIMA forecast method to solve deterministic problem (5.1a)-(5.1v). The technique consists in offering the obtained $q_t^{+^*}$ at the minimum price $\pi_t^{+\min}$ and $\sum_k P_k^{c^{\max}} - q_t^{+^*}$ at the maximum price $\pi_t^{+\max}$. It should be noted that this offering technique guarantees with 95% confidence level (the confidence level from forecasting method) that the awarded reserve offer is $q_t^{+^*}$.

Results are obtained and compared in Table 5.5. Note that the energy offering strategy as presented in section 5.6 is also applied in both cases in the third step of simulation, for the sake of fair comparison between reserve offering strategies. Using the proposed method, the total revenue from participating in reserve market is increased from 5197 CHF to 6846 CHF (30% improvement). Moreover, the cost of energy provision including the energy trading cost plus the operational cost is increased by approximately 6.5%. This energy cost reduction alongside with the reserve revenue augmentation leads to reduction of the total cost of ERC. As it can be seen in Table 5.5 the total cost using the proposed offering strategy is 15% lower than traditional deterministic approach. Note that this is "in-sample comparison".

Finally we compare the two offering technique using the actual Swiss energy and reserve market prices on the third week of May 2014 (From 12 to 16). Note that this is an "out of sample" comparison. The results are provided in Table 5.6. The weekly average cost using the proposed method is 9337 CHF which is 23% lower than the weekly average cost using the deterministic method. Even though the reserve revenue using the deterministic method is higher than the proposed method, the total cost is reduced due to consideration of the energy price variation in the proposed reserve offering strategy. It should be noted that high reserve prices at the beginning days of this week lead to very high reserve revenues and consequently very low total cost. In particular on Monday the total cost obtained from the proposed method is negative which means the total energy and reserve trading alongside with operational cost is profitable on this day.

Table 5.6 – Comparing of the offering methods using actual prices

| | Deterministic offering | | Proposed offering | |
|---|---|---|---|---|
| Day | Total Cost | Reserve Revenue | Total Cost | Reserve Revenue |
| Mon | 745 | 28002 | -3626 | 31676 |
| Tue | 5673 | 27774 | 3689 | 24436 |
| Wed | 9204 | 23560 | 7312 | 21568 |
| Thu | 20412 | 12322 | 20494 | 9104 |
| Fri | 25186 | 6369 | 18819 | 9823 |
| average | 12245 | 19605 | 9337 | 19321 |

## 5.8 Summary and Conclusion

This chapter provides an appropriate offering strategy method for an Electric Railway Company (ERC) to participate in reserve markets.

First, the problem of energy and reserve scheduling for ERC is modeled in a deterministic way. The results show that participating in upward and downward tertiary reserve markets is interesting for ERC since it can sell its surplus reserve capacity in the market without threatening the security of supply. As illustrated in the case study section ERC can compensate one fourth of its total cost from participating in the reserve market.

Second, a robust optimization technique is used to solve the energy and reserve scheduling problem taking into account the uncertain energy and reserve prices as well as the uncertain hourly energy demand of the electric railway substations. Moreover, the proposed method provides the control parameters ($\Gamma^{\mathrm{L}}_{it}$) to set the level of robustness of the solution against uncertainties in the energy demands of ERC.

Third, based on the solution of the robust energy and reserve scheduling, a reserve offering curve construction algorithm considering the correlation between upward and downward reserve prices is proposed.

Finally, the effectiveness of the proposed reserve offering method is compared with another offering strategy reported in the literature that is based on the solution of the deterministic scheduling. In this respect a realistic case study based on the characteristic of an ERC in Switzerland is presented.

# 6 Capacity Expansion of Interconnecting Converters

## Chapter Overview

*The power demand of ERPS is expected to increase in the next years. Increasing the capacity of the interconnecting converters is a reasonable solution to deal with this problem. The aim of this chapter is to propose and to investigate several methodologies to assess the capacity expansion of the interconnecting converters. In this respect, the effect of increasing the capacity of the interconnecting converters on the daily operation cost of ERC has been studied. Afterward, the effect of adding new interconnecting converters on the short circuit ratio of ERPS substations has been investigated. Finally, a cost-reliability approach has been proposed to find the optimal size and location of new interconnecting converters.*

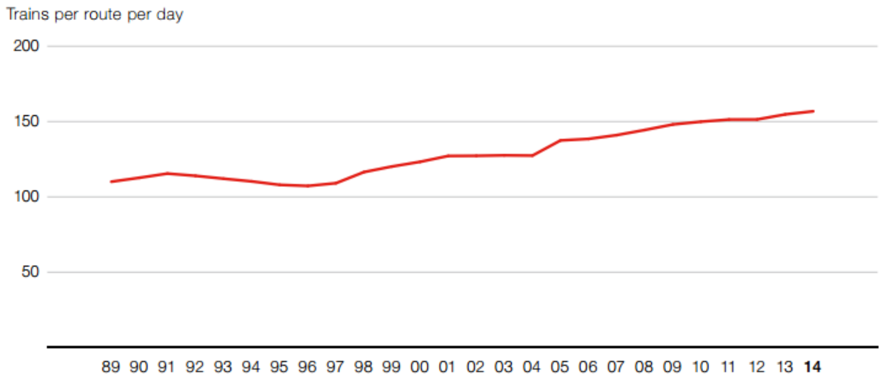


Figure 6.1 – The average number of trains per route per day in Switzerland [95]

## 6.1 Introduction

The railway companies (in particular ERCs) aim to improve the commercial railway transportation services in order to increase the number of passengers and the amount of freight services. To satisfy the railway system demand, ERCs have to either increase the number of circulating trains or increase the speed of the trains. As a result, the power consumption of ERPSs increases year by year. For instance in Switzerland, the average number of trains per route per day is increased from 125 in 2000 to 155 in 2014 as depicted in figure 6.1. Moreover, figure 6.2 shows the increase of passengers and freight services of Swiss railway system in last ten years.

On the other hand, the self-generation capacity of ERC's is not expected to rise in the future. This generation system is mainly composed of the hydro power plants and its expansion is limited due to the geographical and the environmental factors. Despite, the generation expansion in public grid side is more feasible and economic. In fact, the interconnection enables ERC to access to the vast and diverse generation resources that are connected to the public 50 Hz grid. Therefore, the capacity expansion of the interconnecting converters between the two grids plays a decisive role for ERC to satisfy its increasing future power demand [94]. Moreover, as we already discussed in this thesis, the interconnection presents great advantages for both of the power grids. The most important benefits are reliability enhancement, sharing ancillary service resources and energy trading opportunities due to the peak demand diversity.

Within the above context, the aim of this chapter is: 1) to investigate the technical effect and economic effect of increasing the capacity of interconnecting converters and 2) to propose a preliminary model to find the optimal location and size of new converters as well as the size of capacity expansion of the existing converters.

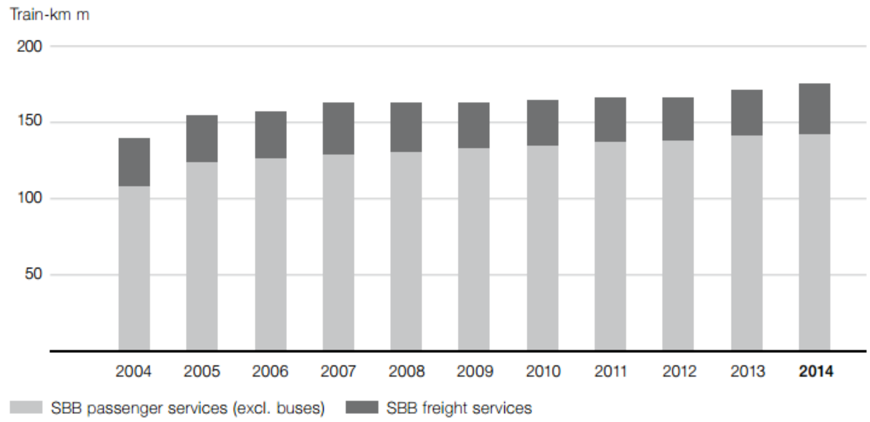


Figure 6.2 – Passenger and freight services in Swiss railway system [95]

To investigate the economic effect of increasing the capacity of the interconnecting converters, the daily energy and reserve scheduling problem under a given set of prices have been solved, taking into account different values for the capacity of the interconnecting converters (more details are presented in section 6.2).

The value of short circuit Ratio (SCR) at a substation, implicitly depicts the strength and the capabilities of the grid on the substation. Hence, SCR is considered as a technical criteria to investigate the technical effect of expanding the interconnecting converters (more details are presented in section 6.3).

Finally an optimization formulation based on a cost-reliability approach is proposed to address the capacity expansion problem. Solving the optimization problem, the possible solutions which satisfy a list of technical constraints, are evaluated under two main criteria:

- Minimizing the investment cost of the interconnections

- Achieving an acceptable reliability level

These two criteria are often contradictory, since a high reliability level is achieved by either increasing the reserve capacity or reducing the component failure rate with redundancies in the system, which implies a large investment costs. In section 6.4, we investigate several ways to deal with this contradiction by incorporating the reliability index within the optimization problem formulation.

## 6.2 Operation Cost Analysis

In this section, we analyze the effect of increasing the capacity of the interconnecting converters on the operation cost of ERC. In this respect, the deterministic energy and reserve scheduling problem as presented in chapter 5 is solved, considering different values for the capacity of the interconnecting converters. Here the energy and reserve prices are fixed and we focus on the total daily operation cost.

In the case study presented in chapter 5 we have seen that the total cost is the cost of energy and reserve provision of ERC's generators, plus the net cost of energy trading through the interconnecting converters, minus the revenue from selling the upward and the downward tertiary reserve services.

The effect of increasing the capacity of the interconnecting converters on the total daily operation cost of ERC is presented in figure 6.3(a). As it can be seen, increasing the capacity of interconnecting converters from 25 MW to 100 MW, drastically decreases the total operation cost. In contrast, capacity expansion from 100 MW to 175 MW slightly decreases the total cost. In fact, the capacity of 175 MW is a saturation point, where any further capacity expansion does not decrease the total cost. This is due to the fact that, considering the given load level, at this capacity of the interconnecting converter, ERC can freely allocate all its resources to minimize the total cost.

Figure 6.3(b) depicts the different cost components of the total operation cost. As it can be seen, increasing the capacity of the interconnecting converters improves the revenue from selling reserve and decreases the cost of energy trading.

We can conclude that, increasing the capacity of the interconnecting converters can effectively decrease the daily operation cost. Note that the operation cost reduction during the amortization period of the new converters, can decrease the long term cost of ERC. However, for a better evaluation, we should consider the expensive investment cost of installing new interconnecting converters. Next, in section 6.4, this problem has been investigated.

## 6.3 Short Circuit Current Analysis

The short circuit ratio for a substation (bus) can be defined as the ratio between the short circuit level (MVA) and the substation rated power [96]. The value of SCR at each substation implicitly depicts the strength and the capabilities of the grid on the substation. Taking the rated power of the substation as the base, the reciprocal of per unit equivalent impedance of

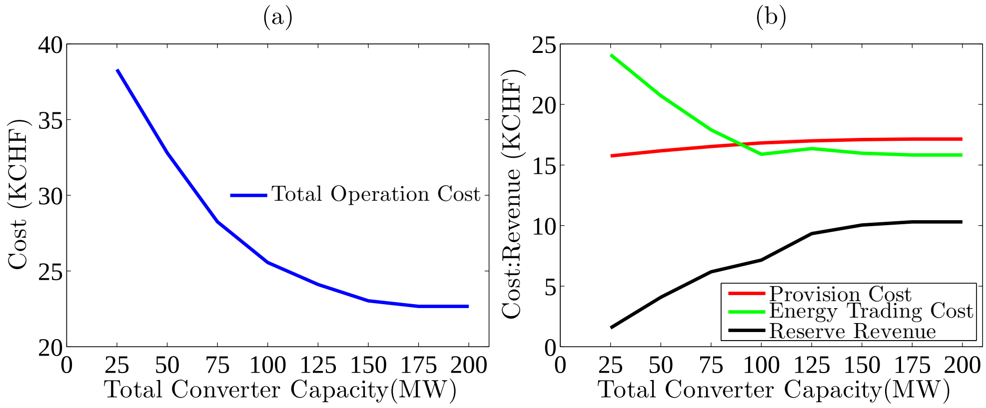


Figure 6.3 – Effect of interconnecting converter expansion: (a) total daily operation cost of ERC and (b) the cost and revenue components.

the network, as viewed from the substation is the SCR at the substation [97].

$$SCR_i = \frac{I_i^{SC}}{I_i^{\text{rated}}} \tag{6.1}$$

where $I_i^{SC}$ and $I_i^{\text{rated}}$ are the short circuit current and the rated (nominal) current at substation $i$, respectively.

We consider the per unit short circuit current of the bus $i$ using a common base, instead of the short circuit ratio at $SCR_i$, to have a relative comparison among different substations. In short, the short circuit current at bus $i$ (i.e., $I_i^{SC}$), can be calculated in a simplified manner as

$$I_i^{SC} = \frac{E_i^{th}}{Z_i^{th}} \tag{6.2}$$

where $E_i^{th}$ and $Z_i^{th}$ are the thevenin equivalent voltage and impedance of the network seen from bus $i$. Taking the rated base voltage, we can assume that the value of $E_i^{th}$ is equal to 1 pu. Moreover, the value of $Z_i^{th}$ is equal to the diagonal element of the network impedance matrix at bus $i$ ($Z_i^{th} = z_{ii}$).

$$I_i^{SC} = \frac{1}{z_{ii}} \tag{6.3}$$

For the purpose of short circuit current calculation, the interconnection can be modeled using the equivalent model from the connection point. The equivalent impedance $Z_{\text{eq}}$ includes the impedance of the frequency converter, the connecting transmission line, the transformers and the equivalent impedance of the public grid seen from its connected bus. The equivalent impedance of the public grid is very small, since the network is highly meshed. Moreover, the impedance of the transmission line and transformers are low in comparison with the frequency converters. Hence,

$$Z_{eq} \approx X_{\text{conv}} \tag{6.4}$$

We can modify the impedance matrix of the ERPS considering the per unit value of $X_{\text{conv}}$ to calculate the effect of adding the interconnecting converter on the per unit short circuit current of the ERPS substations. Note that the rated (nominal) power of the interconnecting converter ($P_{\text{conv}}^{\text{rated}}$) is proportional to the reverse of per unit value of $X_{\text{conv}}$.

$$P_{\text{conv}}^{\text{rated}} \propto \frac{1}{X_{\text{conv}}} \tag{6.5}$$

Let us define $Y^{\text{old}}$ and $Y^{\text{new}}$ as the ERPS admittance matrix before and after adding a new interconnecting converter to bus $j$, respectively. We have

$$Y^{\text{old}} = \begin{bmatrix} y_{11} & y_{12} & \cdots & y_{1n} \\ y_{21} & y_{22} & \cdots & y_{2n} \\ \vdots & \vdots & \ddots & \vdots \\ y_{n1} & y_{n2} & \cdots & y_{nn} \end{bmatrix} \tag{6.6}$$

$$Y^{\text{new}} = \begin{bmatrix} y_{11} & \cdots & y_{1j} & \cdots & y_{1n} \\ \vdots & \vdots & \ddots & \vdots & \\ y_{j1} & \cdots & y_{jj} + \frac{1}{X_{\text{conv}}} & \cdots & y_{jn} \\ \vdots & \vdots & \ddots & \vdots & \\ y_{n1} & \cdots & y_{nj} & \cdots & y_{nn} \end{bmatrix} \tag{6.7}$$

Now we can obtain the diagonal element of the new impedance matrix using the inverse of the new admittance matrix as follows:

$$z_{ii}^{\text{new}} = Y^{\text{new}-1}(i,i) \tag{6.8}$$

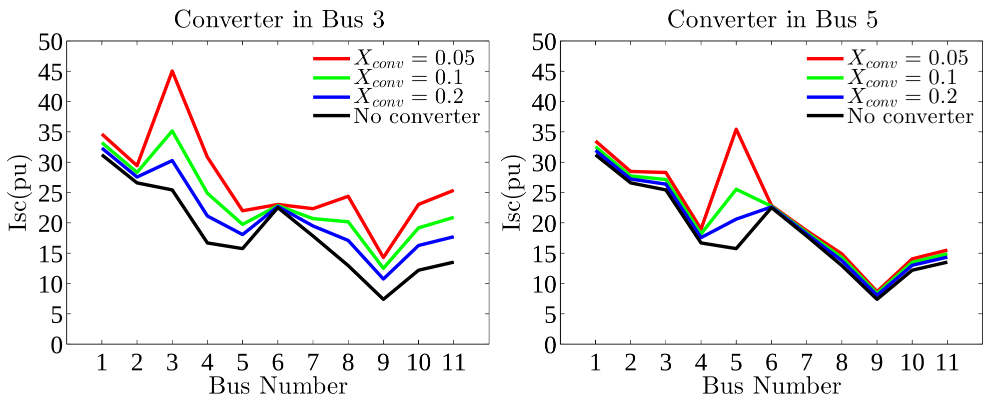


Figure 6.4 – Effect of adding a new interconnecting converter on the nodal short circuit currents

Hence,

$$I_i^{\text{SC,new}} = \frac{1}{z_{ii}^{\text{new}}} = \frac{1}{Y^{\text{new}-1}(i,i)} \tag{6.9}$$

### 6.3.1 Case Study

Taking the Swiss ERPS network in the western part of Switzerland, figure 6.4 depicts the per unit short circuit current at every bus when a new interconnecting converter is located at buses 3 and 5, separately. Moreover the short circuit currents before adding the interconnecting converter are also presented in this figure. Note that the base current and the base voltage for per unit calculation are 757A and 132KV, respectively.

Figure 6.5(a) presents the improvement in the total per unit short circuit current of all buses ($\Delta I_{\text{tot}}^{\text{SC}}$) while a converter is located in different buses. As it can be seen, from SCR point of view, bus 4 is the best option for adding a new interconnecting converters.

$$\Delta I_{\text{tot}}^{\text{SC}} = I_{\text{tot}}^{\text{SC,new}} - I_{\text{tot}}^{\text{SC,old}}; \qquad I_{\text{tot}}^{\text{SC,new}} = \sum_j I^{\text{SC,new}} \tag{6.10}$$

In general, from SCR point of view, two types of solution (size and location of converters) can be considered. In the first type of solutions, there will be only few but large converters that are connected at the strongest (from SCR point of view) buses of the network. As we have seen earlier, in this case bus 4 is the best solution. In the second type of solutions, there are more but small converters that are connected at both of the strong and weak nodes of the network. To evaluate this solution, we have equally distributed the total interconnection capacity ($1/X_{conv}$) among all the buses. Figure 6.5(b) presents the obtained improvement

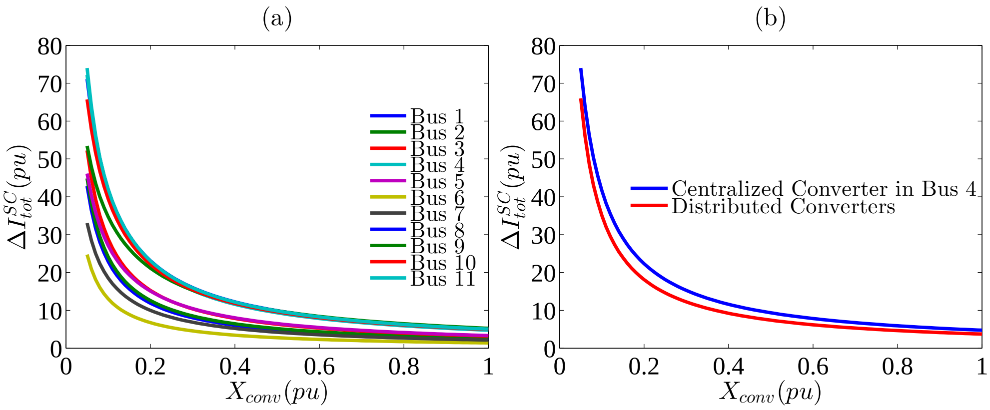


Figure 6.5 – (a) Effect of adding a new interconnecting converter on the total per unit short circuit current (b) Centralized converter vs distributed converters

in total per unit short circuit current of the system derived from adding these distributed converters. Moreover the results are compared with the case that a single converter (with the size equal to the total size of the distributed converters) is located in bus 4. As it can be seen in this figure, the results for a centralized converter is slightly better than the results for the distributed converters.

More discussions and case studies on the effect of adding new interconnecting converters on SCR of the ERPS substations are presented in [98]. Note that the SCR analysis provides some insight on the technical aspects of interconnecting converter capacity expansion problem, However, it does not consider some very important aspects such as the system reliability and the investment cost. These aspects have been addressed in the next section of this chapter.

## 6.4 Cost-Reliability Approach

This section proposes a way to find the optimal locations and capacities for the new interconnections and the optimal capacity expansion for the existing interconnections.

The problems of transmission capacity expansion [99, 100, 101] and substation expansion planning [102, 103, 104] have been deeply investigated in power system literature. However, the problem of interconnection expansion planning between two different networks is not effectively investigated.

The high cost of the elements involved in the interconnections between the ERPS and the public power grid makes it crucial to develop an economic analysis of the problem alongside with the technical analysis.

Here an optimization formulation based on a cost-reliability approach is proposed to address the capacity expansion problem. Solving the optimization problem, the possible solutions which satisfy a list of technical constraints, are evaluated under two main criteria:

- Minimizing the investment cost of the interconnections

- Achieving the acceptable reliability level

These two concepts are often contradictory since a high reliability level is achieved by increasing the reserve capacity or reducing the component failure rate with redundancies in the system, which implies a large investment costs. Here we propose several ways to deal with this contradiction by modifying the role of the reliability indexes within the problem formulation.

The reliability level of a power system can be measured by means of different indexes. Two well known indexes are used in this section, the "loss of load probability" (LOLP) and the "expected load not served" (ELNS).

The LOLP indicates the probability that the available generation and interconnection capacity cannot cover the load of the system. It can also be seen as the portion of the time that the system will suffer from some loss of load. This index can be computed adding the outage probabilities for every possible combination of single or simultaneous outage, only if it causes some loss of load.

The rest of this section is organized as follows: The problem description is presented in section 6.4.1. The calculation and incorporation of the reliability indexes into the optimization problem are discussed in section 6.4.2. Next, the expansion of the interconnection between the Swiss ERPS and public grid in the western part of Switzerland is considered as a case study in section 6.4.3

### 6.4.1 Problem Description

#### Investment Cost

The investment cost is the installation cost of new interconnections and the expansion cost of the existing ones. The cost of installation of new interconnections involves the cost of the transmission line, which depends on the capacity and the distance between the connected substations in both sides, and the cost of the interconnecting converters, which depends on the capacity of the interconnection. The cost of expansion of existing interconnections depends on the expansion capacity. Therefore, the investment cost can be formulated as

$$c^{\text{inv}} = \sum_{(i,j)\notin\mathscr{E}} \left(c^{\text{L}}_{ij} u_{ij} D_{ij} + c^{\text{IC}}_{ij} u_{ij}\right) + \sum_{(i,j)\in\mathscr{E}} c^{\text{E}}_{ij} \tag{6.11}$$

where $i$ and $j$ are the index for substations in the ERPS and the public grid sides, respectively. The pair of substations $(i, j)$ is a candidate for locating a new interconnecting converter or expanding the capacity of the existing converter. Note that $\mathscr{E}$ is the set of substation pairs where an interconnecting converter is already existing. In the first term of (6.11), the binary variable $u_{ij}$ represents the state of the interconnection between substations $i$ and $j$. After solving the optimization problem, if $u_{ij} = 1$, there will be a new interconnection between these substations. The parameter $D_{ij}$ is the distance between substations. The optimization variables $c^{\text{L}}_{ij}$ and $c^{\text{IC}}_{ij}$ represent the transmission line and the interconnecting converter costs, respectively. Here in (6.12) and (6.13) these cost variables are modeled as a linear function of the rated power (size) of the interconnection.

$$c^{\text{L}}_{ij} = A^{\text{L}} + B^{\text{L}} p_{ij} \tag{6.12}$$

$$c^{\text{IC}}_{ij} = B^{\text{IC}} p_{ij} \tag{6.13}$$

where $A^{\text{L}}, B^{\text{L}}$ and $B^{\text{IC}}$ are the linear cost coefficients corresponding to transmission lines and interconnecting converters, respectively. The optimization variable $p_{ij}$ is the rated power of the interconnection in the candidate substation pair $(i, j)$.

The cost of capacity expansion for the existing interconnections $c^{\text{E}}_{i,j} : (i, j) \in \mathscr{E}$ can be formulated as a linear function of the size of the capacity expansion ($p^{\text{E}}_{i,j}$) as follows:

$$c^{\text{E}}_{ij} = B^{\text{E}} p^{\text{E}}_{ij} \tag{6.14}$$

where the value of the expansion cost coefficient $B^{\text{E}}$, is slightly lower than the value of $B^{\text{IC}}$. In general, it is difficult to estimate the cost of the components. The estimations made in this work are based on the historical financial data or market data in Switzerland.

Finally, it should be noted that the presented investment cost formulation in (6.11) is nonlinear as it includes the production of binary and continuous variables (e.g., $u_{ij}$ and $c^{\text{L}}_{ij}$). In this respect, a linearization technique as described in the Appendix B is applied to tackle this non-linearity.

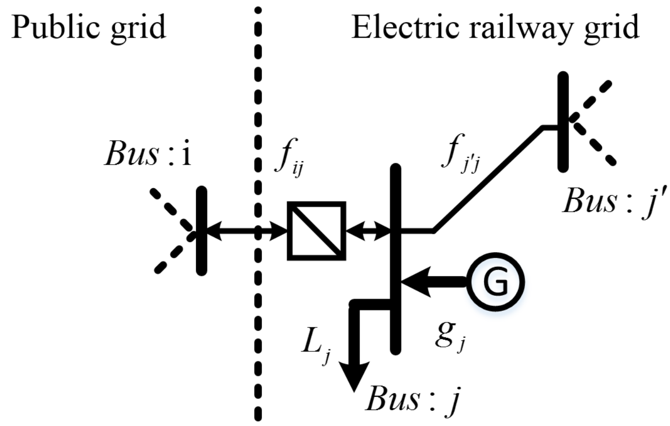


Figure 6.6 – Power flows associated with the bus $j$ of ERPS

### Technical constraints

The main technical constraints of the problem are, the nodal power balance, voltage level constraint of the candidate substations and power flow limits of the transmission lines.

**Power Balance** The power balance at each substation of ERPS as presented in figure 6.6 is formulated in (6.15).

$$\sum_i f_{ij} + \sum_{j'} f_{j'j} + g_j = L_j, \quad \forall j \tag{6.15}$$

where $f_{ij}$ and $f_{j'j}$ are the power flow from the public grid substation $i$ and the ERPS substation $j'$ to the substation $j$. The variable $g_j$ and the parameter $L_j$ are the generated power and the power demand at bus $j$. Here in this problem, the generated power is simply constrained by the rated power of the generator ($G_j$).

$$0 \le g_j \le G_j, \quad \forall j \tag{6.16}$$

**Power Flow Limit** The optimal location and capacity of the interconnections must ensure the transmission of energy to the load points, avoiding any line congestion during a normal operation state. This implies that the power flow through each line of ERPS must be constrained by the maximum transmission capacity of the line (6.17). Also, the power flow between the two grids at each interconnection is limited to the capacity of the interconnection (6.18)-(6.19).

$$-F_{j'j}^{\max} \le f_{j'j} \le F_{j'j}^{\max}, \quad \forall j \tag{6.17}$$

where $F_{j'j}^{\max}$ is the capacity of the transmission line between buses $j$ and $j'$.

$$-p_{ij} \le f_{ij} \le p_{ij}, \quad \forall (i,j) \notin \mathscr{E} \tag{6.18}$$

$$-(p_{ij}^{\mathrm{E}} + P_{ij}^{\mathrm{E}}) \le f_{j'j} \le p_{ij}^{\mathrm{E}} + P_{ij}^{\mathrm{E}}, \quad \forall (i,j) \in \mathscr{E} \tag{6.19}$$

where the parameter $P_{ij}^{\mathrm{E}}$ represents the capacity of the existing converters.

**Voltage Level Constraint** The high voltage network of the public grids includes several voltage levels (e.g., 380 KV and 220 KV). In fact, it is not possible to connect a low power converter to a very high voltage substation and vice versa. Hence, the capacity of the interconnection is also constrained by the voltage level of the substation in the public grid side. Here the public grid substations are partitioned into three groups depending on their appropriate interconnection capacity range. Since each group has its allowed capacity range, we have

$$\underline{P^{\mathrm{V1}}} \le p_{ij} \le \overline{P^{\mathrm{V1}}}, \quad i \in \mathscr{S}^{\mathrm{V1}} \tag{6.20}$$

$$\underline{P^{\mathrm{V2}}} \le p_{ij} \le \overline{P^{\mathrm{V2}}}, \quad i \in \mathscr{S}^{\mathrm{V2}} \tag{6.21}$$

$$\underline{P^{\mathrm{V3}}} \le p_{ij} \le \overline{P^{\mathrm{V3}}}, \quad i \in \mathscr{S}^{\mathrm{V3}} \tag{6.22}$$

where $\underline{P^{\mathrm{Vk}}}$ and $\overline{P^{\mathrm{Vk}}}$ are the lower and the upper bound of the appropriate capacity range for the set of public grid substation $\mathscr{S}^{\mathrm{Vk}}$ $(k = 1, 2, 3)$.

**Reliability Criteria**

There are two approaches to include the reliability criteria in the optimization model. The first approach introduces a new constraint in the problem formulation that sets a minimum acceptable reliability level. This level can be defined using both of the reliability indexes. However, the ELNS provides a better idea of the system reliability since it considers the loss of load probability resulting from the different outages and the amount of load curtailed as a consequence of those outages.

$$ELNS \leq ELNS^{\text{desired}} \tag{6.23}$$

The second approach presents a way to find a balance between the investment cost and the desired reliability level. This balance can be achieved considering both of the issues in the objective function: a cost is associated to each expected megawatt not served and this cost is added to the investment cost in the updated objective function.

$$\min c^{\text{inv}} + c^{\text{ELNS}} \tag{6.24}$$

In order to be able to compare both of the costs, the $c^{\text{ELNS}}$ has to be defined as an operating cost, i.e. it must be evaluated over the amortization time ($T$) of the new interconnecting converters:

$$c^{\text{ELNS}} = \sum_{t=1}^{T} ELNS(t) \cdot UC \tag{6.25}$$

Where $UC$ is the estimated unitary cost of load not served in $[CHF/MW]$. It is important to remark that the $UC$ must consider not only the energy price but also the consequences that a lack of supply has on the demand.

Like the previous approach, here it is possible to incorporate the demand features of the power system (i.e. the sensitivity of the demand against a loss of load) in the formulation, by modifying the value of the $UC$. The advantage of this approach is that it evaluates the two main issues of the problem and finds the best solution that balances both of the costs.

### 6.4.2 Reliability Index Calculations

The reliability of the system can be checked by its answer to the following question: when a contingency occurs, are the remaining elements able to handle the new situation in order to satisfy the loads? In this respect, to calculate the reliability index for ERPS, the availability of generators and interconnecting converters are considered.

Here we assume that the system is compacted in one node including all the generation sources and the loads.

The probability of the outage of a single element of the system (generator or interconnecting converter) can be calculated as the probability of that element being unavailable times the rest of the elements being available:

$$\Phi_k^1 = U_k \cdot \prod_{r=1;\ r\neq k}^{n} A_r \tag{6.26}$$

where $A_r$ and $U_k$ are the availability and the unavailability of the elements $r$ and $k$, respectively. With the same reasoning, we can calculate the probability of the simultaneous outages of two elements ($k$ and $w$) as

$$\Phi_{kw}^2 = U_k \cdot U_w \cdot \prod_{r=1;\ r\neq k,w}^{n} A_r \tag{6.27}$$

Since the purpose of the problem is to determine the optimal number and capacity of interconnections, we can generalize these equations to include every possible interconnection. This requires the addition of a set of binary variables $u_k$ associated with every possible element of the system, i.e. all the generators and all the possible interconnecting converters. These variables will take the value 1, if the element $k$ is finally scheduled in the optimal solution. In other words, they will be 1 for all the generators (since they are already part of the system) and 1 or 0 for the possible interconnections depending on whether they are included or not in the optimal solution. For the interconnection between substations $i$ and $j$, $u_k$ is equal to $u_{ij}$.

Hence, the probability of a single and double outage can be generalized as

$$\Phi_k^1 = U_k u_k \cdot \prod_{r=1;\ r\neq k}^{n} 1 - u_r U_r \tag{6.28}$$

$$\Phi_{kw}^2 = U_k u_k \cdot U_w u_w \cdot \prod_{r=1;\ r\neq k,w}^{n} 1 - u_r U_r \tag{6.29}$$

The same reasoning can be used to calculate the probabilities of the simultaneous outages of more than two components.

Note that the outage of certain elements of the system might be acceptable as long as the remaining elements can wholly supply the load without loss of continuity (i.e. it does not cause a loss of load). Consequently, in order to assess the reliability level of the system, a new set of binary variables $\sigma_k$ is included in the problem. The variable $\sigma_k$ indicates whether the outage of element $k$ causes a loss of load ($\sigma_k = 1$) or not ($\sigma_k = 0$). This variable can be modeled by the following linear inequalities.

$$\frac{L - \sum_{r=1;\ r\neq k}^{n} P_r}{\sum_{r=1}^{n} P_r} \leq \sigma_k \leq 1 + \frac{L - \sum_{r=1;\ r\neq k}^{n} P_r}{\sum_{r=1}^{n} P_r} \tag{6.30}$$

Where $L$ represents the total load of the system and $P_r$ is the capacity of the element $r$. From the previous expression, when element $k$ is out, if the rest of the elements can cover the load ($\sum_{r=1;\ r\neq k}^{n} P_r > L$), the lower boundary of $\sigma_k$ will be relaxed but the upper boundary will be lower than one; hence, $\sigma_k$ will be 0. Otherwise, if the remaining capacity cannot cover the load ($\sum_{r=1;\ r\neq k}^{n} P_r < L$), the lower boundary will be greater than zero and the upper boundary will be relaxed; hence, $\sigma_k$ will be 1.

Since a double outage has also been considered in this study, a second set of binary variables must be defined in order to indicate the presence of the loss of load caused by a double outage. These variables ($\sigma_{kw}$) are modeled as follows

$$\frac{L-\sum_{r=1;\ r\neq k,w}^{n} P_r}{\sum_{r=1}^{n} P_r} \leq \sigma_{kw} \leq 1+\frac{L-\sum_{r=1;\ r\neq k,w}^{n} P_r}{\sum_{r=1}^{n} P_r} \tag{6.31}$$

Now the LOLP index can be computed by adding the outage probabilities for every possible combination of single or simultaneous outages, only if it causes some loss of load. The formulation is as follows

$$LOLP = \sum_{k=1}^{n} \sigma_k \Phi_k^1 + \sum_{k=1}^{n} \sum_{w>k}^{n} \sigma_{kw} \Phi_{kw}^2 + \ldots \tag{6.32}$$

The ELNS can be obtained by multiplying the probability of every single or double outage state by the loss of load caused by the outage.

$$ELNS = \sum_{k=1}^{n} \sigma_k \Phi_k^1 \cdot \left( L - \sum_{r=1;\ r\neq k}^{n} P_r \right) + \sum_{k=1}^{n} \sum_{w>k}^{n} \sigma_{kw} \Phi_{kw}^2 \cdot \left( L - \sum_{r=1;\ r\neq k,w}^{n} P_r \right) + \ldots \tag{6.33}$$

These two indexes provide useful information about the reliability level of the system. However, the expressions above present one obstacle from computational point of view; they are not linear with respect to the variables of the problem ($\sigma_k, \sigma_{kw}, u_k, P_r$). This obstacle can be solved by linearizing the equations. The linearization technique is presented in the Appendix B.

As we discussed in chapters 4 and 2, the load of ERPS is highly fluctuating. There are many parameters influencing the load level. Therefore, we consider the load of the system in a probabilistic way in order to improve the accuracy of the proposed method. This means that the load does not have a deterministic value, hence, it can be represented by a discrete probability distribution function as follows

$$\rho_m = \text{Probability}(L_{m-1} < L \leq L_m) \tag{6.34}$$

Table 6.1 – Maximum load at ERPS substations

| Substation | R1 | R2 | R3 | R4 | R5 | R6 | R7 | R8 | R9 | R10 | R11 | Sum |
|---|---|---|---|---|---|---|---|---|---|---|---|---|
| $L$(MW) | 43.6 | 50 | 30 | 43.6 | 21.8 | 21.8 | 15 | 21.8 | 21.8 | 10.9 | R11 | 310.3 |

$$\sum_{m=1}^{N_L} \rho_m = 1 \tag{6.35}$$

where $N_L$ is the total number of the load levels. For each load level ($L_m$), the value of reliability indexes $LOLP_m$ and $ELNS_m$ could be found using the equations (6.32)-(6.33). Then, the values of reliability indexes of the system considering the load variations are as follows:

$$LOLP = \sum_{m=1}^{N_L} \rho_m LOLP_m \tag{6.36}$$

$$ELNS = \sum_{m=1}^{N_L} \rho_m ELNS_m \tag{6.37}$$

Note that the above discrete probability distribution function does not affect the power balance equation in (6.15). In fact, in the power balance equation, the load $L_j$ is the maximum power demand at substation $j$.

### 6.4.3 Case study

The Swiss ERPS in the western part of Switzerland is considered as a case study. ERPS in this region has 11 substations (R1,...,R11) at 132 KV, 12 transmission lines and 2 generators. The maximum load of the ERPS substations is presented in Table 6.1. The hydro power generators are connected to bus R1 (92.6 MW) and R2 (107 MW). Five load levels are considered to model the load variations at each substation. Figure 6.7 shows the discrete probability distribution function of the daily load at substation R4. The public grid in this region includes 20 substations at 220 KV and 2 substations at 380 KV (N1,...,N22), 29 transmission lines and 6 generators.

It can be seen in Table 6.1 that the load of the railway system in this region is less than its generation. The aim of this case study is to find the size and the location of new interconnecting converters to cover the load with minimum investment cost. This cost minimization is constrained by the technical constraints (6.15)-(6.22) and the reliability constraint (6.23).

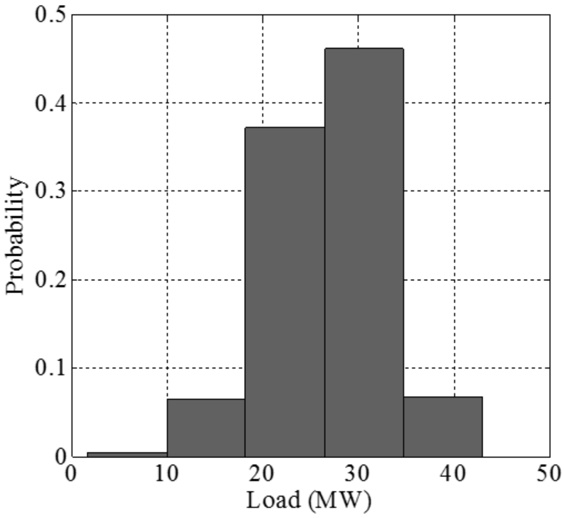


Figure 6.7 – Discrete probability distribution of the load at substation R4

Table 6.2 – Cost coefficients and unavailability parameters

| $B^{\mathrm{IC}}(\frac{\mathrm{CHF}}{\mathrm{MW}})$ | $A^{\mathrm{L}}(\frac{\mathrm{CHF}}{\mathrm{Km}})$ | $B^{\mathrm{L}}(\frac{\mathrm{CHF}}{\mathrm{MW.Km}})$ | $U^{\mathrm{converter}}$ | $U^{\mathrm{generator}}$ |
|---|---|---|---|---|
| 737500 | 475000 | 250 | 0.02 | 0.05 |

Note that, to find the reliability index in (6.23) as function of the optimization variables, the equations (6.29)-(6.33) and (6.36)-(6.37) have to be considered as equality and inequality constraints in the optimization problem.

The economic parameters (cost function coefficients) and the reliability parameters (unavailability of the converters and generators) are presented in Table 6.2. The only applied voltage level constraint is that the minimum capacity of the candidate interconnection to be connected at a 380 KV substation is 25 MW. A schematic of the geographic distribution of the substations in the two grids is depicted in figure 6.8. The distances between the substations of the two grids vary from 2.7 Km to 106 Km. It is also assumed that the public power grid can support the converters with a maximum capacity lower than 100 MW.

Table 6.3 – The optimal location and size of new interconnecting converters

| $ELNS^{\text{desired}}$ | Capacity (MW) | Public grid substation | ERPS substations |
|---|---|---|---|
| 0.1 MW | 74.1 | P18 | R2 |
| | 36.6 | P10 | R10 |
| | 36.6 | P8 | R6 |
| 0.01 MW | 20.9 | P18 | R2 |
| | 89.8 | P2 | R1 |
| | 89.8 | P8 | R6 |

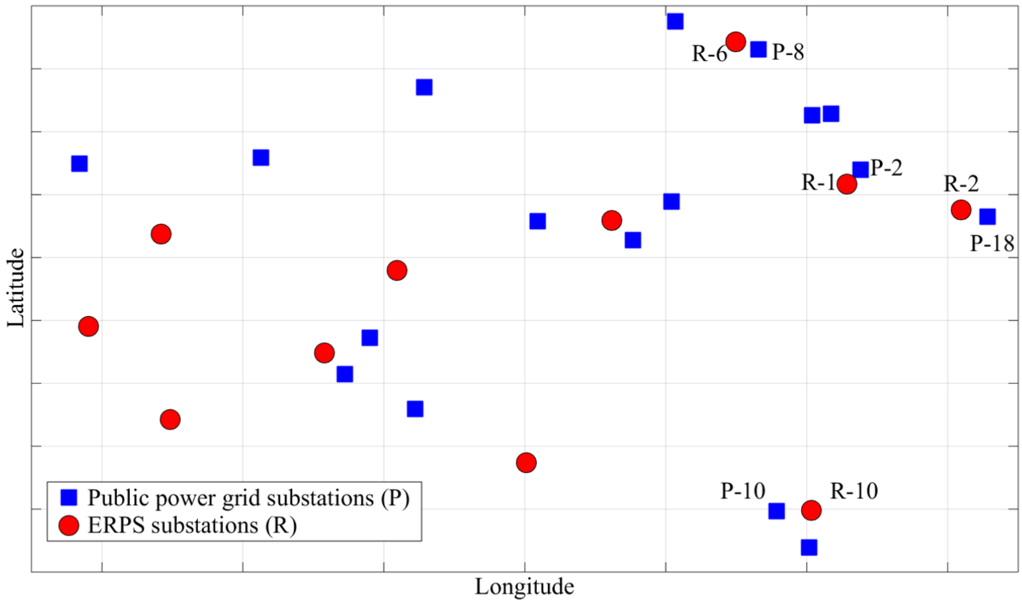


Figure 6.8 – Location of the substations

The linearized optimization problem has been implemented in the GAMS environment. Table 6.3 shows the optimum location and the optimum size of the new converters while two desired values for ELNS of the railway system have been considered. The investment costs for $ELNS^{\text{desired}}$ equal to 0.1 and 0.01 are 11.3 MCHF and 15.3 MCHF, respectively.

The solution of the optimization problem depends on the desired value of reliability indexes. Therefore, a sensitivity analysis has been done to investigate the effect of $ELNS^{\text{desired}}$ on the solution. Figure 6.9 and figure 6.10 show the change in the minimum investment cost and the total capacity of new converters by changing the desired value of ELNS. Not surprisingly, both of the figures indicate that the high total size and consequently the high investment cost are required to achieve the high reliability level.

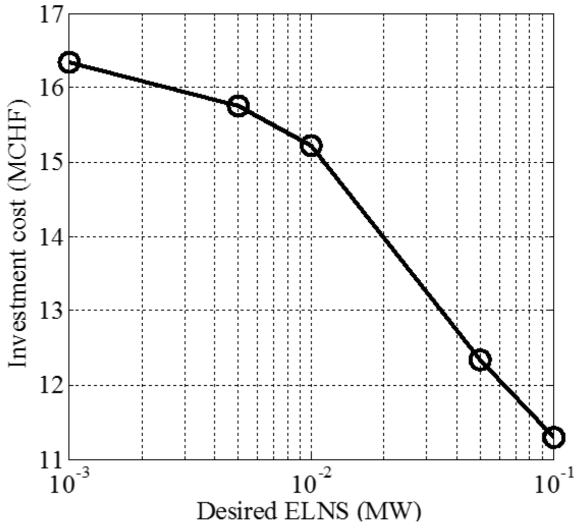


Figure 6.9 – Minimum investment cost as a function of desired level of ELNS

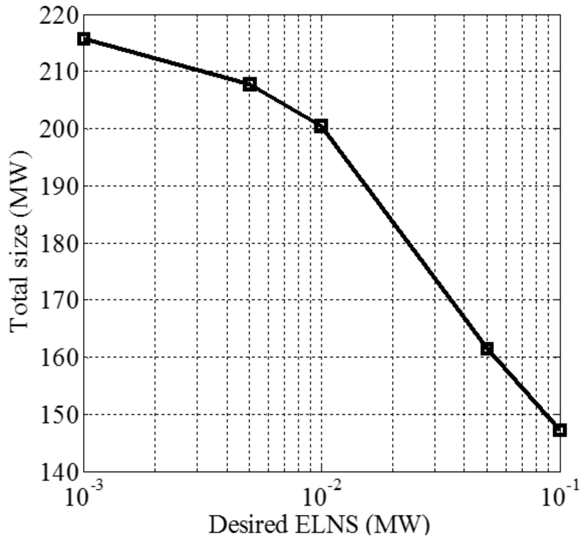


Figure 6.10 – Total optimal size of the interconnecting converters as function of desired level of ELNS

## 6.5 Summary and Conclusion

In this chapter, several methodologies to assess the capacity expansion of the interconnecting converters has been investigated.

First, the effect of increasing the capacity of the interconnecting converters on the daily operation cost of ERC has been studied. The study shows that in certain cases (depending on the capacity of the existing converters) the capacity expansion leads to a huge operation cost reduction.

Second, the effect of adding new interconnecting converters on the short circuit ratio of ERPS substations has been investigated. The results show that adding a centralized converter in a strong substation of the system is more beneficial than adding several distributed converters all over the system, in terms of improving the system total per unit short circuit current.

Finally a cost-reliability approach has been proposed to find the optimal size and location of new interconnecting converters. This has allowed us to provide ERC with a set of optimal solutions according to the different economic and technical criteria.

# 7 Conclusions

The first aim of this thesis is to develop appropriate methods and strategies aiming to allocate and dispatch the energy and reserve services in the interconnected system including electric railway and public power grids. The second aim is to propose and to assess models for finding the optimal interconnecting converter capacity expansion in order to maximize the benefits that can be delivered from the interconnection. In this respect, the following three main problems have been studied in this thesis.

1. Joint energy and reserve scheduling for an electric railway power system under uncertainties (Operation)
2. Offering strategy methods for an electric railway company in energy and reserve markets (Market Strategy)
3. Capacity expansion of the interconnecting converters in interconnected system including electric railway and public power grids (Capacity Expansion)

Next, in this closing chapter, a summary and a list of relevant conclusions drawn from these studies are presented. Finally, in continuation of this work, some topics are suggested for future possible research.

## 7.1 Summary and Conclusions

### Joint energy and reserve scheduling for an electric railway power system under uncertainties

In this study the problem of joint energy and reserve scheduling in an ERPS has been addressed. In this problem, the variation of energy demand at each substation from its forecast value is an uncertain parameter. To investigate the characteristics of this uncertain parameter, a short term load forecast method based on ARIMA time series is applied using realistic data from Swiss ERPS . The results of this study, demonstrate the spatial and the temporal correlations among the energy demand of ERPS substations.

Next, joint energy and reserve scheduling problem has been formulated as a two stages optimization problem including first (day ahead) and second (balancing) stages. Two mathematical approaches, namely, adaptive robust optimization (ARO) and stochastic optimization (SO) are proposed for dealing with uncertainties in this scheduling problem.

The uncertainty and risk management using ARO approach is more conservative and risk averse. This method, effectively considers the temporal and spatial correlation between energy demand forecast error at the ERC substations. In fact, the day-ahead obtained schedule (solution) guarantees that the balancing problem is feasible for any realization and optimal for the worst realization of the uncertain energy demand at substations within the uncertainty set. Since the uncertainty set is obtained considering the nodal load forecast error, the obtained schedule can guarantee the security of supply with a very high level of confidence. In contrast, the uncertainty management using SO approach is based on a probabilistic representation of the uncertain parameters. Here, the level of the security of the system depends on the value of maximum acceptable expected load not served ($ELNS^{\max}$).

Moreover, the proposed ARO approach provides the control parameters to control the level of robustness of the obtained solution against the energy demand variations. This robustness is desirable for ERCs where security of supply is the first objective. However, the main drawback of this approach is that the computation tractability imposes that the second stage problem has to be linear including only continuous variables.

On the contrary, the proposed two stages stochastic optimization method is more flexible in the sense that both of the first and second stage formulation can contains binary variables. Here, the two stage problem formulation is improved to include some detailed technical considerations such as interconnecting converter losses and the aggregation of energy imbalances over all converters. Moreover, the proposed method covers the uncertainties associated with the availability of generators and interconnecting converters in the balancing stage.

The numerical results show that ERC can effectively utilize the interconnecting converters for energy trading and selling reserve without threatening its security of supply.

Finally, these two approaches have been compared considering different criteria such as uncertainty and risk management approach, required information from the uncertain parameter, the obtained total cost, solution computation time and modeling limitations derived from computation tractability.

### Offering strategy methods for an electric railway company in energy and reserve markets

This study provides an appropriate offering strategy method for an Electric Railway Company (ERC) to participate in energy and reserve markets.

First, the problem of energy and reserve scheduling for ERC is modeled in a deterministic way. The results show that participating in upward and downward tertiary reserve markets is interesting for ERC since it can sell its surplus reserve capacity in the market without threatening the security of supply. The numerical results show that ERC can compensate one fourth of its total cost from participating in the reserve market.

Second, a discrete robust optimization technique is used to solve the energy and reserve scheduling problem taking into account the uncertain energy and reserve prices as well as the uncertain hourly energy demand of the electric railway substations. Moreover the proposed method provides the control parameters to set the level of robustness of the solution against uncertainties in the energy demands of ERC.

Third, based on the solution of the robust energy and reserve scheduling, a reserve offering curve construction algorithm considering the correlation between upward and downward reserve prices is proposed.

Finally, the effectiveness of the proposed reserve offering method is compared with another offering strategy reported in the literature that is based on the solution of the deterministic scheduling. In this respect, a realistic case study based on the characteristic of an ERC in Switzerland is presented.

### Capacity expansion of the interconnecting converters in interconnected system including electric railway and public power grids

In this study, methodologies to assess the capacity expansion of the interconnecting converters has been investigated.

First, the effect of increasing the capacity of the interconnecting converters on the daily operation cost of ERC has been studied. The study shows that in certain cases (depending on the capacity of the existing converters) the capacity expansion leads to the huge operation cost reduction.

Second, the effect of adding new interconnecting converters on the short circuit ratio of ERPS substations has been investigated. The results show that adding a centralized converter in a strong substation of the system is more beneficial than adding several distributed converters all over the system, in terms of improving the system total per unit short circuit current.

Finally, a cost-reliability approach has been proposed to find the optimal size and location of new interconnecting converters. This has allowed us to provide ERC with a set of optimal solutions according to the different economic and technical criteria.

## 7.2 Future Works

In the continuation of this work, the following topics are suggested for future possible research:

- The presented load forecast technique in chapter 4 should be enhanced by considering the information regarding the time table of trains along with time-series energy demand data.
- Referring to the capabilities of the interconnecting converters, this work was mainly dedicated to the bidirectional capability for energy exchanges. The converters can provide additional services such as voltage control and fast black start. Considering these capabilities to enhance the security of the interconnected system might be subject of interest for future research.
- The reserve services (ancillary services in general) exchanges between ERC and TSO is modeled based on the reserve market scheme. Considering the reserve service exchanges between the two system out of the market (based on a bilateral relationship) is an interesting topic for future research.
- The proposed energy and reserve offering strategy considers only the daily energy and reserve markets. To propose a general framework considering the weekly reserve markets and intra-day power markets is an interesting research topic. Moreover, this supplementary research is essential for the successful practical application of the proposed offering strategy method.
- The cost-reliability approach for capacity expansion problem presented in chapter 6 can be refined and complemented by considering the operation cost during the amortization time along with the investment cost. For this purpose, a long term load and energy price forecasts should be provided.

# Appendices

## A Solution Algorithms

In this appendix, two solution algorithms concerning the adaptive robust optimization approach for solving the min-max problem (4.27) are presented.

### A.1 Primal Cut Algorithm

This solution method is relying on the fact that the solution of the right hand maximization problem in (4.27) is at one of the vertex of the problem feasibility set [105]. Since the feasibility set for $\Delta\mathbf{L}$ (Uncertainty set (4.27d)) is independent from the feasibility set of the dual variables $\lambda, \mu$, the worst case realization of uncertain energy demand variations is at the uncertainty set vertex.

Let us define $\mathbf{\Delta L}_m$ the vertexes of the feasibility set $\mathbf{B\Delta L} \le \mathbf{b}$ for the uncertain energy demand variations of the ERC substations (the extended formulation is presented in (4.23)). For each vertex $m$, a corresponding set of second stage decision variables are assigned as $\mathbf{y}_m$. Hence, using primal cut algorithm, the problem (4.27) can be formulated as follows:

$$\min_{\mathbf{x},\mathbf{y}_m,\beta} \mathbf{c_x x} + \beta \tag{1a}$$

$$\text{s.t.} \quad \beta \ge \mathbf{c_y y}_\mathrm{m}, \quad \forall \mathrm{m} \tag{1b}$$

$$\mathbf{P y}_m + \mathbf{Q x} = \mathbf{\Delta L}_m, \quad \forall m \tag{1c}$$

$$\mathbf{N y}_m + \mathbf{M x} \le \mathbf{d}, \quad \forall m \tag{1d}$$

$$\mathbf{A x} = \mathbf{L} \tag{1e}$$

$$\mathbf{G x} \le \mathbf{g} \tag{1f}$$

The primal cut solution method formulation as presented in (1) is straight forward and easy to follow. The authors in [106] apply this method to solve the robust energy and reserve dispatch considering the uncertain wind power generation for few number of buses. The computational time and tractability of this method depends on the number of feasibility (uncertainty set) vertexes. The energy and reserve scheduling problem for an ERC as presented in section 4.3 includes the energy variations at each bus during each 15 minutes period. Moreover the complicated uncertainty set (4.23) also increase drastically the number of vertexes by considering the temporal and spatial correlations in the energy demand variations at substations. Therefore this primal cut algorithm is not computationally tractable for the application of adoptive robust optimization in energy and reserve scheduling of an ERC.

## A.2 Benders-Dual Cutting-Plane Algorithm

The Benders-dual cutting-plane algorithm in this section is relying on the fact that the solution of the inner bilinear maximization problem in (4.27) belongs to a set of finite cardinality $N$, which are independent from the first stage decisions. Let us indicate the element of this set as $(\mathbf{\Delta L}_m, \boldsymbol{\lambda}_n, \boldsymbol{\mu}_n)$, with $n = 1, ..., N$, the min-max problem ((4.27)) can be reformulated as:

$$\min_{\mathbf{x},\beta} \mathbf{c_x x} + \beta \tag{2a}$$

$$\text{s.t.} \quad \beta \geq \boldsymbol{\lambda}_{\mathrm{n}}^{\mathrm{T}} \mathbf{\Delta L}_{\mathrm{n}} + \boldsymbol{\mu}_{\mathrm{n}}^{\mathrm{T}} \mathbf{d} - (\boldsymbol{\lambda}_{\mathrm{n}}^{\mathrm{T}} \mathbf{Q} + \mu_{\mathrm{n}}^{\mathrm{T}} \mathbf{M}) \mathbf{x}, \quad \forall \mathrm{n} \tag{2b}$$

$$\mathbf{Ax} = \mathbf{L} \tag{2c}$$

$$\mathbf{Gx} \leq \mathbf{g} \tag{2d}$$

In the above master problem (2), the term $\beta$ is bounded by the piecewise linear function of the decision variables $\mathbf{x}$ with the cut which is derived from the following subproblem:

$$\max_{\mathbf{\Delta L},\boldsymbol{\lambda},\boldsymbol{\mu}} \boldsymbol{\lambda}^{\mathrm{T}}(\mathbf{\Delta L} - \mathbf{Qx}^*) + \boldsymbol{\mu}^{\mathrm{T}}(\mathbf{d} - \mathbf{Mx}^*) \tag{3a}$$

$$\text{s.t.} \quad \mathbf{P}^{\mathrm{T}} \boldsymbol{\lambda} + \mathbf{N}^{\mathrm{T}} \boldsymbol{\mu} = \mathbf{c}_{\mathbf{y}}^{\mathrm{T}} \tag{3b}$$

$$\boldsymbol{\mu} \leq \mathbf{0} \tag{3c}$$

$$\mathbf{B}\Delta\mathbf{L} \leq \mathbf{b} \tag{3d}$$

Here the set of fixed variables $\mathbf{x}^*$ are obtained from the solution of the master problem in the previous iteration. This bilinear maximization problem can be linearized using the dual variables ($\boldsymbol{\gamma}$) of the uncertainty set constraint (3d). This linearization is relying on the fact that maximization problem regarding $\mathbf{\Delta L}$ is linear. Therefore using the strong duality theorem, at the optimal point we have:

$$-\boldsymbol{\lambda}^{\mathrm{T}} \mathbf{\Delta L} = \mathbf{b}^{\mathrm{T}} \boldsymbol{\gamma} \tag{4}$$

Using equation (4) in the bilinear problem (3) we have:

$$\max_{\boldsymbol{\Delta}\mathbf{L},\boldsymbol{\lambda},\boldsymbol{\mu},\boldsymbol{\gamma}} -\boldsymbol{\lambda}^{\mathrm{T}}(\mathbf{Qx}^{*}) - \boldsymbol{\mu}^{\mathrm{T}}(\mathbf{d}-\mathbf{Mx}^{*}) + \mathbf{b}^{\mathrm{T}}\boldsymbol{\gamma} \tag{5a}$$

$$\text{s.t.} \quad \boldsymbol{\gamma} \geq 0 \perp \mathbf{b} - \mathbf{B}\boldsymbol{\Delta}\mathbf{L} \geq 0 \tag{5b}$$

$$\mathbf{B}^{\mathrm{T}}\boldsymbol{\gamma} = -\boldsymbol{\lambda} \tag{5c}$$

$$\mathbf{P}^{\mathrm{T}}\boldsymbol{\lambda} + \mathbf{N}^{\mathrm{T}}\boldsymbol{\mu} = \mathbf{c}_{\mathbf{y}}^{\mathrm{T}} \tag{5d}$$

$$\boldsymbol{\mu} \leq \mathbf{0} \tag{5e}$$

The orthogonal condition in (5b) can be handled using a set of corresponding auxiliary binary variables ($\mathbf{u}^{\gamma}, \mathbf{u}^{\mathrm{b}}$). Each auxiliary variable in $\mathbf{u}^{\gamma}$ is equal to 1 if the corresponding inequality $\boldsymbol{\gamma} \geq 0$ is true, otherwise it is equal to 0. Similarly each auxiliary variable in $\mathbf{u}^{\mathrm{b}}$ is equal to 1 if the corresponding inequality $\mathbf{b} - \mathbf{B}\boldsymbol{\Delta}\mathbf{L} \geq 0$ is true, otherwise it is equal to 0. Note that for each element of the uncertainty set, only one of these binary variables is equal to 1. To ensure this condition we use big M lemma, as a result the linear form of the subproblem can be formulated as follows:

$$\max_{\boldsymbol{\Delta}\mathbf{L},\boldsymbol{\lambda},\boldsymbol{\mu},\boldsymbol{\gamma}} -\boldsymbol{\lambda}^{\mathrm{T}}(\mathbf{Qx}^{*}) - \boldsymbol{\mu}^{\mathrm{T}}(\mathbf{d}-\mathbf{Mx}^{*}) + \mathbf{b}^{\mathrm{T}}\boldsymbol{\gamma} \tag{6a}$$

$$\text{s.t.} \quad 0 \leq \boldsymbol{\gamma} \leq \mathrm{M}^{\mathrm{big}}\mathbf{u}^{\gamma} \tag{6b}$$

$$0 \leq \mathbf{b} - \mathbf{B}\boldsymbol{\Delta}\mathbf{L} \leq M^{\mathrm{big}}\mathbf{u}^{b} \tag{6c}$$

$$\mathbf{u}^{\gamma} + \mathbf{u}^{b} = 1 \tag{6d}$$

$$\mathbf{B}^{\mathrm{T}}\boldsymbol{\gamma} = -\boldsymbol{\lambda} \tag{6e}$$

$$\mathbf{P}^{\mathrm{T}}\boldsymbol{\lambda} + \mathbf{N}^{\mathrm{T}}\boldsymbol{\mu} = \mathbf{c}_{\mathbf{y}}^{\mathrm{T}} \tag{6f}$$

$$\boldsymbol{\mu} \leq \mathbf{0} \tag{6g}$$

where $M^{\mathrm{big}}$ is a large enough positive number.

Next we use an iterative algorithm [107, 106] to solve the min-max problem based on the solutions of the master and the subproblem. This algorithm guarantees to converge to the optimal solutions in finite number of steps.

1. Set upper and lower bounds $UB = +\infty$ and $UB = -\infty$, and initialize the iteration index $i \leftarrow 1$.

2. Define the relaxed master problem (MP) as the minimization of (2) and fix a lower bound for $\beta$, a reasonable lower bound could be lower than the expected objective value of the sub problem. Fix the solution of relaxed MP ($\mathbf{x}_1^*, \beta_1^*$).

3. Solve the sub problem (either (3) or (6), the solutions are the same) while the first stage decisions are fixed. Let $z_i^{\mathrm{SP}*}$ the optimal value of subproblem (SP) objective function. Update the upper bound $UB = \min\left\{UB, \mathbf{c_x x}_i^* + z_i^{\mathrm{SP}*}\right\}$. Add to the relaxed MP the bender cut (2b) corresponding to the SP solution ($\mathbf{\Delta L}^*, \boldsymbol{\lambda}^*, \boldsymbol{\mu}^*$) determined at this stage.

4. Solve the relax MP. Fix $\mathbf{x}_{i+1}^*$ at the solution and $z_{i+1}^{\mathrm{MP}*}$ at the objective function value. Update $LB = z_{i+1}^{\mathrm{MP}*}$.

5. If $UB - LB \leq \epsilon$, where $\epsilon$ is a small predefined tolerance value, then stop. Otherwise, update $i \leftarrow i+1$ and go back to 3.

## B Linearization Technique

The linearization technique presented in [108] and [109] is used in the proposed optimization problem in chapter 6: 1) to transform a product of binary variables into a set of additional inequalities with a new continuous variable, and 2) to express the bilinear product of a binary variable and a continuous variable in as a set of additional linear constraints.

Let $x$ be the product of $n$ binary variables $u_1, \ldots, u_n$. Assuming that $x$ is a continuous variable, this product ($x = \prod_{i=1}^{n} u_i$) is equivalent to the $n+2$ following linear inequalities:

$$x \geq 0 \tag{7}$$

$$x \leq u_i \qquad i = 1, \ldots, n \tag{8}$$

$$x \geq \sum_{i=1}^{n} (u_i - n + 1) \tag{9}$$

Generally, the basic idea for modeling the bilinear product of a bounded continuous variable $y \in \left[y^{\min}, y^{\min}\right]$ and binary variable $x$ is to introduce a new continuous variable h such that $h = xy$. This product is equivalent to the additional linear constraints as follows:

$$xy^{\min} \leq h \leq xy^{\max} \tag{10}$$

$$y - y^{\max}(1-x) \leq h \leq y - y^{\min}(1-x) \tag{11}$$

Note that if $x = 0$, then the first constraint (10) implies that $h = 0$ ,while the second constraint (11) is relaxed. Otherwise, when $x = 1$, the second constraint implies that $h = y$, while the first constraint is inactive.

# Bibliography


[1] Y. G. Rebours, D. S. Kirschen, M. Trotignon, and S. Rossignol, "A survey of frequency and voltage control ancillary services—part ii: economic features," *Power Systems, IEEE Transactions on*, vol. 22, no. 1, pp. 358–366, 2007.

[2] A. Burger, M. Scherer, M. Buser, and P. Wenk, "Kooperationsszenarien für bahnstrom- und landesversorgungsnetz," *Bulletin des SEV VSE Including Jahresheft*, vol. 103, no. 12, p. 12, 2012.

[3] D. Bertsimas, E. Litvinov, X. A. Sun, J. Zhao, and T. Zheng, "Adaptive robust optimization for the security constrained unit commitment problem," *Power Systems, IEEE Transactions on*, vol. 28, no. 1, pp. 52–63, 2013.

[4] A. Street, A. Moreira, and J. Arroyo, "Energy and reserve scheduling under a joint generation and transmission security criterion: An adjustable robust optimization approach," *Power Systems, IEEE Transactions on*, vol. 29, pp. 3–14, Jan 2014.

[5] R. Billinton, *Reliability evaluation of power systems.* New York: Plenum Press, 1996.

[6] H.-S. Park and C.-H. Jun, "A simple and fast algorithm for k-medoids clustering," *Expert Systems with Applications*, vol. 36, no. 2, pp. 3336–3341, 2009.

[7] D. Bertsimas and M. Sim, "Robust discrete optimization and network flows," *Mathematical programming*, vol. 98, no. 1-3, pp. 49–71, 2003.

[8] S. Danielsen, *Electric Traction Power System Stability.* PhD thesis, NTNU-Norwegian University of Science and Technology, Trondheim, 2010.

[9] C. Heising, J. Fang, R. Bartelt, V. Staudt, and A. Steimel, "Modelling of rotary converter in electrical railway traction power-systems for stability analysis," in *Proceedings of Electrical Systems for Aircraft, Railway and Ship Propulsion (ESARS)*, pp. 1–6, IEEE, 2010.

[10] M. Oettmeier, C. Heising, R. Bartelt, V. Staudt, and A. Steimel, “Flux-based multivariable control of a static converter feeding a 16.7-hz single-phase load,” in *Industrial Electronics, 2009. IECON'09. 35th Annual Conference of IEEE*, pp. 492–497, IEEE, 2009.

[11] L. Abrahamsson and L. Soder, “Basic modeling for electric traction systems under uncertainty,” in *Universities Power Engineering Conference, 2006. UPEC'06. Proceedings of the 41st International*, vol. 1, pp. 252–256, IEEE, 2006.

[12] M. Olofsson, G. Andersson, and L. Söder, “Optimal operation of the swedish railway electrical system,” in *Proceedings of the International Conference on Electric Railways in a United Europe*, no. 405, pp. 64–68, 1995.

[13] M. Olofsson, L. Söder, and G. Andersson, “Optimal power flow in a traction power supply system,” in *Proceedings of12th Power Systems Computation Conference, August 19-23, 1996, Dresden, Germany*, 1996.

[14] A. Steimel, *Electric traction-motive power and energy supply: basics and practical experience.* Oldenbourg Industrieverlag, 2008.

[15] F. Kiessling, R. Puschmann, A. Schmieder, and E. Schneider, *Contact Lines for Electric Railways. Planning, Design, Implementation, Maintenance.* Publicis Publishing, 2009.

[16] B. Bhargava, “Benefits of a low frequency, low voltage railway electrification system,” in *Railroad Conference, 1996., Proceedings of the 1996 ASME/IEEE Joint*, pp. 177–184, IEEE, 1996.

[17] L. F. Rangel, “Competition policy and regulation in hydro-dominated electricity markets,” *Energy Policy*, vol. 36, no. 4, pp. 1292–1302, 2008.

[18] K. C. Almeida and A. J. Conejo, “Medium-term power dispatch in predominantly hydro systems: An equilibrium approach,” *Power Systems, IEEE Transactions on*, vol. 28, no. 3, pp. 2384–2394, 2013.

[19] D. De Ladurantaye, M. Gendreau, and J.-Y. Potvin, “Strategic bidding for price-taker hydroelectricity producers,” *Power Systems, IEEE Transactions on*, vol. 22, no. 4, pp. 2187–2203, 2007.

[20] X. Guan, E. Ni, R. Li, and P. B. Luh, “An optimization-based algorithm for scheduling hydrothermal power systems with cascaded reservoirs and discrete hydro constraints,” *Power Systems, IEEE Transactions on*, vol. 12, no. 4, pp. 1775–1780, 1997.

[21] R. Boeck, O. J. Gaupp, P. Daehler, E. Baerlocher, J. Werninger, and P. Zanini, “Bremen's 100-mw static frequency link,” *ABB REVIEW*, pp. 4–17, 1996.

[22] B. Robertson and T. Rogers, "Performance of the single-phase synchronous machine," *American Institute of Electrical Engineers, Transactions of the*, vol. 67, no. 1, pp. 194–196, 1948.

[23] S. Danielsen and T. Toftevaag, "Experiences with respect to low frequency instability from operation of advanced electrical rail vehicles in a traction power system with rotary converters," in *Proceedings of the MET2007 8th International Conference "Drives And Supply Systems For Modern Electric Traction", Warsaw, Poland*, pp. 51–57, 2007.

[24] G. Linhofer, P. Maibach, and N. Umbricht, "The railway connection: Frequency converters for railway power supply," *ABB Review*, vol. 4, pp. 49–55, 2009.

[25] J. R. Rodríguez, J. W. Dixon, J. R. Espinoza, J. Pontt, and P. Lezana, "Pwm regenerative rectifiers: state of the art," *Industrial Electronics, IEEE Transactions on*, vol. 52, no. 1, pp. 5–22, 2005.

[26] M. Malinowski, "Sensorless control strategies for three-phase pwm rectifiers," *Rozprawa doktorska, Politechnika Warszawska, Warszawa*, 2001.

[27] "Bahnstromversorgung BLS: Statische Umrichter für die Netzkupplung BKW/BLS in Wimmis," tech. rep., BKW FMB Energie AG: Internal, 2003.

[28] P. wenk, K. Brunner, W. Sattinger, T. Arnold, R. Notter, and M. Scherer, "Möglichkeiten der technischen Zusammenarbeit zwischen SBB und Swissgrid, Schwerpunkt: Austausch von Systemdienstleistungen an der Schnittstelle," tech. rep., SBB and Swissgrid, 06 2010.

[29] P.-H. Hsi and S.-L. Chen, "Electric load estimation techniques for high-speed railway (hsr) traction power systems," *Vehicular Technology, IEEE Transactions on*, vol. 50, no. 5, pp. 1260–1266, 2001.

[30] G. Garcia, M. A. Rios, and G. Ramos, "A power demand simulator of electric transportation systems for distribution utilities," in *Universities Power Engineering Conference (UPEC), 2009 Proceedings of the 44th International*, pp. 1–5, IEEE, 2009.

[31] "Sbb consumption." http://www.sbb.ch/en/group/sbb-as-business-partner/offers-for-rus/energy.html. Accessed: 2015-04-01.

[32] M. Beck and M. Scherer, "Swissgrid: Overview of ancillary services," 2010.

[33] "Entso-e: Operation handbook, appendix 1. load-frequency control and performance," 2014.

[34] D. Kirschen, *Fundamentals of power system economics.* Chichester, West Sussex, England Hoboken, NJ: John Wiley & Sons, 2004.

[35] A. A. Khatir, R. Cherkaoui, and M. Zima, "Literature survey on fundamental issues of frequency control reserve (fcr) provision," *Swiss Electric Research*, 2010.

[36] M. Shahidehpour, *Market operations in electric power systems forecasting, scheduling, and risk management.* New York: Institute of Electrical and Electronics Engineers, Wiley-Interscience, 2002.

[37] A. Wood, *Power generation, operation, and control.* New York: J. Wiley & Sons, 1996.

[38] K. W. Cheung, P. Shamsollahi, D. Sun, J. Milligan, and M. Potishnak, "Energy and ancillary service dispatch for the interim iso new england electricity market," in *Power Industry Computer Applications, 1999. PICA'99. Proceedings of the 21st 1999 IEEE International Conference*, pp. 47–53, IEEE, 1999.

[39] J. F. Restrepo and F. D. Galiana, "Unit commitment with primary frequency regulation constraints," *Power Systems, IEEE Transactions on*, vol. 20, no. 4, pp. 1836–1842, 2005.

[40] T. Zheng and E. Litvinov, "Contingency-based zonal reserve modeling and pricing in a co-optimized energy and reserve market," *Power Systems, IEEE Transactions on*, vol. 23, no. 2, pp. 277–286, 2008.

[41] M. A. O. Vazquez, *Optimizing the spinning reserve requirements.* PhD thesis, University of Manchester, 2006.

[42] A. Ahmadi-Khatir, M. Bozorg, and R. Cherkaoui, "Probabilistic spinning reserve provision model in multi-control zone power system," *Power Systems, IEEE Transactions on*, vol. 28, no. 3, pp. 2819–2829, 2013.

[43] R. Allan and R. Billinton, "Probabilistic assessment of power systems," *Proceedings of the IEEE*, vol. 88, no. 2, pp. 140–162, 2000.

[44] R. Billinton and M. Fotuhi-Firuzabad, "A basic framework for generating system operating health analysis," *Power Systems, IEEE Transactions on*, vol. 9, no. 3, pp. 1610–1617, 1994.

[45] A. Abiri-Jahromi, M. Fotuhi-Firuzabad, and E. Abbasi, "Optimal scheduling of spinning reserve based on well-being model," *Power Systems, IEEE Transactions on*, vol. 22, no. 4, pp. 2048–2057, 2007.

[46] C. Maurer, S. Krahl, and H. Weber, "Dimensioning of secondary and tertiary control reserve by probabilistic methods," *European Transactions on Electrical Power*, vol. 19, no. 4, pp. 544–552, 2009.

[47] M. Scherer, M. Zima, and G. Andersson, "An integrated pan-european ancillary services market for frequency control," *Energy Policy*, vol. 62, pp. 292–300, 2013.

[48] R. Billinton and R. N. Allan, *Reliability Evaluation of Power Systems.* 2nd ed. Plenum Press, 1996.

[49] R. Allan and R. Billinton, "Power system reliability and its assessment. iii. distribution systems and economic considerations," *Power Engineering Journal*, vol. 7, pp. 185 –192, aug 1993.

[50] F. Lee, Q. Chen, and A. Breipohl, "Unit commitment risk with sequential rescheduling," *Power Systems, IEEE Transactions on*, vol. 6, pp. 1017 –1023, aug 1991.

[51] H. Gooi, D. Mendes, K. Bell, and D. Kirschen, "Optimal scheduling of spinning reserve," *Power Systems, IEEE Transactions on*, vol. 14, pp. 1485 –1492, nov. 1999.

[52] D. Chattopadhyay and R. Baldick, "Unit commitment with probabilistic reserve," in *Power Engineering Society Winter Meeting, 2002. IEEE*, vol. 1, pp. 280 – 285 vol.1, 2002.

[53] M. Ortega-Vazquez, D. Kirschen, and D. Pudjianto, "Optimising the scheduling of spinning reserve considering the cost of interruptions," *Generation, Transmission and Distribution, IEE Proceedings-*, vol. 153, no. 5, pp. 570 – 575, 2006.

[54] F. Bouffard and F. Galiana, "An electricity market with a probabilistic spinning reserve criterion," *Power Systems, IEEE Transactions on*, vol. 19, no. 1, pp. 300 – 307, 2004.

[55] F. Aminifar, M. Fotuhi-Firuzabad, and M. Shahidehpour, "Unit commitment with probabilistic spinning reserve and interruptible load considerations," *Power Systems, IEEE Transactions on*, vol. 24, no. 1, pp. 388–397, 2009.

[56] F. Bouffard, F. D. Galiana, and A. J. Conejo, "Market-clearing with stochastic security-part i: formulation," *Power Systems, IEEE Transactions on*, vol. 20, no. 4, pp. 1818–1826, 2005.

[57] F. D. Galiana, F. Bouffard, J. M. Arroyo, and J. F. Restrepo, "Scheduling and pricing of coupled energy and primary, secondary, and tertiary reserves," *Proceedings of the IEEE*, vol. 93, no. 11, pp. 1970–1983, 2005.

[58] J. M. Morales, A. J. Conejo, and J. Pérez-Ruiz, "Economic valuation of reserves in power systems with high penetration of wind power," *Power Systems, IEEE Transactions on*, vol. 24, no. 2, pp. 900–910, 2009.

[59] D. Bertsimas, D. B. Brown, and C. Caramanis, "Theory and applications of robust optimization," *SIAM review*, vol. 53, no. 3, pp. 464–501, 2011.

[60] O. Alizadeh Mousavi, M. Bozorg, R. Cherkaoui, and M. Paolone, "Investigation of the blackouts complexity regarding spinning reserve and frequency control in interconnected power systems," in *Proceedings of the 12th International Conference on Probabilistic Methods Applied to Power Systems (PMAPS)*, no. EPFL-CONF-183288, pp. 1–6, IEEE Power Engineering Society, 2012.

[61] O. A. Mousavi, M. Bozorg, R. Cherkaoui, and M. Paolone, "Inter-area frequency control reserve assessment regarding dynamics of cascading outages and blackouts," *Electric Power Systems Research*, vol. 107, pp. 144 – 152, 2014.

[62] A. Ahmadi Khatir, *Reserve services management in multi-area power system under uncertainty.* PhD thesis, EPFL, 2013.

[63] S. S. Oren, "Design of ancillary service markets," in *System Sciences, 2001. Proceedings of the 34th Annual Hawaii International Conference on*, pp. 9–pp, IEEE, 2001.

[64] H.-P. Chao and R. Wilson, "Multi-dimensional procurement auctions for power reserves: Robust incentive-compatible scoring and settlement rules," *Journal of Regulatory Economics*, vol. 22, no. 2, pp. 161–183, 2002.

[65] "Swiss ancillary service market." http://www.swissgrid.ch/. Accessed: 2015-04-01.

[66] F. Abbaspourtorbati and M. Zima, "Procurement of frequency control reserves in self-scheduling markets using stochastic programming approach: Swiss case," in *European Energy Market (EEM), 2013 10th International Conference on the*, pp. 1–6, IEEE, 2013.

[67] "Introduction to balance group model." http://www.swissgrid.ch/. Accessed: 2015-04-01.

[68] E. Vrettos, F. Oldewurtel, M. Vasirani, and G. Andersson, "Centralized and decentralized balance group optimization in electricity markets with demand response," in *PowerTech (POWERTECH), 2013 IEEE Grenoble*, pp. 1–6, IEEE, 2013.

[69] M. Bozorg and R. Cherkaoui, "Energy and reserve scheduling for electric railway power system using stochastic optimization," in *Proceedings of PowerTech (POWERTECH), 2015 IEEE Eindhoven*, IEEE, 2015.

[70] T. Kulworawanichpong, *Optimising AC electric railway power flows with power electronic control.* PhD thesis, University of Birmingham, 2004.

[71] T. Ho, Y. Chi, J. Wang, K. Leung, L. Siu, and C. Tse, "Probabilistic load flow in ac electrified railways," in *Electric Power Applications, IEE Proceedings-*, vol. 152, pp. 1003–1013, IET, 2005.

[72] S. Kazempour, M. Hosseinpour, and M. Moghaddam, "Self-scheduling of a joint hydro and pumped-storage plants in energy, spinning reserve and regulation markets," in *Power Energy Society General Meeting, 2009. PES '09. IEEE*, pp. 1–8, July 2009.

[73] M. Rahimiyan, L. Baringo, and A. Conejo, "Energy management of a cluster of interconnected price-responsive demands," *Power Systems, IEEE Transactions on*, vol. 29, pp. 645–655, March 2014.

[74] R. A. Jabr, "Worst-case robust profit in generation self-scheduling," *Power Systems, IEEE Transactions on*, vol. 24, no. 1, pp. 492–493, 2009.

[75] H. K. Alfares and M. Nazeeruddin, "Electric load forecasting: literature survey and classification of methods," *International Journal of Systems Science*, vol. 33, no. 1, pp. 23–34, 2002.

[76] G. Mbamalu and M. El-Hawary, "Load forecasting via suboptimal seasonal autoregressive models and iteratively reweighted least squares estimation," *Power Systems, IEEE Transactions on*, vol. 8, no. 1, pp. 343–348, 1993.

[77] G. Box, G. Jenkins, and G. reinsel, *Time Series Analysis: Forecasting and Control*. Wiley, 2008.

[78] G. Juberias, R. Yunta, J. Garcia Moreno, and C. Mendivil, "A new arima model for hourly load forecasting," in *Transmission and Distribution Conference, 1999 IEEE*, vol. 1, pp. 314–319, IEEE, 1999.

[79] A. Lorca and X. Sun, "Adaptive robust optimization with dynamic uncertainty sets for multi-period economic dispatch under significant wind," *Power Systems, IEEE Transactions on*, vol. 30, pp. 1702–1713, July 2015.

[80] E. Richard, "Gams-a user's guide." GAMS Development Corporation, Washington, DC, USA, 2010.

[81] M. Bozorg, E. Hajipour, and S. H. Hosseini, "Interruptible load contracts implementation in stochastic security constrained unit commitment," in *Probabilistic Methods Applied to Power Systems (PMAPS), 2010 IEEE 11th International Conference on*, pp. 796–801, IEEE, 2010.

[82] E. Hajipour, M. Bozorg, and M. Fotuhi-Firuzabad, "Stochastic capacity expansion planning of remote microgrids with wind farms and energy storage," *Sustainable Energy, IEEE Transactions on*, vol. 6, no. 2, pp. 491–498, 2015.

[83] J. Sumaili, H. Keko, V. Miranda, A. Botterud, and J. Wang, "Clustering-based wind power scenario reduction," in *Proceedings of the 17th Power Systems Computation Conference*, 2011.

[84] G. Li, J. Shi, and X. Qu, "Modeling methods for genco bidding strategy optimization in the liberalized electricity spot market–a state-of-the-art review," *Energy*, vol. 36, no. 8, pp. 4686–4700, 2011.

[85] E. Ni, P. B. Luh, and S. Rourke, "Optimal integrated generation bidding and scheduling with risk management under a deregulated power market," *Power Systems, IEEE Transactions on*, vol. 19, no. 1, pp. 600–609, 2004.

[86] A. J. Conejo, F. J. Nogales, and J. M. Arroyo, "Price-taker bidding strategy under price uncertainty," *Power Systems, IEEE Transactions on*, vol. 17, no. 4, pp. 1081–1088, 2002.

[87] T. Li, M. Shahidehpour, and Z. Li, "Risk-constrained bidding strategy with stochastic unit commitment," *Power Systems, IEEE Transactions on*, vol. 22, no. 1, pp. 449–458, 2007.

[88] S.-E. Fleten and T. K. Kristoffersen, "Stochastic programming for optimizing bidding strategies of a nordic hydropower producer," *European Journal of Operational Research*, vol. 181, no. 2, pp. 916–928, 2007.

[89] J. Garcia-Gonzalez, R. R. de la Muela, L. M. Santos, and A. M. González, "Stochastic joint optimization of wind generation and pumped-storage units in an electricity market," *Power Systems, IEEE Transactions on*, vol. 23, no. 2, pp. 460–468, 2008.

[90] L. Baringo and A. J. Conejo, "Offering strategy via robust optimization," *Power Systems, IEEE Transactions on*, vol. 26, no. 3, pp. 1418–1425, 2011.

[91] "Epex spot exchange rules." http://www.epexspot.com/en/extras/download-center/. Accessed: 2015-04-01.

[92] "Ucte operations handbook: P1–policy 1: Load-frequency control and performance [c]; version: v3. 0 rev," 2009.

[93] A. J. Conejo, J. Contreras, R. Espinola, and M. A. Plazas, "Forecasting electricity prices for a day-ahead pool-based electric energy market," *International Journal of Forecasting*, vol. 21, no. 3, pp. 435–462, 2005.

[94] M. Bozorg, D. Lopez, and R. Cherkaoui, "Converter placement in the interconnection of railway power grid and public power grid based on cost-reliability approach," in *PowerTech (POWERTECH), 2013 IEEE Grenoble*, pp. 1–6, IEEE, 2013.

[95] "Sbb facts and figures 2014." https://www.sbb.ch/en/group/the-company/facts-and-figures. Accessed: 2015-04-01.

[96] Y. Liu and Z. Chen, "Short circuit ratio analysis of multi-infeed hvdc system with a vsc-hvdc link," in *IECON 2011-37th Annual Conference on IEEE Industrial Electronics Society*, pp. 949–954, IEEE, 2011.

[97] X.-F. Wang, Y. Song, and M. Irving, *Modern power systems analysis.* Springer Science & Business Media, 2010.

[98] D. L. Duran, "Optimal converter placement in the interconnection of a power system and a railway network," Master's thesis, Comillas Pontifical University, Madrid, Spain, 2012.

[99] G. Latorre, R. D. Cruz, J. M. Areiza, and A. Villegas, "Classification of publications and models on transmission expansion planning," *Power Systems, IEEE Transactions on*, vol. 18, no. 2, pp. 938–946, 2003.

[100] N. Alguacil, A. L. Motto, and A. J. Conejo, "Transmission expansion planning: a mixed-integer lp approach," *Power Systems, IEEE Transactions on*, vol. 18, no. 3, pp. 1070–1077, 2003.

[101] M. Rider, A. Garcia, and R. Romero, "Power system transmission network expansion planning using ac model," *IET Generation, Transmission & Distribution*, vol. 1, no. 5, pp. 731–742, 2007.

[102] I. J. Ramírez-Rosado and J. L. Bernal-Agustín, "Reliability and costs optimization for distribution networks expansion using an evolutionary algorithm," *Power Systems, IEEE Transactions on*, vol. 16, no. 1, pp. 111–118, 2001.

[103] M. S. Sepasian, H. Seifi, A. A. Foroud, S. H. Hosseini, and E. M. Kabir, "A new approach for substation expansion planning," *Power Systems, IEEE Transactions on*, vol. 21, no. 2, pp. 997–1004, 2006.

[104] E. Carrano, R. Takahashi, E. Cardoso, R. Saldanha, and O. Neto, "Optimal substation location and energy distribution network design using a hybrid ga-bfgs algorithm," in *Generation, Transmission and Distribution, IEE Proceedings-*, vol. 152, pp. 919–926, IET, 2005.

[105] B. Zeng and L. Zhao, "Solving two-stage robust optimization problems using a column-and-constraint generation method," *Operations Research Letters*, vol. 41, no. 5, pp. 457–461, 2013.

[106] M. Zugno and A. J. Conejo, “A robust optimization approach to energy and reserve dispatch in electricity markets,” tech. rep., Technical University of Denmark, 2013.

[107] A. Thiele, T. Terry, and M. Epelman, “Robust linear optimization with recourse,” *Rapport technique*, pp. 4–37, 2009.

[108] H. P. Williams, *Model Building in Mathematical Programming.* Wiley, 2013.

[109] C. A. Floudas, *Nonlinear and Mixed-Integer Optimization: Fundamentals and Applications (Topics in Chemical Engineering).* Oxford University Press, USA, 1995.

# Curriculum Vitae


## Mokhtar BOZORG

Power System Research Group
École Polytechnique Fédérale de Lausanne (EPFL)

Date of Birth: 11th February 1986
Place of Birth: Tehran, Iran.

Address: Avenue Jomini 4
CH-1004 Lausanne

Tel: +41 78 737 7833

Email: mokhtar.bozorg@gmail.com
mokhtar.bozorg@epfl.ch


## Education

| | |
|---|---|
| 2011 – 2015 | **Ph.D. in Electrical Engineering**, EPFL, Lausanne, Switzerland.<br>Thesis title: Energy and Reserve Management in Interconnected Systems including Electric Railway and Public Power Grids: Operation, Market Strategies and Capacity Expansion. |
| 2008 – 2010 | **M.Sc. in Electrical Engineering,** Sharif University of Technology, Tehran, Iran.<br>Major: Management and control of power systems<br>Thesis title: Uncertainty Management in Operation and Planning of Combined Heat and Power units using Monte Carlo Approach to Stochastic Optimization. |
| 2004 – 2008 | **B.Sc. in Electrical Engineering,** Sharif University of Technology, Tehran, Iran.<br>Major: Power engineering |

## Professional Experience

| | |
|---|---|
| 2011 – 2015 | EPFL<br>Position: Assistant Doctorate |
| 2010 – 2011 | Tehran Urban Planning and Research Center<br>Position: Junior Researcher |
| 2008 – 2009 | “Namad Mobtaker” Consultant Engineers Company, Tehran, Iran.<br>Position: Consultant Engineer |

## Research Interest

Electricity Markets
Power System Optimization and Control
Risk and Uncertainty Management in Power Systems
Integration of Renewable Energy Sources into Power Grids

## Languages

Persian: Mother tongue
English: Fluent
French: Very good knowledge

# List of Publications

## <u>Journal Papers</u>


[J6] **M. Bozorg**, A. Ahmadi Khatir and R. Cherkaoui, "Developing offer curves for an electric railway company in reserve markets based on robust energy and reserve scheduling", Under minor revision in *IEEE Transactions on Power Systems*.

[J5] A. Ahmadi-Khatir**, M. Bozorg** and R. Cherkaoui. "Probabilistic spinning reserve provision model in multi-control zone power system", *IEEE Transactions on Power Systems*, vol. 28, no. 3 (2013): 2819-2829.

[J4] O. A. Mousavi, **M. Bozorg**, and R. Cherkaoui, "Preventive reactive power management for improving voltage stability margin." *Electric Power Systems Research* 96 (2013): 36-46.

[J3] Mousavi, O. Alizadeh, R. Cherkaoui, and **M. Bozorg**, "Blackouts risk evaluation by Monte Carlo Simulation regarding cascading outages and system frequency deviation." *Electric Power Systems Research* 89 (2012): 157-164.

[J2] E. Hajipour, **M. Bozorg** and M. Fotuhi-Firuzabad, "Stochastic Capacity Expansion Planning of Remote Microgrids with Wind Farms and Energy Storage", *IEEE Transactions on Sustainable Energy*, vol. 6, no. 2 (2015): 491-498.

[J1] O. A. Mousavi, **M. Bozorg**, R. Cherkaoui, and M. Paolone, "Inter-area frequency control reserve assessment regarding dynamics of cascading outages and blackouts." *Electric Power Systems Research* 107 (2014): 144-152.


## <u>Conference Papers</u>


[C7] **M. Bozorg** and R. Cherkaoui, "Converter placement in the interconnection of railway power grid and public power grid based on cost-reliability approach." In *proceedings of the 11th IEEE PowerTech (POWERTECH)*, 29 June - 2 July, 2015, Eindhoven, Netherlands.

[C6] O. A. Mousavi, R. Cherkaoui and **M. Bozorg**, "Statistical analysis of optimal energy and security controls under different sources of uncertainties" In *Proceedings of the 12th International Conference on Probabilistic Methods Applied to Power Systems (PMAPS)*, 7-10 July, 2014, Durham, United Kingdom.

[C5] **M. Bozorg**, D. Lopez, and R. Cherkaoui. “Converter placement in the interconnection of railway power grid and public power grid based on cost-reliability approach.” In *10th IEEE PowerTech Conference, 16-20 June, 2013, Grenoble*, France. 153

[C4] O. A. Mousavi, **M. Bozorg**, R. Cherkaoui, and Mario Paolone, “Investigation of the blackouts complexity regarding spinning reserve and frequency control in interconnected power systems.” In *Proceedings of the 11th International Conference on Probabilistic Methods Applied to Power Systems (PMAPS)*, 10-14 June, 2012, Istanbul, Turkey.

[C3] O. A. Mousavi, **M. Bozorg**, A. Ahmadi-Khatir and R. Cherkaoui, “Reactive power reserve management: preventive countermeasure for improving voltage stability margin.” In *Power and Energy Society General Meeting*, 22-26 July, San Diego, California, USA.

[C2] **M. Bozorg** and M. Ehsan, “Uncertainty Management in Optimal Sizing of CHP for Residential Complexes Based on Monte Carlo Approach to Stochastic Programming”, In *Proceedings of the International Conference on Energy Sources and Smart Grids Development*, 17-19 December, 2010, Jilin, China.

[C1] **M. Bozorg**, E. Hajipour, and S. H. Hosseini, “Interruptible load contracts implementation in stochastic security constrained unit commitment.” In *Proceedings of the 10th International Conference on Probabilistic Methods Applied to Power Systems (PMAPS)*, 14-17 June, 2010, Singapore.